CORE
Metadata, citation and similar papers at core.ac.uk
Provided by ScholarBank@NUS

STUDY OF TMCTS BASED PECVD CARBON-DOPED LOW DIELECTRIC CONSTANT MATERIAL

XIE JIELIN

NATIONAL UNIVERSITY OF SINGAPORE

2004

STUDY OF TMCTS BASED PECVD CARBON-DOPED LOW DIELECTRIC CONSTANT MATERIAL

XIE JIELIN
(B.Sc. NWU)

A THESIS SUBMITTED

FOR THE DEGREE OF MASTER OF SCIENCE

DEPARTMENT OF PHYSICS

NATIONAL UNIVERSITY OF SINGAPORE

2004

Acknowledgements

First of all, I would like to thank Professor Jianyi Lin from the Department of Physics. As my supervisor, Professor Lin gives his ongoing support and important guidance on this project. Thanks are extended to academic staff from Physics Department and Surface Lab. This project could not have been finished without their support. Many thanks are due to Mr. Xiaobin Wu, Dr. Jizhong Luo, Mr. Liu Rong, Ms. Yanjiao Liu and Dr. Luwei Chen for their kindly support during sample analysis.

Next, I wish to thank Dr.Yihua Wang from Institute of Microelectronics (IME). Dr. Wang contributes many good ideas to this project. He also gives many helps on data explanation. Special thanks to IME DSIC-MD department manager Mr. Rakesh Kumar. The supports and guidance from him are very important for this project. Thanks are also extended to my colleagues Mr. Babu Narayanan, Mr. Minrui Wang, Dr. Chaoyong Li, Ms. Yuan Yijing Stella, Ms. Shurui Wang and Ms. Li Weihong Cartherine for their helps during sample preparation.

Finally, I want to express thanks to my dear wife and my lovely son. The supports during my study from them are appreciable.

Table of Contents

Chapter 1 Introduction 1

1.1 Moore's Law 1

1.2 Why low-k material 3

1.3 What is low-k material 5

1.3.1 Spin-on low-k Dielectric (SOD) 5

1.3.2 PECVD low-k material 9

1.4 The requirements of dielectric in microelectronics and the research topic of the thesis 12

1.5 Outline of the thesis 16

Chapter 2 Literature Review 17

2.1 Structure of carbon doped oxide (SiOCH) low-k film 17

2.2 Basic properties of SiOCH low-k film 20

2.2.1 Dielectric constant and Pore-Related properties 20

2.2.2 Optical properties 25

2.2.3 Other physical and electrical properties 25

2.2.4 Resistance to plasma treatment 29

2.3 Integration issues of SiOCH low-k film 29

Chapter 3 Experimental 33

3.1 Principle of Plasma Enhanced Chemical Vapor Deposition (PECVD) 33

3.2 Novellus Concept two Sequel Express PECVD system 35

3.3 C-V 495 system 38

3.4 Fourier Transform Infrared (FTIR) Spectroscopy 41

3.5 Atomic Force Microscopy (AFM) 43

3.6 X-Ray Photoemission Spectroscopy (XPS) 44

3.7 Secondary Ion Mass Spectroscopy (SIMIS) 46

3.8 FSM 7800TC Stress Measurement System 47

3.9 Tetramethylcyclotelrasiloxane (TMCTS), the precursor for PECVD 49

3.10 Experiment conditions 50

3.10.1 The growth of CORAL films on Si (100) 51

3.10.2 Thermal treatment 51

3.10.3 Dilute HF treatment 52

3.10.4 Plasma treatment 52

Chapter 4 The effects of thermal, dilute HF and plasma treatments on CORAL film 54

4.1 The growth of CORAL 54

4.2 Thermal treatment 55

4.2.1 Thickness and Refractive Index (RI) 55

4.2.2 Chemical bonding in CORAL films 61

4.2.3 Roughness and stress 65

4.2.4 Chemical composition of CORAL films 70

4.2.5 K value and leakage current 78

4.3 Dilute HF treatment 80

4.3.1 Thickness and RI 81

4.3.2 Surface roughness 82

4.3.3 Chemical bonding 83

4.3.4 K value and leakage current 84

4.4 Plasma treatment 89

4.4.1 Forming gas (4%H_2+N_2) plasma treatment 89

4.4.2 Oxygen plasma treatment 93

4.4.3 Fluoride gas plasma treatment 96

4.4.4 Ammonia and Helium plasma treatment 97

Chapter 5 Conclusion 98

5.1 Thermal treatment 98

5.2 Dilute HF treatment 99

5.3 Plasma treatment 100

Reference 102

Summary

Carbon doped silicon oxide (SiOCH), a low dielectric constant (low-k) material is one of good dielectric candidates for advanced interconnect technology. Good thermal stability of dielectric and resistance to plasma treatment are required due to many thermal processes and plasma processes are involved during IC fabrication. On the other hand, reducing k value of bulk dielectric is critical as it plays an important role on effective k value of the final product. Therefore, we carry out this project, focusing on the synthesis of carbon-doped SiOCH, and its post-growth thermal treatment, dilute HF treatment (intending to reduce k value) and plasma treatment.

Firstly, Tetramethylcyclotelrasiloxane (TMCTS) based PECVD carbon doped low-k material (CORAL) was thermally annealed at temperatures from 400°C to 800°C in N_2. It was found that thermal stability temperature of CORAL film is 600°C. At above 600°C annealing, the thermal energy can break Si-CH_3, Si-C, Si-H and C-H bonds, as detected by XPS, FTIR, leads to outgasing, which results in film composition change, weight loss and thickness shrinkage. Film composition changes especially carbon loss and oxygen incorporation can degrade its reliability extremely. Carbon is desorbed in the form of CH_4, CO and other hydrocarbon.

Secondly, dilute HF wet etch method was employed intending to reduce dielectric constant of CORAL film. The chemical structure, surface roughness and leakage current etc. of CORAL film after dilute HF treatment were investigated. The Si-O bonds

decreased after dilute HF etch due to the main structure Si-O skeleton of CORAL film was attacked. This method can reduce k value of CORAL film about 14% by introducing pores in it. One of the concerns of this method is the introduction of hole trapping sites at the interface of Si/CORAL. These sites can increase leakage current of the treated CORAL film.

Finally, the properties of CORAL film after H_2/N_2, O_2, fluoride gas, NH_3 and He plasma treatment were investigated. CORAL film is unstable after H_2/N_2 and O_2 plasma treatment whereas it remains stable after fluoride gas, NH_3 and He plasma treatment. In H_2/N_2 plasma, heavy N^+ ions bombarded the CORAL film to generate silicon dangling bonds. The H^+ ions and water in the atmosphere then transferred the Si dangling bonds to OH bonds that can degrade film properties including increased k value and leakage current. In O_2 plasma, the function groups of CORAL film were destroyed by oxygen radicals. This process results in thickness decreased which was attributed to gas desorption and OH bonds incorporation due to moisture uptake. As mentioned above, the incorporated OH bonds result in k value and leakage current increased.

List of Figures

Figure 1-1 Moore's law (Courtesy of Intel Corporation)

Figure 1-2 Dependence of signal delay on device size

Figure 1-3 Generation vs. Delay (Courtesy of Intel)

Figure 2-1 OSG structure and SiO_2 structure

Figure 2-2 The dielectric constant as a function of the ratio of the precursor flow rates

Figure 2-3 Dual damascene Cu/low-k via first process in ULSI

Figure 3-1 Schematic of PECVD reactor designed by Reinberg (Coutesy of the Electrochemical Society, Inc.)

Figure 3-2 Sequel Express process module

Figure 3-3 Novellus Concept two Sequel Express PECVD system

Figure 3-4 Schematic of mercury (Hg) probe

Figure 3-5 C-V curve of MOS structure

Figure 3-6 Equivalent circuit of two terminals MOS structure

Figure 3-7 Michelson Interferometer

Figure 3-8 Schematic of TappingMode AFM

Figure 3-9 Schematic of electron analyzer

Fig. 3-10 Schematic of SIMIS instrument

Figure 3-11 Schematic of stress measurement system configuration

Figure 3-12 Chemical structure of TMCTS

Figure 4-1 Thickness and RI of CORAL after annealing

Figure 4-2 Gas desorption of CORAL

Figure 4-3 TGA from RT to 800°C of CORAL

Figure 4-4 Thickness after 10 thermal cycles @ 425°C of CORAL

Figure 4-5 RI trend after thermal cycle at 425°C of CORAL

Figure 4-6 TGA @ 425°C for 6 hours of CORAL film

Figure 4-7 FTIR spectra of CORAL after annealing

Figure 4-8 Shoulder shift after annealing of CORAL

Figure 4-9 C-H_3 to Si-O peak area ratio as determined from FTIR spectra after annealing of CORAL

Figure 4-10 C-H to Si-O peak area ratio as determined from FTIR spectra after annealing of CORAL

Figure 4-11 Si-C to Si-O peak area ratio as determined from FTIR spectra after annealing of CORAL

Figure 4-12 FTIR spectra of CORAL after 10 thermal cycles @ 425°C

Figure 4-13 Surface roughness (R_{MS}) of CORAL film after annealing

Figure 4-14 Dependence of stress on annealing temperature on CORAL film

Figure 4-15 XPS wide scan of as-deposit CORAL film

Figure 4-16 SIMIS analysis of as-deposit CORAL film

Figure 4-17 Oxygen to silicon ratio of CORAL film after annealing

Figure 4-18 Carbon to silicon ratio of CORAL film after annealing

Figure 4-19 XPS narrow scan Si 2p of CORAL film after annealing

Figure 4-20 XPS narrow scan C 1s of CORAL film after annealing

Figure 4-21 K value of CORAL after annealing

Figure 4-22 Field break down voltage of CORAL after annealing

Figure 4-23 Thickness and RI of CORAL film after etching in 1% dilute HF

Figure 4-24 CORAL surface after 1% dilute HF treatment

Figure 4-25 Surface Roughness of CORAL film after dilute HF treatment

Figure 4-26 Si-O peak of CORAL film decreases after dilute HF etching

Figure 4-27 K value trend of CORAL film after1% dilute HF treatment

Figure 4-28 C-V curve of CORAL after etching in dilute HF

Figure 4-29 Leakage current of CORAL after 1% dilute HF etching

Figure 4-30 FTIR spectra of CORAL film after forming gas plasma treatment

Figure 4-31 Peak area ratio of Si-CH3 to Si-O as determined from FTIR spectra after forming gas plasma treatment

Figure 4-32 Peak area ratio of Si-H to Si-O as determined from FTIR spectra after forming gas plasma treatment

Figure 4-33 Peak area ratio of C-H to Si-O as determined from FTIR spectra after forming gas plasma treatment

Figure 4-34 K value of CORAL after forming gas plasma treatment

Figure 4-35 Leakage current of CORAL film after forming gas plasma treatment

Figure 4-36 Thickness of CORAL after Oxygen plasma treatment

Figure 4-37 FTIR spectra of CORAL after Oxygen plasma treatment

Figure 4-38 K value of CORAL after Oxygen plasma treatment

Figure 4-39 Leakage current of CORAL after Oxygen plasma treatment

List of Tables

Table 1-1 Spin-on dielectric material candidates

Table 1-2 PECVD dielectric material candidates

Table 1-3 Properties required for new inter metal dielectrics

Table 2-1 MPU Interconnect Technology Requirements for low-k material—Near-term

List of Pictures

Picture 1-1 6-level Metal Structure (Courtesy of IBM)

Picture 3-1 Multi-station of Concept two Sequel Express PECD system (courtesy of Novellus System Inc.)

Picture 4-1 SEM cross section thickness analysis of CORAL film

Picture 4-2 AFM images of CORAL film surface after annealing

Picture 4-3 AFM images of CORAL film grain after annealing

Acronyms

AFM	Atomic Force Microscopy
BD	Blackdiamond
BEOL	Back-End of the Line
CMP	Chemical Mechanical Polish
C-V	Capacitance-Voltage
DLC	Diamond-like Carbon
ECP	Electrochemical Plating
FSG	Fluorosilicate Glass
FTIR	Fourier Transform Infrared
HMDSO	Methyldisiloxane
HSQ	Hydrogen Silsesquioxane
IC	Integrate Circuit
ILD	Interlayer Dielectric
ITRS	International Technology Roadmap for Semiconductor
LFC	Liquid Flow Controller
Low-k	Low Dielectric Constant
LSI	Small Scale Integration
MFC	Mass Flow Controller
MIS	Metal Insulator Semiconductor
MOS	Metal Oxide Semiconductor

1MS	Methylsilane
2MS	Dimethylsilane
4MS	Tetramethylsilane
MSI	Medium Scale Integration
MSQ	Methyl Silsesquioxane
OSG	Organosilicate Glass
PECVD	Plasma Enhanced Chemical Vapor Deposition
PRS	Photo-resist Strip
PVD	Physical Vapor Deposition
RF	Radio Frequency
RI	Refractive Index
RIE	Reaction Ion Etch
SEM	Scan Electron Microscopy
SIMS	Secondary Ion Mass Spectrometry
SOD	Spin-on low-k Dielectric
TGA	Thermal Gravity Analysis
TMCTS	Tetramethylcyclotelrasiloxane
TPD	Temperature Programmed Desorption
ULSI	Ultra-large Scale Integration
VLSI	Very Large Scale Integration
XPS	X-Ray Photoemission Spectroscopy
Z3MS	Trimethylsilane

Chapter 1 Introduction

Very recently, a novel dielectric material, i.e. low dielectric constant (low-k) material, has been developed to replace the conventional SiO_2 as the interlayer dielectric (ILD) in Integrate Circuits (ICs). In this thesis, a typical low-k dielectric material, carbon-doped silicon oxide was synthesized by plasma-enhanced chemical vapor deposition. Its thermal stability and its structural properties as function of hydrofluoric acid (HF) treatment and plasma treatments are carefully studied in order to understand the correlations between the k value, structure and various fabrication processes.

1.1 Moore's Law

The invention of transistors in 1947 opened the field of electronic circuit designs. Since 1958, engineers began to develop Integrated Circuits (ICs). The IC complexity has advanced from small scale integration (SSI) to medium scale integration (MSI), to large scale integration (LSI), to very large scale integration (VLSI), which has 10^5 or more components per chip, and finally to present ultra-large scale integration (ULSI), which has 10^7 or more components per chip. In order to integrate so many components in one chip, the dimension of each device needs to be decreased.[1,2] Currently, deep sub-micron IC process and technology are popular in wafer fab and 90nm and 65/45nm technologies are under development.[3]

In 1965, Gordon Moore made his famous observation. He observed an exponential growth in the number of transistors per integrated circuit (the doubling of transistors every couple of years) and predicted that this trend would continue. This prediction was called as Moore's Law. Moore's Law still holds true today. Fig1-1 shows the development of Intel CPU that was constrained by Moore's Law.

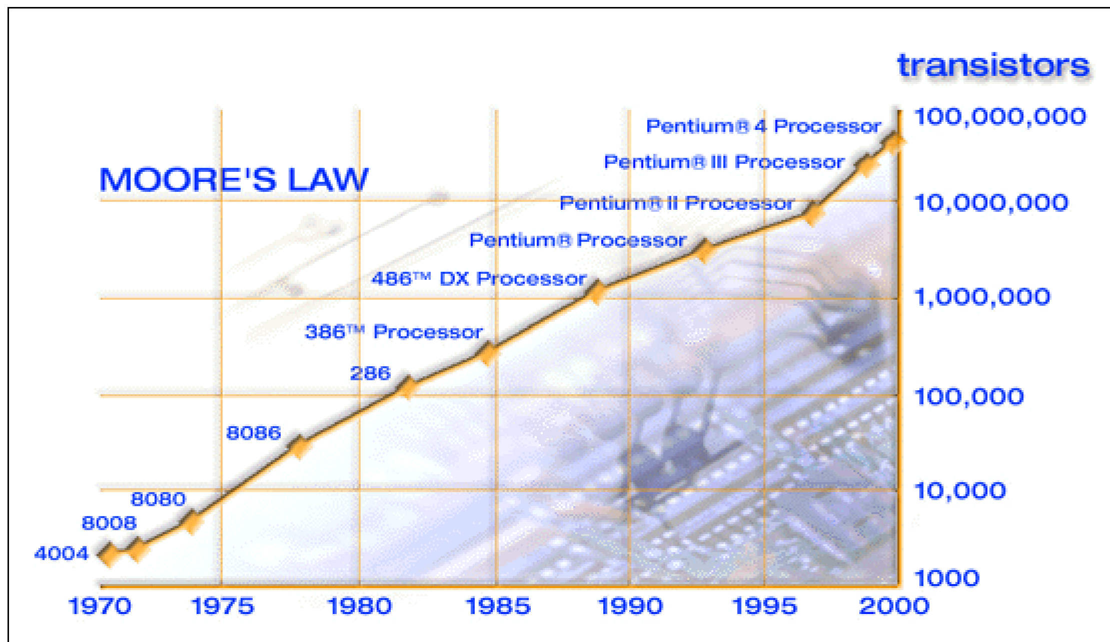

Figure 1-1 Moore's law (Courtesy of Intel Corporation)

To fulfill Moore's Law, many new technologies and new materials had been developed. Recent years, a novel dielectric—low dielectric constant (low-k) material is developed to replace the conventional silicon dioxide as the interlayer dielectric (ILD) due to the requirement of operating speed of IC.

1.2 Why low-k material

With the dimension of IC decreased, the wire density is increased. This will lead to an increase number of metal levels. Thus, the interconnect parasitics are increased, especially, the metal line cross-talk capacitance, line to line capacitance and metal resistance. Fig.1-2 shows the dependence of signal delay on device size. It was shown that below a certain distance of the interconnecting lines, the signal delay is no longer dominated by the intrinsic gate delay of the transistor, but by capacitive resistance of the interconnect array. Clearly, below certain device size, the delay caused by the total resistance of the interconnection becomes more important than the gate delay. In other words, RC (Resistance & parasitic Capacitance) delay becomes the limitation of the device operating speed. RC delay can be calculated using the following equation:

$$T=RC=2\rho\varepsilon\varepsilon_0[4L^2/P^2+L^2/T^2]$$

Where T—signal delay time

R—the resistance of metal

C—the parasitic capacitance

ρ—the specific resistance of the metal

ε—the dielectric constant of the dielectric

ε_0—the dielectric constant of vacuum

L—the length of the metal

P—the distance between two metal lines

T—the thickness of dielectric

According to this equation, there are three ways to decrease the RC delay: changing the layout (decreasing L/P or L/T), decreasing the specific resistance of the metal and decreasing the dielectric constant of the interlayer dielectric (ILD).[4]

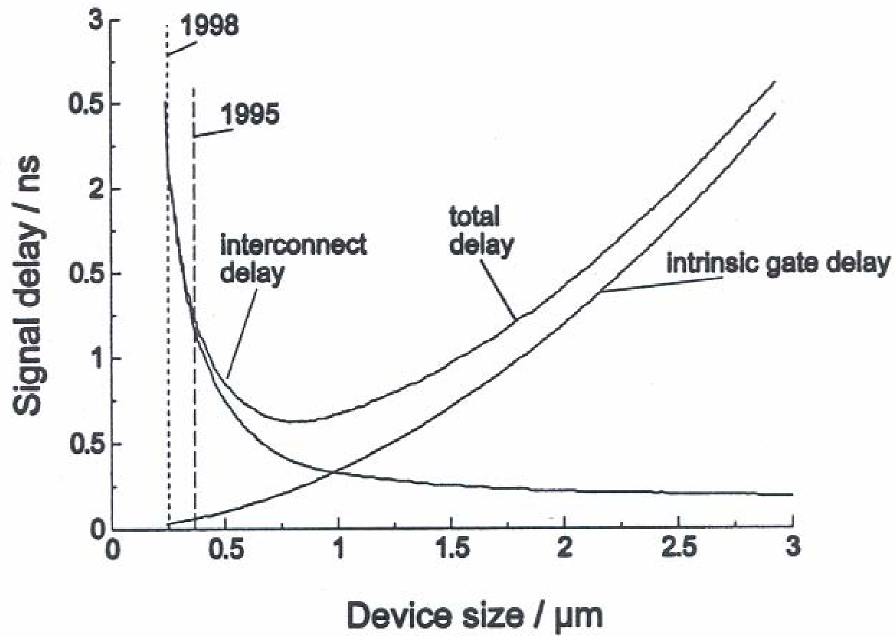

Figure 1-2 Dependence of signal delay on device size [4]

In advanced interconnect technology, Cu and low permittivity (low-k) dielectrics were introduced to the interconnect scheme. Copper was introduced to reduce resistance as it has lower specific resistance than aluminum alloys (1.65 μΩ.cm vs 2.66μΩ.cm) while dielectrics with low permittivity were used instead of conventional SiO_2 aiming at reducing capacitance. [5]

In summary, the purpose of using low-k materials as ILD is to decrease RC delay, improve operating speed of ICs. Fig. 1-3 indicates that at below 0.2μm technology node, using Cu and low-k (k~2.7) interconnect scheme can decrease total delay effectively.

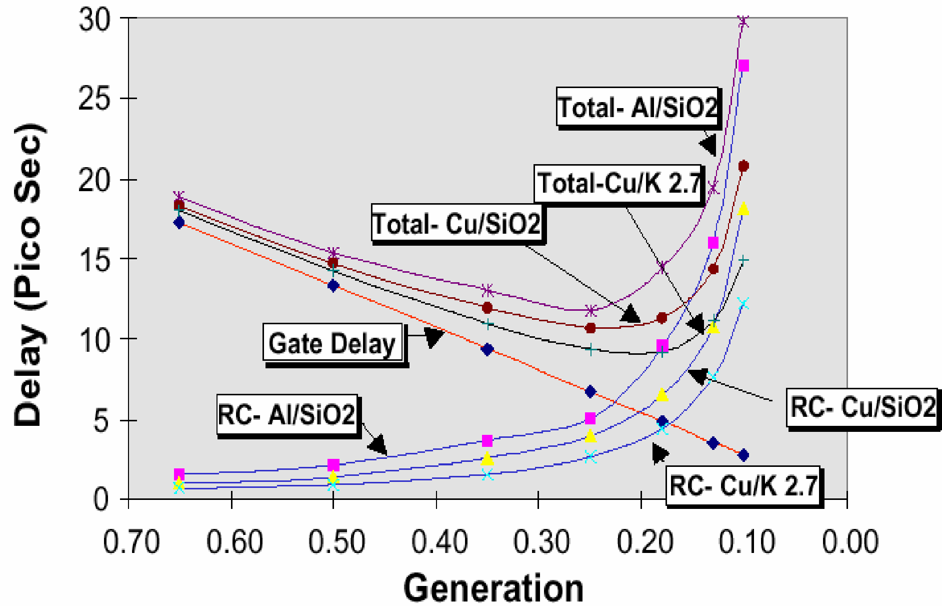

Figure 1-3 Generation vs. Delay (Courtesy of Intel)

1.3 What is low-k material

Low-k material is one kind of dielectric materials, such as diamond-like carbon (DLC) and hydrogen silsesquioxane (HSQ), which have lower dielectric constant than silicon dioxide (Thermal SiO_2 k=3.9, CVD SiO_2=4.1~4.2). This material is used to insulate adjacent metal lines on a chip, and it is vital in reducing "cross talk" between those lines, especially as line density increases. Low-k material can be grouped to two, based on the methods to obtain these materials. The two methods are Spin-on Deposition and Plasma Enhanced Chemical Vapor Deposition (PECVD) processes.

1.3.1 Spin-on low-k Dielectric (SOD)

Many organic or inorganic low-k films like Hydrogen silsesquioxane (HSQ), Methyl silsesquioxane (MSQ) and SiLK™ resin from Dow Chemical etc. are created by spin-on process. Table 1-1 provides a list of industry recognized spin-on dielectric material candidates for the 0.13µm and 0.1µm technology nodes.

Table 1-1 Spin-on dielectric material candidates

Material	**Process**	**K value**	**Remark**
Polyimides	Spin-on	3.1 – 3.4	Organic Polymers
Hydrogen silsesquioxane(HSQ)	Spin-on	2.9 – 3.2	Inorganic Polymers
B-staged Polymers (CYCLOTENE and SiLK)	Spin-on	2.6 – 2.7	
Fluorinated Polyimides	Spin-on	2.5 – 2.9	
Methyl silsesquioxane (MSQ)	Spin-on	2.6 – 2.8	Organic Polymers
Poly (arylene ether) (PAE)	Spin-on	2.6 – 2.8	Organic Polymers
PTFE	Spin-on	1.9	
Aerogels/Xerogels (porous silica)	Spin-on	1.1 – 2.2	
Porous HSQ	Spin-on	1.7 – 2.2	Porous Material
Porous SiLK	Spin-on	1.5 – 2.0	Porous Material
Porous MSQ	Spin-on	1.8 – 2.2	Porous Material
Porous PAE	Spin-on	1.8-2.2	Porous Material

Typical Spin-on dielectric SiLK™ from Dow Chemical is used by IBM for their 0.13 micron process. It was reported that IBM had attained a 3.0 effective k using SiLK ILD (k=2.65) with SiC based barriers and hard mask. Picture 1-1 shows 6-level metal structure from IBM. Spin-on method contends better extendibility to future generations.

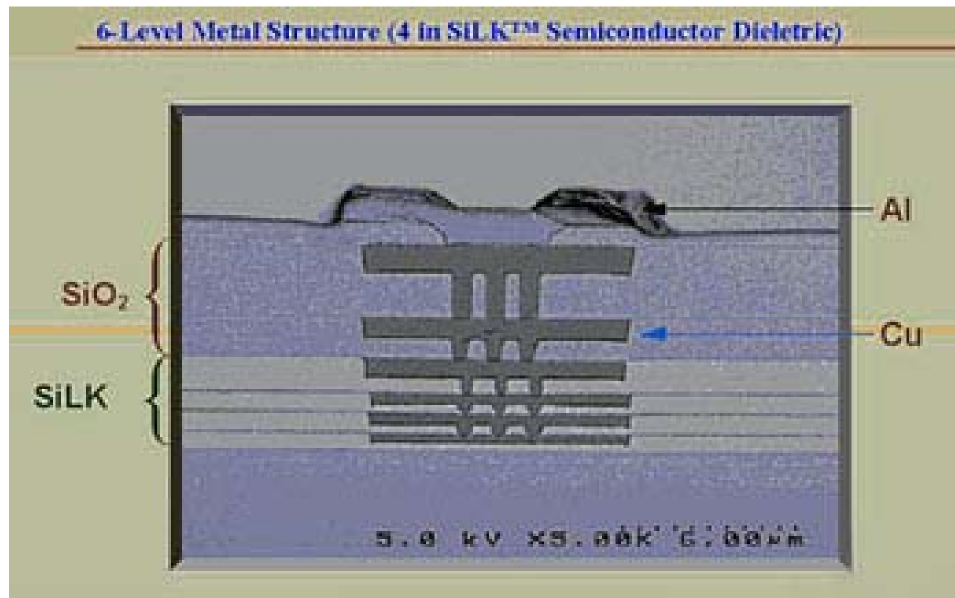

Picture 1-1 6-level Metal Structure (Courtesy of IBM)

One of the most important extensions is the increase of the material's porosity. Ideally, the best low-k dielectric material is no material at all. Air gaps have the lowest k value at 1, but they suffer from low breakdown voltage, low strength and low thermal conductivity. Therefore, the next generation best material is the one with a reduced density, i.e. increased porosity. Hence, there are many companies working on adding porosity to dielectric materials.

Original formulations of SiLK are limited to k = 2.65, but Dow Chemical and IBM are addressing the extendibility of SiLK through an $18 million Advanced Technology Program granted by the National Institute of Standards & Technology. The goal of the program was to develop a porous (closed cell, 10nm pore diameter) version of SiLK with a dielectric constant of 1.5 to 2.0 for 0.1µm semiconductors. Initial results have been promising.

Porous PAE materials have also been developed. Porous FLARE has delivered a k value of 1.9-2.2 with good adhesion. A single layer Cu damascene integration was completed, but Young's modulus was reduced by 50% and there has been some decrease in thermal stability and plasma resistance due to the higher exposed surface area.

Xerogels and aerogels are another classification of porous material. Aerogels are highly porous solids formed by replacement of a liquid in a gel with a gas. This process involves supercritical extraction of a solvent(s) so that there is little shrinkage. On the other hand, xerogels are formed from a gel by drying it with unhindered shrinkage. These nanoporous silica coatings typically have a dielectric constant value between 1.0 and 3.0, depending upon the cure process. NANOGLASS, from Honeywell, is based upon Tetraethoxy-orthosilicate (TEOS). Texas Instruments reported process feasibility using NANOGLASS in Al and single Cu damascene structures. Using 0.3 µm metal lines, the Cu/NANOGLASS devices provided a 36% reduction in capacitance for lines of equal resistance and a 46% decrease in resistance for interconnects of equal capacitance. High temperature testing of NANOGLASS films by Honeywell revealed a stable k of 2.0 in an uncapped film after repeated thermal cycling to 500°C.

Other nanoporous films can be formed via a two-phase controlled nanophase separation of a blend, hybrid or copolymer system. Porosity is controlled by selective removal of sacrificial components. IBM is characterizing porous organosilicates (nanofoams) with k values of < 1.7 at $<40\%$ porosity. These materials demonstrate high thermal stability and process simplicity. These nanoporous inorganic-organic hybrids are created through the

vitrification of low molecular weight silsesquioxane (MSQ) in the presence of highly branched thermally labile aliphatic polyesters of controlled molecular weight and architecture. The thermally labile pore generator decomposes by heating to 350-400°C to leave behind pores in the inorganic oxide. The combined structure contains closed-cell pores in a hydrophobic matrix, minimizing moisture absorption. XLK™ is from Dow Corning and is based upon HSQ. These pores, made by boilingout a solvent during a cure step, lower the dielectric constant of HSQ significantly-to between 2.0 and 2.5, depending on pore size. Also, ammonia treatment has been found to have a crucial influence on film characteristics (hydrophobicity and mechanical properties). In addition to this material, other materials under development are JSR's LKD™ and Catalyst and Chemicals' IPS™.

MesoELK™ from Schumacher involves spin-on deposition of a TEOS-based mesoporous material. The resulting film has a highly organized pore structure with good thermal stability. The mesoporous films potentially offer simplified processing and improved mechanical strength relative to conventional xerogel approaches. [6]

Although there are many porous of spin-on low-k materials available for testing, porous CVD low-k materials have yet to be demonstrated. The requirements of new equipment, film shrinkage, cracking after curing, gap-filling and multilevel structure are big issues of this approach. [7]

1.3.2 PECVD low-k material

One approach of producing low-k materials is doping the insulating SiO_2 films with C or F etc. Table 1-2 gives a list of PECVD low-k dielectric material candidates.

Table 1-2 PECVD dielectric material candidates

Material	Process	K value
Fluorosilicate glass (FSG)	PECVD	3.2-4.0
Diamond-like Carbon (DLC)	PECVD	2.7-3.4
Black Diamond (SiCOH)	PECVD	2.7-3.3
CORAL(SiCOH)	PECVD	2.7-2.8
Parylene-N	PECVD	2.7
Fluorinated DLC	PECVD	2.4-2.8
Parylene-F	PECVD	2.4-2.5

For this group of low-k materials the k value of SiO_2 is reduced either by incorporation into the SiO_2 matrix of atoms and bonds that have a lower polarizability, or by lowing the density of atoms and bonds of the SiO_2-related material, or both. Unlike the Spin-on, PECVD method can reuse existing toolsets and simple integration due to the silicon dioxide-like structure of the deposition film.

With regard to the first effect, there are several polarization components that must be minimized in reducing the dielectric constant. These usually include the electronic, atomic, and orientational responses of the material. The latter two components constitute the nuclear response and are important at lower frequencies ($<10^{13}$ S^{-1}), while the electronic response dominates at higher frequencies. For typical device operating frequency, currently $< 10^9$ S^{-1}, all three components contribute to the dielectric constant and should be minimized for optimum performance.[8]

Fluorosilicate glass (FSG) is the first generation low-k material which is used as the interlayer dielectric (ILD) for 180 and 130nm technology nodes. In this material, k is reduced by substituting some of the oxygen for F, which connects to the rest of the structure through a single chemical bond. Fluorine in FSG lowers the electrical polarizability per volume of silica. It is the major factor lowering k in FSG.[9] The dielectric constant of FSG decreases by increasing the F content until it reaches the minimum and then increases by increasing the F content. The stable FSG film can be deposited at 3–5% of F percentage with SiF as the gas source. At F percentage larger than approximately 4.5%, the dielectric constant of FSG film increases due to the presence of highly polar Si-O–H bonds formed when the films pickup moisture. However, the F percentage to achieve minimum dielectric constant depends on the reagents and the process conditions.[10] As a result, FSG's k value is typically limited to ~3.6 due to chemical instability when fluorine loadings exceed a certain percentage. Solutions capable of delivering k=2.7 for 100nm technology node are largely focused on organosilicate glass.

Carbon-doped low-k oxide materials (SiOCH), also termed organosilicate glass (OSG), can be deposited by PECVD process using a variety of precursors including methylsilane (1MS), dimethylsilane (2MS), trimethylsilane (Z3MS), tetramethylsilane (4MS) or tetramethylcyclotelrasiloxane (TMCTS). In this material, part of the oxygen atoms in the SiO_2 structure is replaced by -CH_x- groups. Because the Si-C bond has less polarizability than the Si-O bond and the reduced density of SiOCH relative to SiO_2, this material has a

lower dielectric constant than SiO_2.[11] Incorporation of $–CH_x$- group has a significant effect on the key physical, thermal and chemical properties of the resulting film.

Black Diamond^{TM} from Applied Materials is a trimethylsilane (Z3MS) based carbon doped oxide low-k material. Report said that Texas Instruments (TI) was combining Black Diamond^{TM} and BLOK^{TM} SiC film for k around 3.0.[4] Recently, Applied Materials Inc. also announced that its Black Diamond^{TM} and BLOK^{TM} low-k dielectric films were used by Toshiba Corp. for volume production of its 90nm CMOS4 process in the Oita, Jap.[12]

CORAL^{TM} is also one kind of carbon doped oxide low-k materials from Novellus. This film was deposited by Novellus-Sequel Concept two system use TMCTS as precursor. It was reported that the k value of this kind of film at 2.7-2.8 levels.[6] This film was evaluated as a good low-k dielectric candidate to replace the conventional SiO_2 as the next generation ILD.

1.4 The requirements for the dielectric in Microelectronics and the research topic of the thesis

Although, many low-k materials were developed recent years, there are few material can be used in microelectronics as ILD. To replace the conventional dielectric silicon dioxide, the new dielectric material should have the similar properties as SiO_2 except the dielectric constant. A dielectric material must meet at least the following criteria: (1) low

permittivity, (2) high breakdown field, (3) low leakage current, (4) no moisture absorption or excessive permeability to moisture, (5) thermal stability to >400°C (6) good adhesion to metal and to dielectric, (7) no metallic contaminants, (8) low defect density, (9) no significant outgassing, and (10) resistance to plasma, no significant change of k value after plasma treatment.[13] Table 1-3, shows qualified requirements of some properties to new dielectric material.

Using low permittivity i.e. low dielectric constant (low-k) material can decrease parasitic capacitance, for example, line to line capacitance and cross talk capacitance etc. So that the operating speed of device will increase. In this project, diluted HF was used to etch the resulting carbon doped low-k film in order to introduce pores into it. The purpose of this research work is to reduce dielectric constant of this film.

As an insulator layer in electronic devices, the dielectric should withstand high breakdown field, and have low leakage current under certain operating voltage. Otherwise the dielectric will be breakdown, resulting in device failure. High leakage current of dielectric will affect the stability of the device.

Moisture uptake, defect density and outgassing of dielectric will degrade its properties like breakdown voltage, leakage current, k value, film thickness etc. result in the function of device failure or unstable.

Thermal reliability of dielectric is always a vital factor since repetitive thermal treatments

Table 1-3 Properties required for new inter metal dielectrics [4]

Property	Value
Dielectric constant	3 (preferably ,2.5)
Dissipation factor at 1 MHz	<0.005
Thermal stability :1% weight loss in N2	>425ºC
Moisture absorption	<1%
Adhesion (to metal, self-adhesion)	Pass tape test after thermal cycles to 450ºC
Coefficient of thermal expansion	<50 ppm
Etch rate	>3 nm/s
Etch selectivity	Oxygen plasma resistance
Stress	<±100 MPa
Gap-fill	No voids at 0.35 µm, aspect ratio = 2
Planarization	80% (regional)
Tensile modulus	>1 GPa
Tensile strength	>200 MPa
Tg	>400ºC
Thickness uniformity within wafer (3σ)	<10%
Thickness uniformity wafer to wafer (3σ)	<5%
Metal content	ppb level
Dielectric breakdown	1 MV/cm
Step coverage	80%
Number of particles>0.3 µm	0.08/cm^2

are involved in IC device processing. In order to withstand metallization, anneal, cure and chip-attach temperatures good thermal stability of the materials is required.[11] This project is also focused on thermal stability of carbon doped PECVD low-k material. Not only the thermal stability of this material under common microelectronic process temperature was considered, but also high temperature annealing (e.g. 700°C and 800°C) was done on this material to understand its thermal properties in depth.

On the other hand, plasma process like dry etch, photo-resist strip (PRS) and sputtering etc. are very common processes in IC fabrication. So the resistance to plasma treatment is also important to dielectric material. Different kinds of plasma treatment (O2, H2/N2, He, NH3 etc.) on TMCTS based PECVD carbon doped low-k material was studied in this project.

The requirement of good adhesion to metal and to dielectric is intent to prevent peeling issue after thermal process (anneal, alloy), plasma process (RIE, PRS, PVD, PECVD), chemical process (cleaning) or mechanical process (CMP).

Contamination especially metal contamination of dielectric is a critical issue. Some metal atoms such as Cu can diffuse easily into Si and dielectric (SiO_2) even at modest temperatures, which leads to degradation of device reliability. Other metal atoms such as Au can diffuse into Si to form deep energy level and decrease the lifetime of carriers, affecting the function of device. Hence it is important to eliminate metal contamination in wafer fab.

1.5 Outline of Thesis

In this thesis, a carbon-doped low-k SiO_2 CORAL^{TM} from Novellus is synthesized and studied in detail. Chapter 2 briefly introduces the basic structure and properties of carbon doped SiO_2 which were previously reported in literature. Experiment details, including the synthesis, characterization and various treatments are described in Chapter 3. Chapter 4 presents the results of the treatments.

A comprehensive study was completed, using SEM to determine the thickness of the CORAL film, Therma-Wave opti-probe to measure the refractive index, FTIR to study chemical bonding, AFM to scale the surface roughness, SSM 495 CV system to find dielectric constant and field breakdown voltage, TGA and TPD to detect the outgassing, XPS and SIMS to investigate surface chemical composition, FSM stress measurement system to know the stress and so on. Based on these data, Chapter 4 discusses the correlations between theses treatments, the material structural properties and its effects on the k value. The conclusion is summarized in Chapter 5.

Chapter 2 Literature Review

2.1 Structure of carbon doped oxide (SiOCH) low-k film

Since carbon doped oxide was developed, many research works have been done on this material. Excellent reviews could be found in literature [18]. This kind of materials was prepared using PECVD process. Conventional precursor including methylsilane (1MS), trimethylsilane (Z3MS) from Dow Corning, tetramethylsilane (4MS) and tetramethylcyclotelrasiloxane (TMCTS) from Schumacher.

M.J. Loboda, PECVD precursor pioneer from Dow Corning, reported a Z3MS based carbon doped low-k material. This low-k oxide is an amorphous film of C–Si–O with hydrogen. The material can be deposited having $k<3$ with key electrical properties and integration characteristics that are similar to SiO_2. It was reported that this material primarily consists of carbon, silicon, oxygen and hydrogen. The content of carbon is 33-40 atom%, silicon content is 18-25 atom%, oxygen content is 17-30 atom% and hydrogen content is 17-30 atom%.[14]

The Z3MS low-k oxide process is a simple modification of the traditional PECVD process to grow SiO_2 using SiH_4 and N_2O as the process gases. Gas flow, power and pressure are consistent with the SiH_4 oxide processes. At high N_2O flow levels, SiO_2 is formed. By reducing the nitrous oxide flow, both Si–CH–Si and Si–O–Si bonding is

retained in the film. The resulting material is a low density oxide of amorphous silicon carbide.[4]

Licheng M. Han et al. characterized carbon doped oxide low-k material prepared by PECVD from Tetramethylsiane (4MS). Fourier transform infrared (FTIR) and X-ray photoemission spectroscopy (XPS) were used to characterize the chemical structure of this thin film. Copolymer thin film from 4MS and SiH_4 precursor and polymer thin film from 4MS were investigated.

Both films prepared from 4MS and 4MS/SiH4 mixed precursor show similar absorption bands, but with different relative intensity. The characteristic peak of these carbon doped film is the symmetric deformation vibration of the CH_3 from Si-CH_3 group at about 1270 cm^{-1}, a broader Si-O-Si peak at about 1040cm^{-1} with a strong shoulder at higher wavenumber of about 1130cm^{-1} and the Si-C, Si-CH_3 wagging stretching vibration at 800cm^{-1}. The different intensity of these peaks is dependent on the deposition conditions.[15]

XPS analysis showed that films from both 4MS and 4MS/SiH4 polymerizations were determined to have a similar atomic ratio of about $Si_{0.25}O_{0.35}C_{0.40}$. The Si 2p spectra were deconvoluted into five different moieties. These five chemically distinct Si atoms are assigned as follows: SiO_4 ~103.4 eV, SiO_3 ~102.2 eV, SiO_2~101.1 eV, SiO_1 ~100.2 eV, and SiO_0 ~99.1 eV, respectively. The major backbone of the network of these films is -O-Si-O-Si-, which is more like a linear polymer and has a lower degree of cross-linking. It

is anticipated that these films show lower mechanical strength such as lower hardness compared with SiO_2. The resolved high resolution C ~1s XPS peaks were assigned into individual contributions of different carbon atoms based on recommended values from Si-, C-, O-, and H-containing polymers. The peak at 282.4 eV is assigned to C~Si_n , n= 2-4, which is in good agreement with SiC. The majority of C moiety is Si-CH_3 at 283.4 eV, which is in good agreement with FTIR spectra. Additionally, there is a high concentration of C-O bonds, which cannot be distinguished from FTIR spectra.[15]

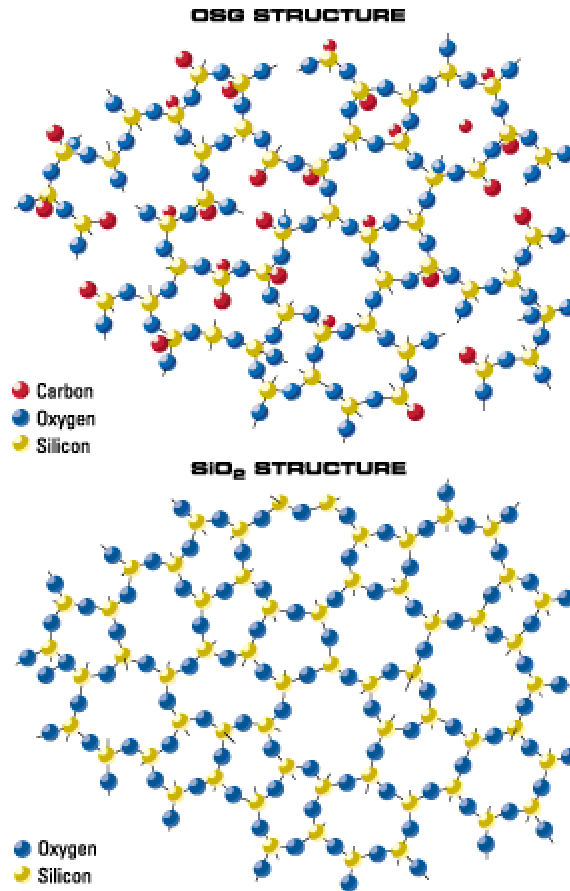

Figure 2-1 OSG structure and SiO_2 structure

Ravi K. Laxman et al. also addressed that the resulting organosilicate glass (OSG) films, also called carbon-doped oxides, have a composition of $Si_wC_xO_yH_z$. The organic groups in OSGs invariably take the form of tetravalent silicon with a wide range of alkyl and alkoxy substitutions. In these films, the silicon-oxygen network seen in glass is occasionally interrupted, in a more or less homogeneous fashion, by the presence of organic, typically methyl (CH_3) groups. Hydrido (H) substitution at silicon can also be present. The film's lower dielectric constant, k, is due to these changes to the SiO_2 network and the reduced density of the OSG film relative to SiO_2. In typical CVD low-k films, 10% to 25% of the oxygen atoms are substituted with organic groups. Fig. 2-1 shows the differences in chemical bonding between amorphous SiO_2 and amorphous OSG (Si:C = 4:1).[16]

2.2 Basic properties of SiOCH low-k film

Basic properties of carbon doped oxide film including dielectric constant, thermal stability, stress, adhesion, break down voltage, leakage current and hardness etc. These properties of SiOCH film which was prepared by PECVD process use different precursor have been presented in many papers.

2.2.1 Dielectric constant and Pore-Related properties

Reducing dielectric constant of carbon doped oxide film was undoubtedly the focus of many researchers. According to the International Technology Roadmap for Semiconductor (ITRS) 2002, the effective k value of low-k material will decrease from

3.0-3.6 currently to 2.3-2.7 in 2007 and the k value of bulk low-k material will decrease from < 2.7 in 2003 to <2.1 in 2007. Table 2-1 provides the prediction of MPU Interconnect Technology Requirements for low-k material—Near-term from ITRS in 2002. [17]

Table 2-1 MPU Interconnect Technology Requirements for low-k material—Near-term

Year of Production	2001	2002	2003	2004	2005	2006	2007
Interlevel metal insulator (minimum expected) —effective dielectric constant (k)	3.0-3.6	3.0-3.6	3.0-3.6	2.6-3.1	2.6-3.1	2.6-3.1	2.3-2.7
Interlevel metal insulator (minimum expected) —bulk dielectric constant (k)	<2.7	<2.7	<2.7	<2.4	<2.4	<2.4	<2.1

As we known, the quantitative relation between the dielectric constant (k) and properties of the molecules is described by the Debye equation:

$$\frac{k-1}{k+2} = \frac{N}{3\varepsilon_0}(\alpha_e + \alpha_d + \frac{\mu^2}{3KT})$$

Where:

k —dielectric constant

N —density of the dielectric

ε_0 —the permittivity of vacuum

α_e —electronic polarization in the molecule

α_d — distortion polarization in the molecule

μ —the orientation polarizability

K —Boltzmann constant

T — the temperature in K

$\frac{\mu^2}{3KT}$ —thermal averaging of permanent electric dipole moments

The dielectric constant of materials is high if its molecules are polar and highly polarizable. This equation shows that k value is smaller if materials do not contain polar molecules. Reduction of density N, polarizabilities α_e and α_d are possible ways to decrease the dielectric constant. Reducing the number of ionic bonds in the material minimizes distortion polarization. The electronic polarization is minimized by lowering the electron density in the material, i.e., introducing smaller elements. As α_e and α_d are almost fixed in carbon doped low-k materials and the possibility to lower the molecular polarizability is limited, reduce density becomes the only way to reduce k value of this kind of material. An important way to reduce the film density is introduction of pores. The dielectric constant k of porous film depends on porosity P (the ratio of pore volume to film volume) as follows:

$$\frac{k-1}{k+2} = (1-P)(\frac{k_1-1}{k_1+2})$$

in which k_1 is the dielectric constant of the film skeleton. [18]

It was reported that for k values in the 2.8-3.2 regime, the pore volumes are typically<10%, effectively producing a dense film. From k=2.5-2.8, the pore volumes

increase to 20-30%, reaching into the percolation threshold where films start to become mesoporous and some of the pores are interconnected. Below k=2.5, the films are mesoporous with 30-50% pore volume and total pore interconnectivity. [19]

D.G. Shamiryan et al. in their paper provided a method for controllable increase of porosity (reduce density in order to decrease the k value) of trimethylsilane based carbon doped oxide (SiOCH) low-k material. Diluted HF was used to etch the SiOCH film. The modified SiOCH film is characterized by FTIR, XPS, and ellipsometric porosimetry. The chemical composition of the modified SiOCH film remains almost the same during etching. No significant thickness loss is observed, while the pore radius and film porosity increase with HF dip time. It was concluded that the increase of the pore radius is caused by isotropic etching inside the pore as well as at the film surface. The very low etch rate of SiOCH film by dilute HF and the large difference between the pore radius and the film thickness allows an increase in the porosity without significant thickness loss. This method is a way to prepare ultralow-k dielectric film with higher chemical stability as compared to oxide and silsesquioxane-based porous materials. [11]

Pore-Related properties of carbon doped oxide low-k material were studied by Yoshimi Shioya et al. In their research work, the effects of bias power on the pore size, pore distribution, relative dielectric constant (k), density, composition and leakage current of PECVD methyldisiloxane (HMDSO) based low-k material were studied. The pore diameter of this film changes from 1.23 to 0.73nm with the application of bias power from 0 to 100W. Pores with an average diameter larger than 0.63 nm were found to

decrease the k value of this PECVD film. The pore volume ratio of this film with different composition was calculated from the measured pore size, k value and density. The k value and the density were found to increase with increasing silicon and oxygen contents and decreasing hydrogen contents in the film at same pore volume ratio. The pore volume ratio of this film with the lowest k value, 2.66, was estimated as 31%. [20]

Another method for reducing k value is named as multiphase deposition. The SiOCH precursor tetramethylcyclotetrasiloxane (TMCTS) is mixed with a thermally unstable CHx phase during deposition. This unstable phase is thermally decomposed and removed from the film during subsequent anneal ~4 h at 400°C, leaving behind pores. The resulting porosity depends on the CHx /TMCTS ratio and can be as high as 30%–40% for a 1/2 ratio. The mean pore size is about 2 nm. Fig.2-2 plots the obtained dielectric constant as a function of CHx /TMCTS ratio.[18]

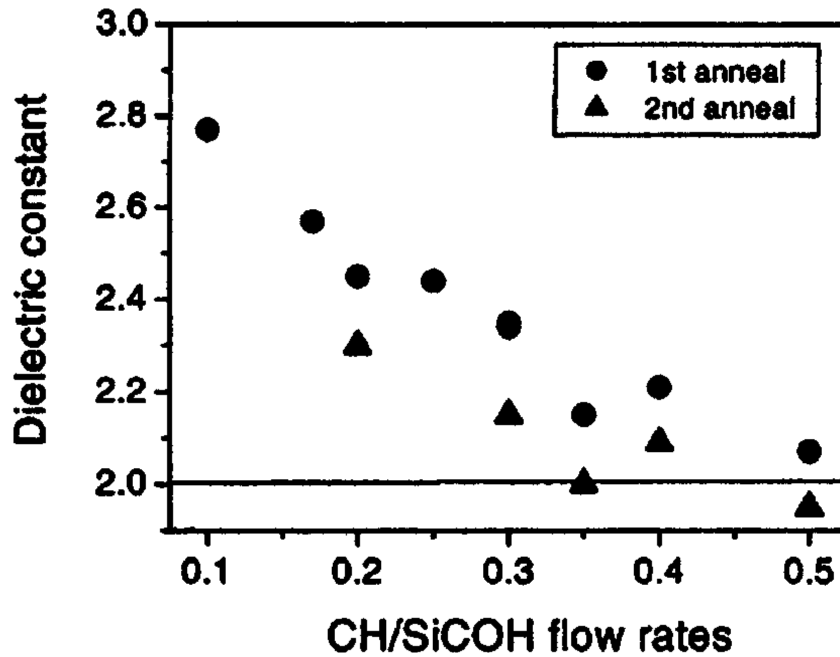

Figure 2-2 The dielectric constant as a function of the ratio of the precursor flow rates

2.2.2 Optical properties

H. Zhou et al. investigated thickness and deposition method dependence of optical properties and glass transition temperature (Tg) of PECVD carbon doped low-k dielectric. The carbon doped silicon dioxide low-k films, 105–1255 nm in thickness, were prepared by plasma-enhanced chemical vapor deposition (PECVD) in a six-station sequential deposition system use multi-station deposition and single station deposition methods respectively. Their optical properties were measured using an optical spectrometer coupled with a hot stage. A decrease in refractive index, n, for films with six sub-layers compared with film with a single layer of similar thickness has been observed. This decreased refractive index is thought to be caused by the different effect of crystallinity of the substrate, as a film interface effect is introduced due to the different deposition methods. Both types of PECVD thin films show an increasing refractive index with increasing thickness, which could be attributed to the increased effective density with the increased thickness indicated from Fourier transform infrared (FTIR) spectroscopy microstructure analysis. Cauchy dispersion function was found to be valid for films within all the thickness range and with different deposition methods from visible spectrum to IR spectrum. The refractive index is found to decrease as the temperature increases from 25 to 450°C at a fixed wavelength for all the films.[21]

2.2.3 Other physical and electrical properties

Ben Pang et al. from Applied Materials Inc. introduced carbon doped oxide Black Diamond (BD)^{TM} in their paper. As they addressed because BD film contains primarily

Table 2-2 Summary of Black Diamond Film Properties

DESCRIPTION	BLANKET FILM
Dielectric Constant – Bulk film (Hg Probe)	<=2.5 @ 1MHz
Uniformity (%, 1σ)	<1.5
Stress (dyne/cm^2) (5k≈film after cure)	4E8 – 8E8 Tensile
Stress Hysteresis (dyne/cm^2)	<2.0E8 RT – 450ºC
Cracking Threshold (µm; blanket film on silicon)	>1.5
ASTM Scratch Tape Test on SiN, SiON, Ta, TaN	Passed
Stud Pull Adhesion Test(Black Diamond on Silicon)	>12kpsi
Thermal Shrinkage (%), post cure film	<2.0 @ 450ºC
2hrs Isothermal TGA	<1% @ 450ºC
n & k @ 633nm @ 248nm @ 193nm	n = 1.46 k = 0 n = 1.50 k = 0 n = 1.59 k = 0
Particles @ >0.2µm size	<0.1/cm^2
Leakage Current (Amps/cm^2)	10^{-9} @ 1MV/cm

silicon and oxygen, it retains many of the beneficial thermal and mechanical properties of silicon oxide. Table 2-2 shows a summary of film properties. The glass transition

temperature of this film is well above 450^oC and isothermal weight loss<1%wt per hour at 450^oC. Reduction of the dielectric constant is achieved primarily through maximizing the free volume in the microstructure. As deposited, the films are stable, but a furnace anneal is required to achieve the lowest dielectric constant value. Annealing can be performed in a vacuum furnace under nitrogen (or forming gas) atmosphere. The purpose of annealing is to out-gas the un-reacted low molecular weight species.[22]

Zhen-Cheng Wu et al. investigated the physical and electrical properties of two species of inorganic C-doped low dielectric constant (low-k) chemical vapor deposited (CVD) organosilicate glasses (OSGs, α-SiCO:H). They are both deposited by plasma-enhanced CVD (PECVD) processes using methylsilane (CH_3SiH_3, 1MS) and trimethylsilane [$(CH3)_3SiH$, Z3MS] based gases as the reagents, and are designated as OSG1 and OSG2, respectively. Experimental results indicate that the thermal stability temperature of OSG1 is 500°C, while that of OSG2 is 600°C, based on the results of thermal annealing for 30 min in an N_2 ambient. The deterioration of the low-k property in OSG1 is predominately due to the thermal decomposition at temperatures above 500°C of methyl (-CH3) groups, which are introduced to lower the density and polarizability of OSGs.[23]

D.Shamiryan et al. studied the properties of PECVD SiOCH low-k films obtained at different deposition conditions. In their work, four CVD SiOCH films deposited at various conditions were used for comparative evaluation. The films were evaluated by RBS, spectroscopic ellipsometry, and ellipsometric porosimetry. Oxygen plasma resistance was studied by spectroscopic ellipsometry and TOF-SIMS analysis after exposure of the films to downstream oxygen plasma. The different deposition conditions

result in different carbon content and different porosity. The film with the highest carbon content has the lowest porosity and vice versa. As carbon content of films increases and their porosity decreases, the SiOCH films become more resistant to oxygen plasma.[24]

Satoshi Sugahara et al. successfully demonstrated chemical vapor deposition of silica film in which some oxygen atoms of the pure silica network are replaced by methylene (-CH_2-) groups. Since this group does not break the original silica network, sufficient mechanical strength of this film is expected. Due to the decomposition reaction of the methylene group with the dense H_2O in the film, the as-deposit film was thermally unstable. However, the resulting film could be dehydrated without decomposition of the methylene group by low temperature annealing in a XeF_2 ambient. The dehydrated film showed not only good insulating and low-k characteristics (resistivity of 10^{15} Ω.cm, break down field of 3.3 MV/cm, and k of 2.8), but also good thermal properties, such as good thermal stability and high thermal conductivity. [25]

Low-k dielectric carbon doped silicon dioxide films created by PECVD using a six-station sequential deposition system exhibit different glass transition behavior from film created by PECVD in a single deposition station. The enhanced glass transition temperature (T_g) for the PECVD thin film of a layer consisting of six sub-layer deposited in a six station sequential deposition system to the T_g for film of a single layer deposited in a single deposition system is traced back to the introduced film interface effect inherent to the different deposition methods. Both types of PECVD thin films rang in thickness from 50 to 1255nm show an increasing T_g with increasing film thickness. The

observed glass transition behavior for film with six sub-layers can be will explained by a theoretical model of thickness dependent T_g for multiple sub-layers obtained by modifying the currently existing theoretical model for the single layer thickness dependent T_g behavior, which explains the observed thickness dependent T_g for single layer PECVD thin film. [26]

2.2.4 Resistance to plasma treatment

Oxygen plasma resistance is a major concern of carbon doped low-k materials as weak oxygen plasma resistance of this film can cause via poisoning (via connection failure). The failure occurs when the SiOCH film is exposed on sidewalls and is directly subjected to oxygen plasma for ashing. The oxygen plasma converts the SiOCH into porous oxides absorbing much moisture. This moisture is released during subsequent metal deposition and prevents via connections. Oxygen plasma resistance of SiOCH film is shown to be strongly dependent on the material structure. [27] Post helium plasma treatment on SiOCH film was found can reduce oxygen plasma damage without film properties change. [28]

2.3 Integration issues of SiOCH low-k film

In advanced interconnects scheme, copper and low-k materials are selected as the next generation metal and interlayer dielectric (ILD) respectively. Dual damascene via first or trench first process is used for backend Cu/low-k integration. Fig. 2-3 shows the dual

damascene via first process used in ULSI. In this process, the wafers are first deposited with multiple dielectric layers (low-k, etch stop and barrier layers), then coated with photoresist and patterned use lithograph process. Next, an anisotropic etch cuts through

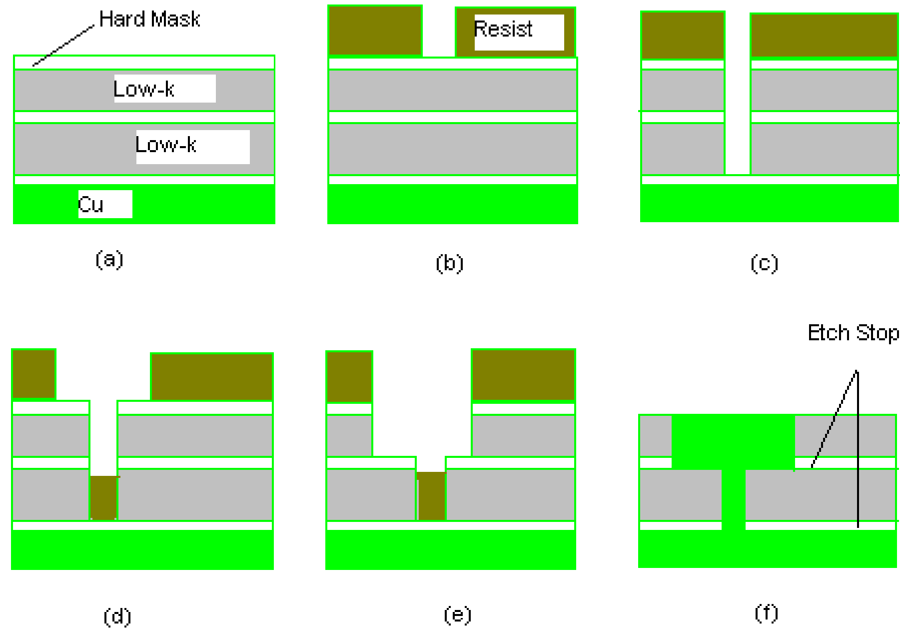

Figure 2-3 Dual damascene Cu/low-k via first process in ULSI
(a) stack layers (low-k material, hard mask, etch layer etc.) deposition (b) and (c) via formation (d) and (e) trench formation (f) Cu/low-k interconnect final structure

the surface hard mask and etches down through the ILD (low-k material) and the embedded etch stop, and stops on the bottom barrier layers. After that, the via photoresist is stripped use oxygen plasma. Again, after new photoresist is coated and patterned, an anisotropic etch cuts through the surface hard mask and down through the ILD, stopping at the embedded hard mask. This etch forms the trench. The photoresist is then stripped

and the barrier at the bottom of the via is opened with a very soft, low-energy etch that will not cause the underlying Copper to sputter into the via. Finally, the Tantalum, Copper seed layer and bulk Copper are deposited using PVD (Physical Vapor Deposition), ECP (Electrochemical Plating) process and planarized using CMP (Chemical/Mechanical Polishing). [29]

During integrated low-k materials into ICs, researchers and engineers are facing many challenges and process issues. These challenges can be roughly divided into the mechanical part—like material strength, adhesion of the low-k material to different other layers and Chemical Mechanical Polish (CMP) compatibility—and chemical issues like compatibilities with etches, dry and wet cleans. In addition, there are further challenges waiting in reliability testing and packaging even if the copper/low-k dual damascene shows good electrical parameters in electrical tests at the end of the wafer fabrication process.[30]

O.Louvean et al. investigated issues arising from ashing and cleaning on SiOCH low-k film. The porosity of these materials makes them prone to absorb nitrogen or amine containing by-products from the asing (photoresist strip) and cleaning operations. These amines tend to be released in the next photolithograph step, creating a poisoning of the chemically amplified photoresist, which will block its development. A combination of dry and wet treatments can be a solution to limit these problems, enabling to shorten the plasma exposure time to limit material modification. The subsequent wet cleaning can then be lighter, giving the possibility of using ‘amine-free’ products. Apart from the ash

process, improvements can come from development of the photoresists, using additional barrier layer and the double hard-mask integration scheme.[31]

D. Louis et al. also discussed ashing issues and the influence of carbon concentration in SiOCH film to clean process in their paper. Conventional BEOL (Back-End of the Line) stripping processes use an ion depleted dry plasma strip. Oxygen has been used as the principle gas in traditionally plasma downstream strip processes. With SiOCH dielectrics, oxygen could "strip out" the carbon from the low-k film itself. It is essential that the low-k film maintains its physical and chemical properties during the resist and polymer removal steps. Several approaches have been tested to preserve the dielectric characteristics. The use of pure H_2 reductive plasma has been tested and also different treatments to cap the sidewall and protect are reported. On the other hand, increasing the carbon content of SiOCH film influences the cleaning requirement. This study offers a solution combining plasma and wet cleaning steps which is compatible not only with copper but also the carbon doped low-k materials.[32]

Takeshi Furusawa, in his paper, proposed a new carbon doped low-k material to improve the mechanical strength of low-k ILDs.[33] Unlike conventional OSG film which was fragile due to the methyl-groups ($-CH_3$) terminate the Si-O-Si networks, this new film was strong because they do not terminate the networks as the methyl-bonds do. It was shown to be over three-times stronger than conventional ones. The electrical and mechanical properties of the new film are compared with those of the conventional OSG films.

Chapter 3 Experimental

3.1 Principle of Plasma Enhanced Chemical Vapor Deposition (PECVD)

PECVD is a universal process which is used for thin film deposition in microelectronics area. The major advantage of PECVD is its lower temperature capability compared to that of thermal driven CVD. For example, deposition temperature of 700^oC to 900^oC are required to deposit silicon nitride film by thermal CVD, while only 250^oC to 350^oC are sufficient to deposit similar films by PECVD. This lower temperature capability is made possible by the addition of electric energy to the CVD environment, and the effective substitution of this electrical energy for thermal energy. [34]

The first commercially important PECVD reactor was introduced by Reinberg in 1974. The plasma is generated between the two parallel, circular electrodes. The wafers are loaded onto the lower, electrically grounded, electrode. The upper electrode is connected to the rf generator through an impedance matching network. The reactants are fed in from the gas ring, enter the plasma region at its outer edge, and flow radially in toward a pumping port at the center of the lower electrode. Fig. 3-1 Shows the schematic of this reactor.[34]

Although there are many different types of PECVD reactors are available, the basic principle of this process is same. In this process, the ground state reactant gases containing the elements to be deposited are transported to the vicinity of the wafer

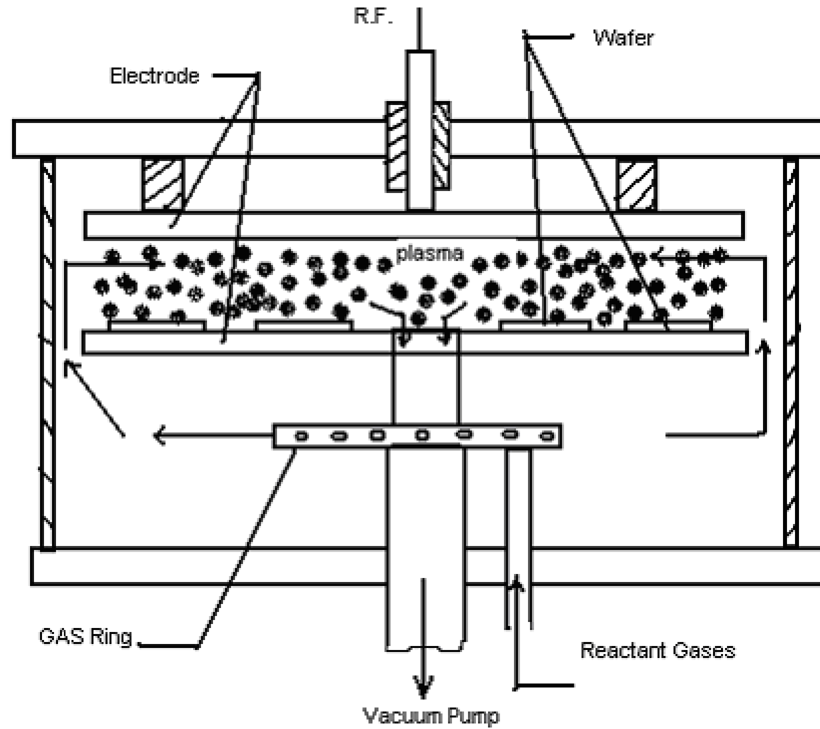

Figure 3-1 Schematic of PECVD reactor designed by Reinberg (Coutesy of the Electrochemical Society, Inc.)

surface where they diffuse to the surface, adsorb on the surface, undergo chemical reactions and surface migration, and eventually yield a solid film. Reaction by products also form, and they desorb, diffuse away into the main gas stream, and transport out of the chamber. This sequence of steps is summarized below:

1. Transport of reactants to the growth region
2. Mass transport of reactants to the wafer surface
3. Adsorption of reactants
4. Physical-chemical reactions yielding the solid film and reaction byproducts
5. Desorption of by products
6. Mass transport of byproducts to the main gas stream

7. Transport of byproducts away from the growth region [34]

When plasma is generated in a CVD environment, a fraction of the ground state reactants in the gas phase undergoes electron impact dissociation and excitation, and highly reactive species are consequently generated. As a result, in addition to the ground state species, these highly reactive species also diffuse to the surface, and undergo similar processes of adsorption, chemical reaction, surface migration, etc. In other words, these highly reactive species follow an alternative deposition pathway which operates in parallel to the existing thermal deposition pathway.[34]

3.2 Novellus Concept two Sequel Express PECVD system

Picture 3- 1 Multi-station of Concept two Sequel Express PECD system (courtesy of Novellus System Inc.)

The CORAL sample studied in this thesis was grown using Concept two Sequel Express PECVD system, which was developed by Novellus Systems, Inc. It has a parallel-plate

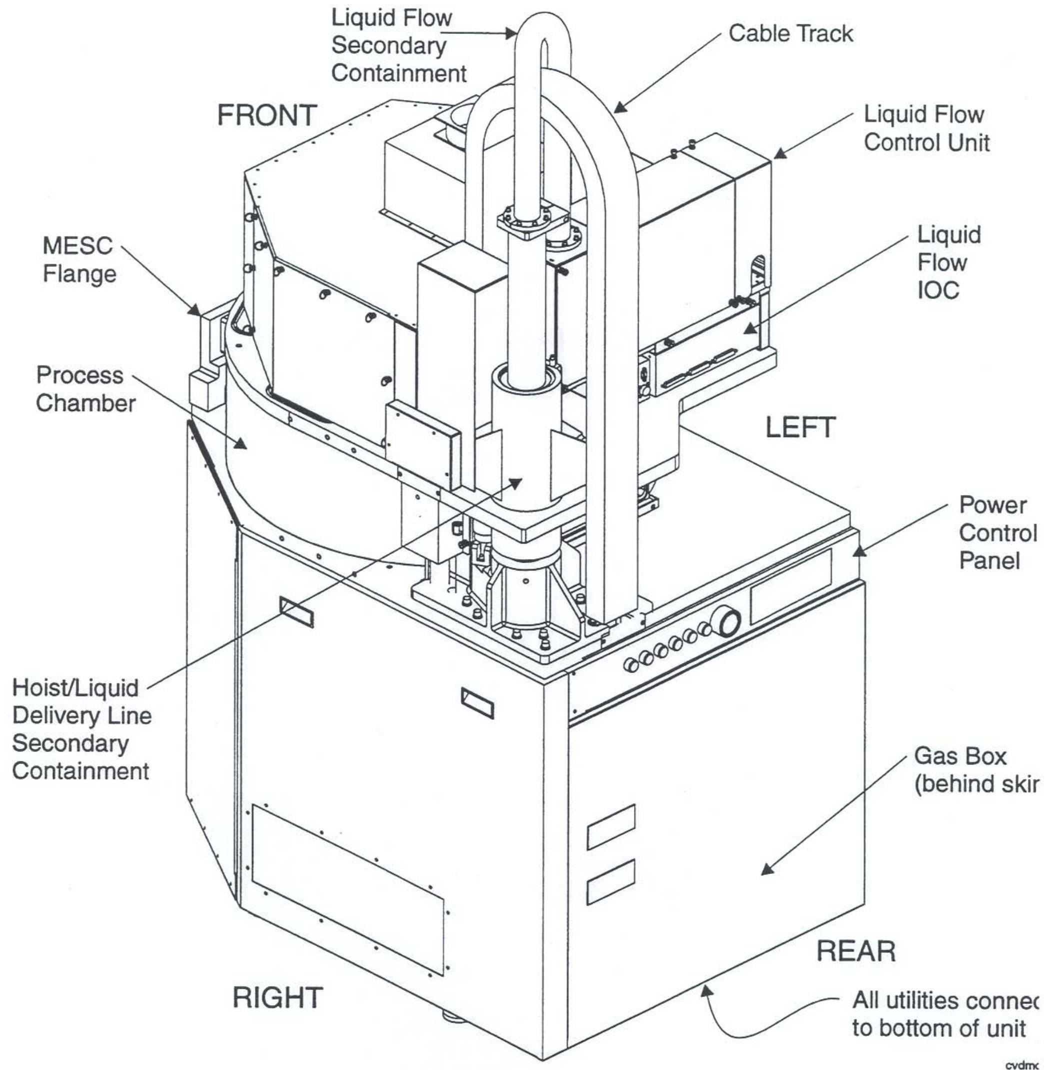

Figure 3-2 Sequel Express process module

reactor (process chamber). The upper electrode is connected to a 13.56MZ radio frequency (RF) generator through matching network and the lower electrode was grounded. The wafers are loaded onto the lower electrode. A 400KHZ low frequency generator is also connected to the lower electrode. The purpose of using low frequency power is to obtain low stress film. All the gases used in this machine are controlled by Mass Flow Controller/Liquid Flow Controller (MFC/LFC).

Sequel system is a dual load lock multi-station deposition system. There are six stations in the process chamber. Gases flow into the chamber through six showerheads. The film was deposited on the wafer layer by layer. In other words, the resulting film was constructed by six sub-layers. Pic. 3-1 shows the six stations in the process chamber.

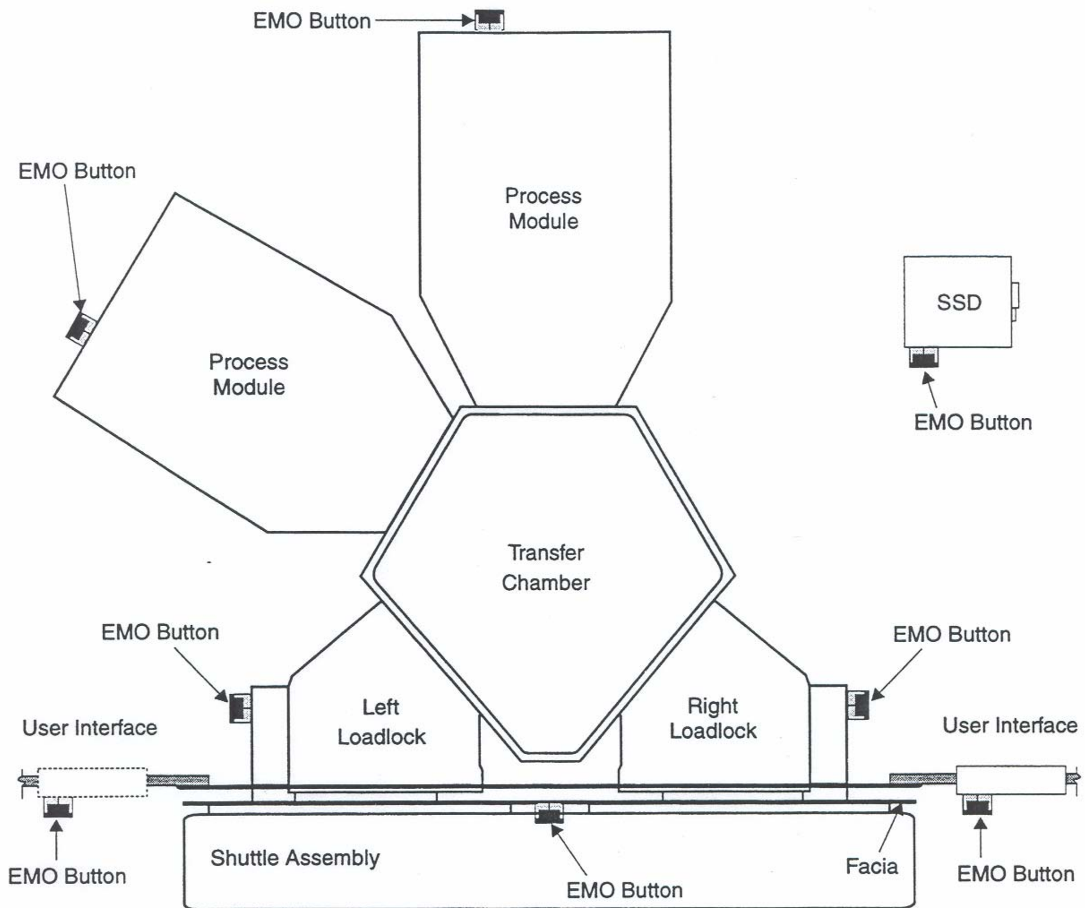

Figure 3-3 Novellus Concept two Sequel Express PECVD system

This system was designed based on 4MS/TMCTS precursor. At room temperature these precursors are liquid. The liquid will be heated to gas state before they flow into the chamber. Fig.3-2 shows the schematic of Sequel Express process module and Fig. 3-3 shows the schematic of the whole system.

3.3 SSM C-V 495 system for k value measurements

Dielectric constant (k value) measurement is very important in this research work. Normally, k value measurement needs MIS (Metal Insulator Semiconductor) structure. Forming this structure is a very tedious work. It needs many steps, like PVD and pattern transfer (litho and etch) process.

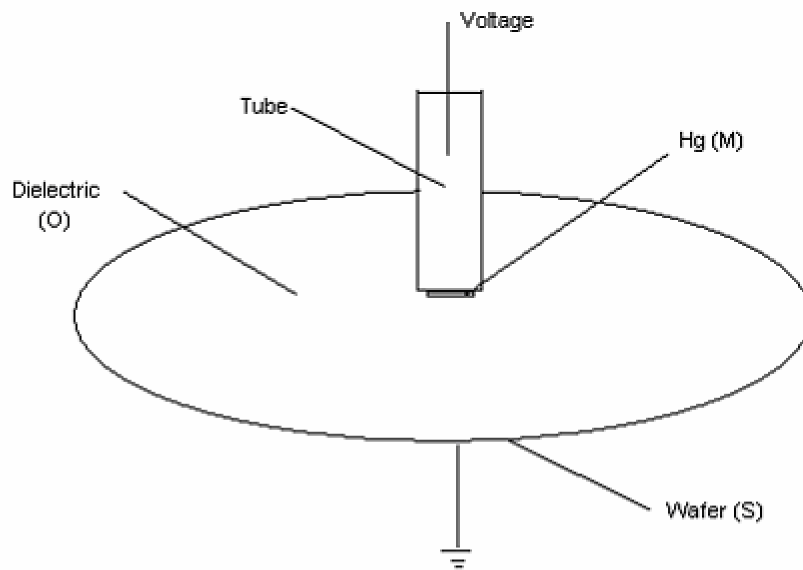

Figure 3-4 Schematic of mercury (Hg) probe

SSM CV-495 system is developed by Solid State Measurement Inc. for k value measurements. It can predict k value of the dielectric through measuring C-V curve of Metal Oxide Semiconductor (MOS) structure. In this machine, mercury (Hg) was used as the gate material. When doing measurement, the mercury probe is down to contact the

dielectric which has been deposited on the silicon wafer. Then a voltage will sweep the gate to get the C-V curve. Fig. 3-4 shows the mercury probe contacts with the dielectric to form a two terminals MOS structure.

As we have known that, C-V curve can be divided into five areas, strong inversion area, moderate inversion area, weak inversion area, depletion area and accumulation area. Fig. 3-5 shows these areas. Use circuit representation, we can give a small-signal equivalent

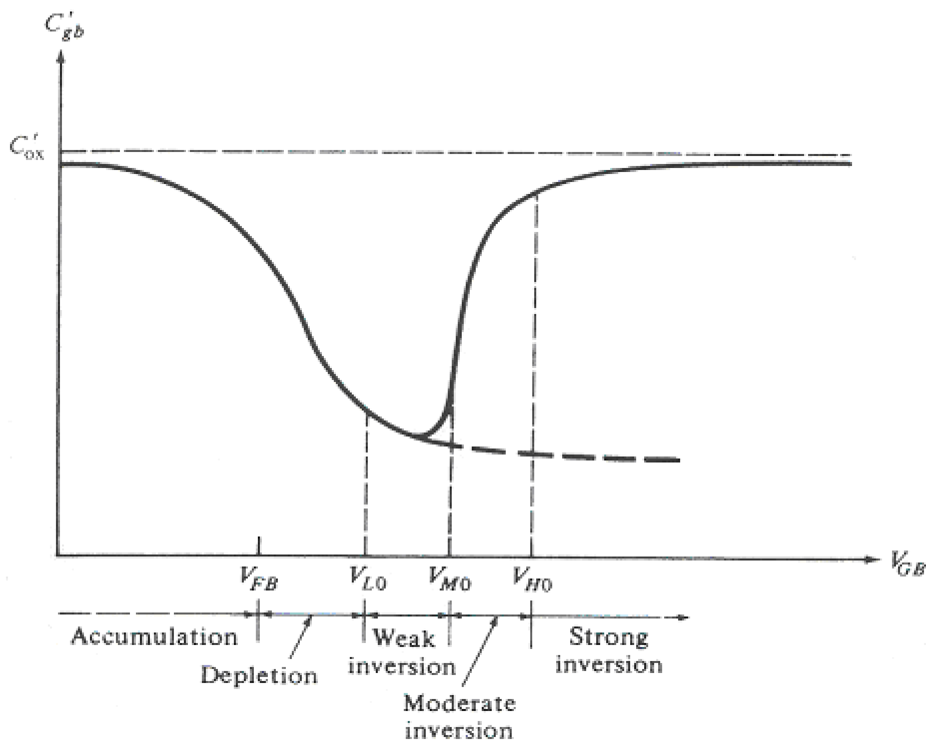

Figure 3-5 C-V curve of MOS structure

circuit, just as Fig. 3-6 shows, for the two terminals MOS structure. It indicates that the total capacitance C_{gb} can be expressed by two capacitors of values C_{ox} and C_c, connected in series. In which C_{ox} is the capacitance of oxide and C_c is the capacitance of semiconductor charge region. We can write C_{gb} as follows:

$$1/Cgb=1/Cox+1/Cc \quad (3.1)$$

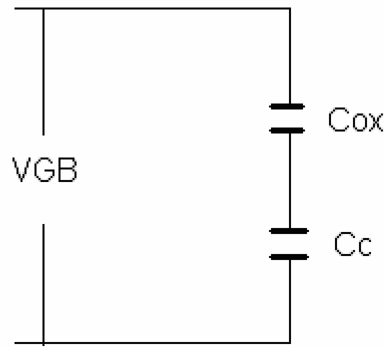

Figure 3-6 Equivalent circuit of two terminals MOS structure

It will be in the case of accumulation when gate voltage (V_{GB}) less than flat band voltage (V_{FB}). Under this condition C_c is very large and the total capacitance C_{gb} is reduced to approximately C_{ox} as see from (3.1). In other words, in accumulation there is an abundance of holes (here, p-type substrate will be assumed) which can provide a conducting path from the substrate bottom through the semiconductor to the surface. For V_{GB} sufficiently smaller than V_{FB}, the resulting negative surface potential attracts huge number of holes immediately below the oxide, in a sense forming the bottom “plate” of the oxide capacitor. As a result, the total incremental capacitance seen between the two terminals of the MOS junction is basically that of the oxide, C_{ox}. [35]

Once we get the capacitance of oxide, we can use formula (3.2) to calculate the k value of oxide.

$$C_{ox}=\varepsilon_0 kA/d$$

$$k=C_{ox}d/\varepsilon_0 A \quad (3.2)$$

where A is the contact area of gate and oxide, d is the thickness of oxide.

Thus, if we know the contact area of mercury and low-k dielectric and the thickness of low-k dielectric, using SSM CV-495 system we can get the capacitance of low-k film when the carriers accumulate in the substrate. Further more, we can calculate the k value of low-k film.

3.4 Fourier Transform Infrared (FTIR) Spectroscopy

Bio-Rad FTIR spectroscopy was used to characterize chemical bonding of low-k material. The Michelson interferometer is the basis of a FTIR spectroscopy. The optical layout of this interferometer is shown in Fig. 3-7.

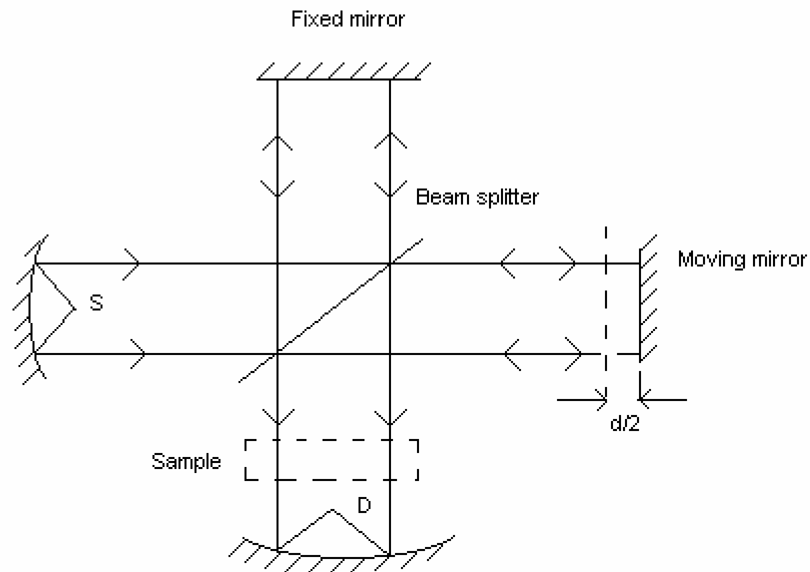

Figure 3-7 Michelson Interferometer (S=source, D=detector)

A beam of radiation from the source S, is focused on a beam splitter which is constructed of material such that about half the beam is transmitted to a moving mirror which reflects the beam back to the beam splitter which then reflects part of this beam through a sample to a detector, D. The other half of the beam from the source is reflected from the beam splitter to a fix mirror which reflects the beam through the beam splitter to the detector, D, via the sample. A suitable material with the necessary optical properties for beam splitting in the mid-infrared is KBr coated with germanium. In the far-infrared polyethylene terephthalate is used.

When the position of the moving mirror produces two beams traveling equal distance and falling on the detector, D, a strong signal should be obtained from the detector. When the moving mirror is scanned through a distance each side of the central position corresponding to zero path distance an interference pattern is registered by the detector. This interference pattern contained spectral information.

The essential equations relate the intensity falling on the detector, I(δ), to the spectral power density at particular wavenumber, ν, given by B(υ) are as follows:

$$I(\delta)=\int_{0}^{+\infty} B(\upsilon)\cos 2\pi\upsilon\delta \cdot d\upsilon \quad (3.3)$$

which is one half of a cosine Fourier transform pair, the other being

$$B(\upsilon)=\int_{-\infty}^{+\infty} I(\upsilon)\cos 2\pi\upsilon\delta \cdot d\delta \quad (3.4)$$

These two equations are interconvertible. They are known as a Fourier Transform pair. Equation (3.3) shows the variation in power density as a function of difference in path-length which is an interference pattern. Equation (3.4) shows variation of intensity as a

function of difference in path length, which is a spectrum. Each can be converted into the other by the mathematical method of Fourier transformation. [36]

3.5 Atomic Force Microscopy (AFM)

AFM, which can be operated in air or water, uses a fine tip to measure surface morphology and properties through an interaction between the tip and surface. Almost all materials can be measured without specific sample preparations. [37]

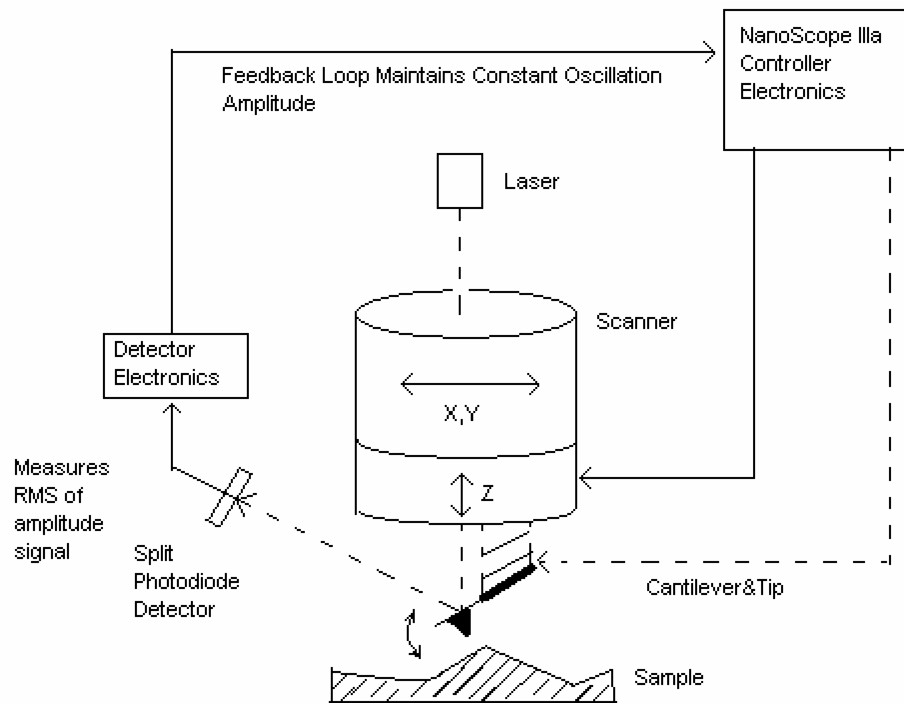

Figure 3-8 Schematic of TappingMode AFM

Veeco Digital-5000 AFM which working under TappingModel^{TM} from Digital Instrument was used to measure surface morphology of low-k film. This machine

operates by scanning a tip attached to the end of an oscillating cantilever across the sample surface. The cantilever is oscillated at or near its resonance frequency with an amplitude ranging typically from 20nm to 100nm. The tip lightly "taps" on the sample surface during scanning, contacting the surface at the bottom of its swing. The feedback loop maintains a constant oscillation amplitude by maintaining a constant RMS of the oscillation signal acquired by the split photodiode detector. The vertical position of scanner at each (x,y) data point in order to maintain a constant "setpoint" amplitude is stored by the computer to form the topographic image of the sample surface. Fig. 3-8 shows schematic of Tapping Model AFM.

3.6 X-Ray Photoemission Spectroscopy (XPS)

X-ray Photelectron Spectroscopy known as XPS or Electron Spectroscopy for Chemical Analysis (ESCA) is used widely in research, development and manufacturing. This technique is able to obtain the chemical composition of various material surfaces up to 1 nm depth. Most of the elements can be detected by determining their binding energy except hydrogen.

By absorbing a photon, an atom gains an energy amount equal to hv. It then releases an electron to regain its original stable energy state. The released electron retains all the energy from the striking photon. It can then escape from the atom, and even further from matter and kinetic energy keeps it moving. With XPS, incident photons usually carry an energy ranging from 1 to 2 KeV. For example, by usual X-ray sources, magnesium and

aluminium emit at 1253.6 and 1486.6 eV respectively. The relative high level of the incident energy causes the matter to release electron from an atom internal shell. Consequently, there will be some atoms lacking electrons in the internal shells from which photoelectrons have been released. To recover from this ionized state the atom can emit another photon (fluorescence) or undergo an Auger transition. The principle of the conservation of energy allows us to write the energy balance equation, valid for the absorption of a photon carrying an energy of hν :

$$h\nu = E_{\text{Kinetic}} + E_{\text{Binding}} + \text{Ø}_{\text{Work function}} \qquad (3.5)$$

Where

hν— X-ray beam incident energy.

E_{Kinetic}— Electron kinetic energy when leaving the specimen.

E_{Binding}— Electron binding energy inside the atom.

In order to obtain E_{Binding}, a analyzer is used to determine E_{Kinetic} . Fig. 3-9 shows the schematic of this analyzer. This analyzer consists of two plates carrying a potential.

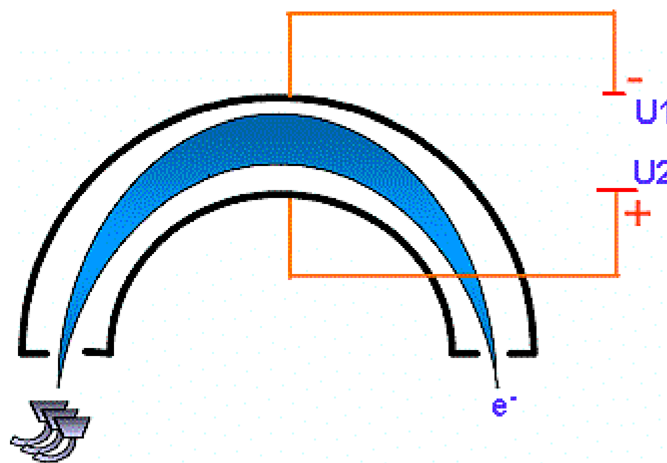

Figure 3-9 Schematic of electron analyzer

When the electron is entering the analyzer it undergoes and electrical field which forces it to travel along the trajectory defined by the following equation:

$$F = qE = m(V^2/R) \qquad (3.6)$$

Where

F— Force,

V—speed,

R—trajectory radius,

E—electrical fields established by U potential,

m—electron mass,

q—electron charge.

According to this equation (3.6), a given electrical field or a given U potential corresponds to a given kinetic energy. The hemispherical analyzer behaves like an energy filter. Thus, $E_{Binding}$ can be calculated by using equation (3.5).[38]

3.7 Secondary Ion Mass Spectrometry (SIMS)

SIMS is a surface analytical technique that uses an ion beam to remove material from a surface. The impact of the primary ions generates neutral atoms and positively and negatively charged secondary ions, that are sputtered from the sample surface. Positive or negative ions can then be mass-separated and detected by an electron multiplier or projected onto a phosphorescent screen in order to measure their spatial distribution on the surface. [39]

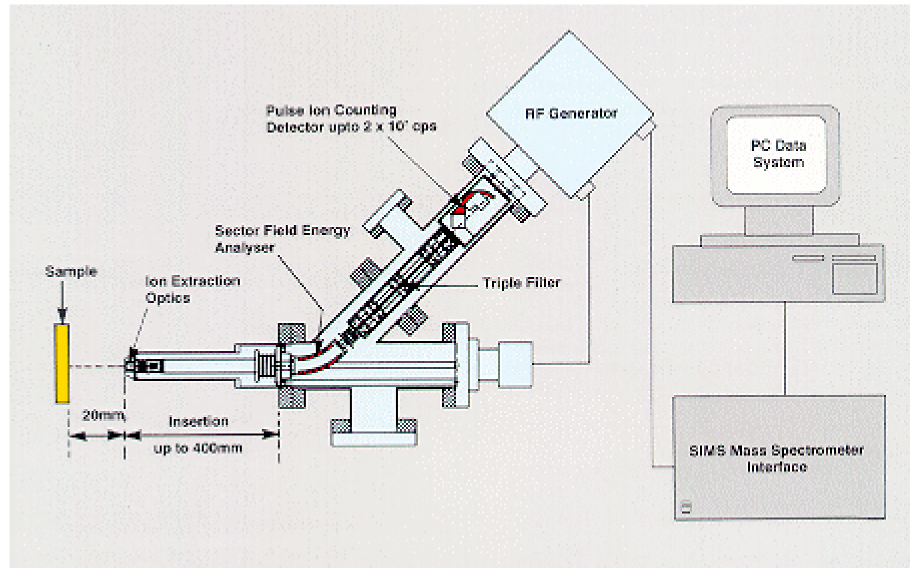

Fig. 3-10 Schematic of SIMIS instrument

Bombardment of a sample surface with a primary ion beam followed by mass spectrometry of the emitted secondary ions constitutes SIMIS. Typical SIMIS instrument use either a duoplasmatron or a surface ionization primary ion source (or both). Primary ions are extracted from the source and passed to the sample through the primary ion column. The column usually contains a primary beam mass filter that transmits only ions with a specified mass to charge (m/z) ratio. Secondary ions are extracted and accelerated toward the ground plate of an electrostatic lens from the sample once they are produced by primary ion beam. After focusing, the secondary ion beam is transferred to the mass spectrometer slits or aperture for analyzing. Fig. 3-10 shows the schematic of SIMS instrument. [40]

3.8 FSM 7800TC Stress Measurement System

Film stress was measured by FSM 7800TC stress measurement system. The FSM 7800TC uses a laser optical lever to measure the change of curvature induced in a wafer due to the deposition film. A schematic of the configuration is shown in Fig. 3-11. The laser scans the surface of the wafer and the beam is deflected by the wafer surface, reflected off a mirror, and detected by a precision position detector. A clean, blank wafer is measured prior to film deposition. Its data is compared to measurements taken on the same sample after film deposition.

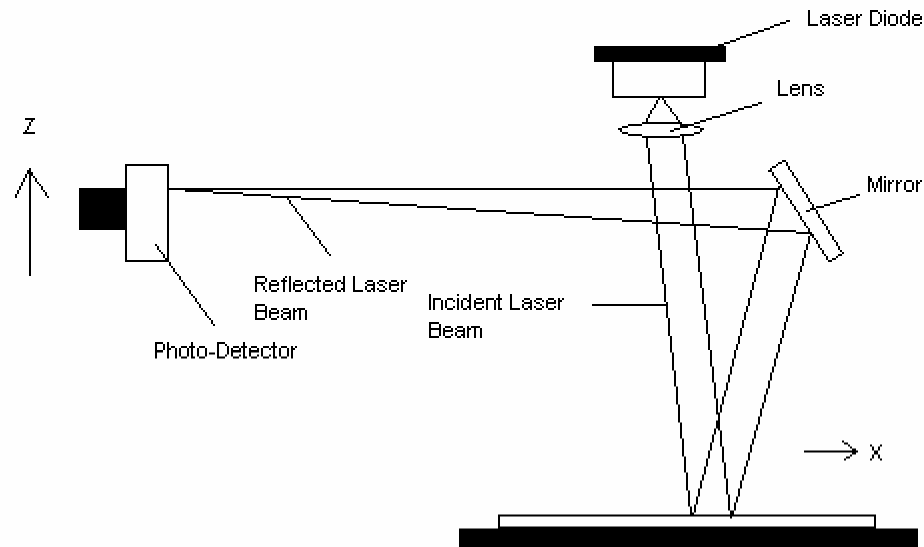

Figure 3-11 Schematic of stress measurement system configuration

The radius of curvature of the sample is determined from the slope of a straight line fitted to point –by-point subtraction data calculated from the before and after deposition scan data. That is:

$$R=2L\,\delta_x/\delta_z$$

The film stress, S is then calculated using the following equation:

$$S=\frac{E(D)^2}{6(1-\nu)RT}$$

Where

E —Young's modulus of the substrate

ν —Poisson's ratio of the substrate

D—thickness of the substrate

R—net radius of curvature

T—thickness of the film (T<< D)

3.9 Tetramethylcyclotelrasiloxane (TMCTS), the precursor for PECVD

TMCTS (TOMCATS™ is the trade mark of this chemical which was given by Schumacher), also called 1, 3, 5, 7, tetramethylcycloterasiloxane or cyclotetrasiloxane 2, 4, 6, 8 tetramethyl is developed by Schumacher as a PECVD precursor for Novellus' CORAL low-k material deposition. It is prepared through hydrolysis of methyldichlorosilane to firstly form a liner siloxane polymer that is endcapped with trimethylsilyl groups (derived from trimethylchlorosilane) according to:

$$(CH_3)Si(H)(Cl_2) + (CH_3)_3Cl \rightarrow (CH_3)_3Si\text{-}O\text{-}[SiHCH_3\text{-}O]_n\text{-}Si(CH_3)_3$$

$$(CH_3)_3Si\text{-}O\text{-}[SiHCH_3\text{-}O]_n\text{-}Si(CH_3)_3 \rightarrow \text{TMCTS + other cyclic compounds [39]}$$

This precursor is a clear, colorless, flammable liquid and has ether-like odor. It has molecular weight 240.51g, melting point 17°C, boiling point 135°C, flash point 24°C (closed cup test), freezing point -65°C and auto-ignition temperature 250°C. The density

of TMCTS is 0.991g/cm^3. At 20°C, its vapor pressure is 7 Torr. The formula of this chemical is: $C_4H_{16}O_4Si_4$. It belongs to organosilicone chemical family.

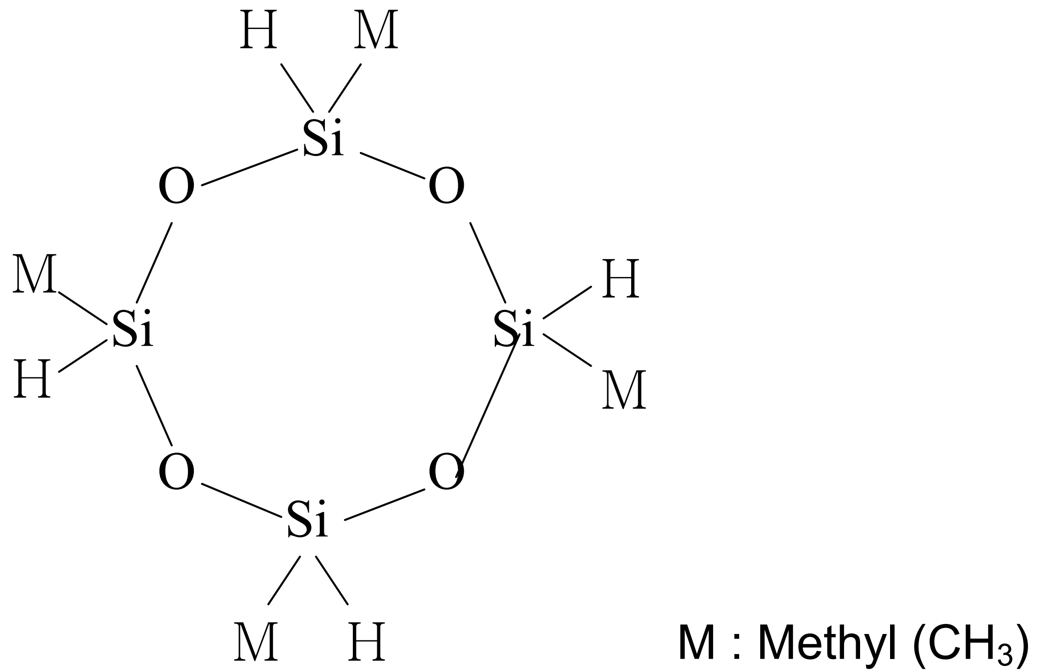

Figure 3-12 Chemical structure of TMCTS

TMCTS has cyclic structure as Fig. 3-12 shows. It was reported that there is a strong relationship between Si-O:Si ratio present in the precursor molecular structure and mechanical strength in the resulting films. As this ratio varies, interplay between k and mechanical properties was observed. TMCTS with a Si-O:Si ratio of 1:1, produces film with relatively poor mechanical properties but k~2.75. However, small additions of oxygen to the TMCTS process moderately improve mechanical properties. [41]

3.10 Experiment conditions

3.10.1 The growth of CORAL films on Si (100)

In this research works, CORAL film was deposited on 8 inch P-type bare silicon (100) test wafer at 400^oC use Novellus-Sequel PECVD system. All the gas flow that used for process were controlled by Mass Flow Controller/Liquid Flow Controller (MFC/LFC) and the flow rate ratio is TMCTS:O_2:CO_2=1(ml):50(sccm):1000(sccm). RF power was introduced using two frequencies, one is 13.56MHZ (High Frequency) and another one is 250 KHZ (Low Frequency). The ratio of high frequency power to low frequency power was 4:3 and the pressure of deposition was 3.9-4.1 Torr.

3.10.2 Thermal treatment

The as-deposited film was annealed at 400^oC, 500^oC, 600^oC, 700^oC and 800^oC in N_2 amient for 30 min respectively. Ten thermal cycles (30 minutes per cycle in N_2) were also done at 425^oC which was an interesting temperature in microelectronics processes. After annealing, the thickness and refractive index of CORAL film was measured use Thermal wave 5240I opti-probe at 673.2nm. Film thickness was also confirmed by Scan Electron Microscopy (SEM). Chemical bonding and surface roughness of CORAL film was characterized by Bio-Rad Fourier Transform Infrared (FTIR) and Atomic Force Microscopy (AFM) respectively. K value and field breakdown voltage were measured using SSM 495 CV system. The element concentration, for example the carbon concentration, was analysis use X-Ray Photoemission Spectroscopy (XPS) and Secondary Ion Spectroscopy (SIMS). Thermal Gravity Analysis (TGA) was also used to characterize this film. Film stress was measured from room temperature to 700^oC use

FSM 7800TC stress measurement system. Film degas at high temperature was detected by Temperature Programmed Desorption (TPD) experiment. TPD and TGA samples were obtained by scraping film from silicon substrate.

3.10.3 Dilute HF treatment

The as-deposited film was etched using 1% (diluted from 49% HF) dilute HF up to 10 minutes. Before etching, film thickness and refractive index (RI) were measured by FilmTek-4000 ellipsometer. To ensure uniform etching, the 1.5x1.5cm sample was put into large volume HF solution.(~250ml) After etching, the samples were rinsed using DI water and then dried by N_2. Again, FilmTek-4000 ellipsometer was used to measure the film thickness and RI. Surface roughness was measured by Vecco Digital-5000 Atomic Force Microcopy (AFM) within 1µmx1µm range, chemical bonding was characterized by Fourier Transform Infrared (FTIR) and k value, leakage current were measured using SSM Hg probe.

3.10.4 Plasma treatment

The as-deposited film was treated by different kinds of plasma including Oxygen plasma, forming gas (4% H_2+N_2) plasma, NH_3 plasma, Helium plasma, Nitrogen plasma and Fluoride gas (CHF_3+CF_4+Ar+O_2) plasma. All the plasma treatments were conducted in Applied Materials Centura 5200 PECVD system DxZ chamber except forming gas plasma and CHF_3+Ar+O_2 plasma treatment that were conducted using Mattson photoresist strip system.

All the plasma treatments used 13.56 MHz RF generator. The temperature of D_XZ chamber was 350°C whereas the temperature of Mattson system was 250°C. O_2 flow rate was controlled at 200sccm, pressure was set to 4 mTorr and the RF power is 900W. Forming gas flow rate was controlled at 5000sccm, pressure was set to 850 mTorr and the RF power is 900W. In CHF_3+CF_4+Ar+O_2 plasma, RF power was 1000W, CHF_3 flow rate was 30sccm, CF_4 flow rate was 40sccm, Ar flow rate was 200sccm and O_2 flow rate was 20sccm. NH_3 flow rate was controlled at 200sccm, pressure was set to 6 mTorr and the RF power was 900W.

After plasma treatment, CORAL film was characterized by Opti-probe, FTIR, AFM and Mercury probe C-V system.

Chapter 4 The effects of thermal, dilute HF and plasma treatments on CORAL film

4.1 The growth of CORAL

CORAL film was deposited on 8 inch p-type bare silicon (100) test wafer at 400°C in the Novellus-Sequel Concept two multi-station PECVD system. There are 6 stations in the process chamber. The film was deposited on the wafer layer by layer. The precursor used in this process is cyclic1,3,5,7-tetramethyl-cycloterasiloxane (TMCTS). TMCTS is prepared through hydrolysis of methyldichlorosilane to firstly form a liner siloxane polymer that is endcapped with trimethylsilyl groups (derived from trimethylchlorosilane) according to:

$$(CH_3)Si(H)(Cl_2) + (CH_3)_3Cl \rightarrow (CH_3)_3Si\text{-}O\text{-}[SiHCH_3\text{-}O]_n\text{-}Si(CH_3)_3$$

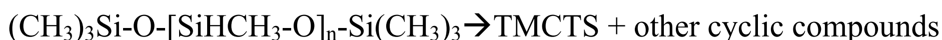

$$(CH_3)_3Si\text{-}O\text{-}[SiHCH_3\text{-}O]_n\text{-}Si(CH_3)_3 \rightarrow \text{TMCTS + other cyclic compounds}$$

This precursor has molecular weight 240.51g., melting point 17°C, boiling point 135°C, flash point 24°C and autoignition temperature 250°C.

All the gas flow was controlled by mass flow controller (MFC) and the flow rate ratio is TMCTS:O2 :CO2=1(ml):50(sccm):1000(sccm). RF power was introduced using two frequencies, one is 13.56MHZ (High Frequency) and another one is 250 KHZ (Low Frequency). The ratio of high frequency power to low frequency power was 4:3 and the pressure of deposition was 3.9-4.1 Torr.

4.2 Thermal treatment

The thermal treatment effect is an important topic of investigation of low-k material since repetitive thermal treatments involved in IC processing, and good thermal stability is required for the materials to withstand metallization, anneal, cure and chip-attach.

The PECVD-grown CORAL films were annealed at various temperatures between 400-800^oC. After thermal annealing the structural, chemical and optical properties of the films were characterized by a variety of tools, as presented below.

4.2.1 Thickness and Refractive Index (RI)

The thickness and refractive index of CORAL film after annealing in N_2 for 30 minutes at various temperatures are plotted in Fig. 4-1. The film thickness is observed to decrease continuously with increasing temperature to 500^oC and above. After annealing at 800^oC 25% film shrinkage is measured. This is confirmed by SEM cross section analysis (see picture 4-1). The film shrinkage is due to the partial destruction of the film at high temperatures. As detected by temperature programmed desorption (TPD), at annealing temperatures above 600^oC, H_2, CO and some other hydrocarbons, as well as large amount of CH_4, are desorbed from CORAL film. In Fig. 4-2 (a) to (d), the desorption of these gases starts at 500—600^oC, and reaches a maximum value at the temperature 780-800^oC. Careful analysis indicates that at temperatures below 600^oC CH_4 is the main constituent

of the desorbed gases. Formation of H_2, CH_4, CO and other hydrocarbon at about

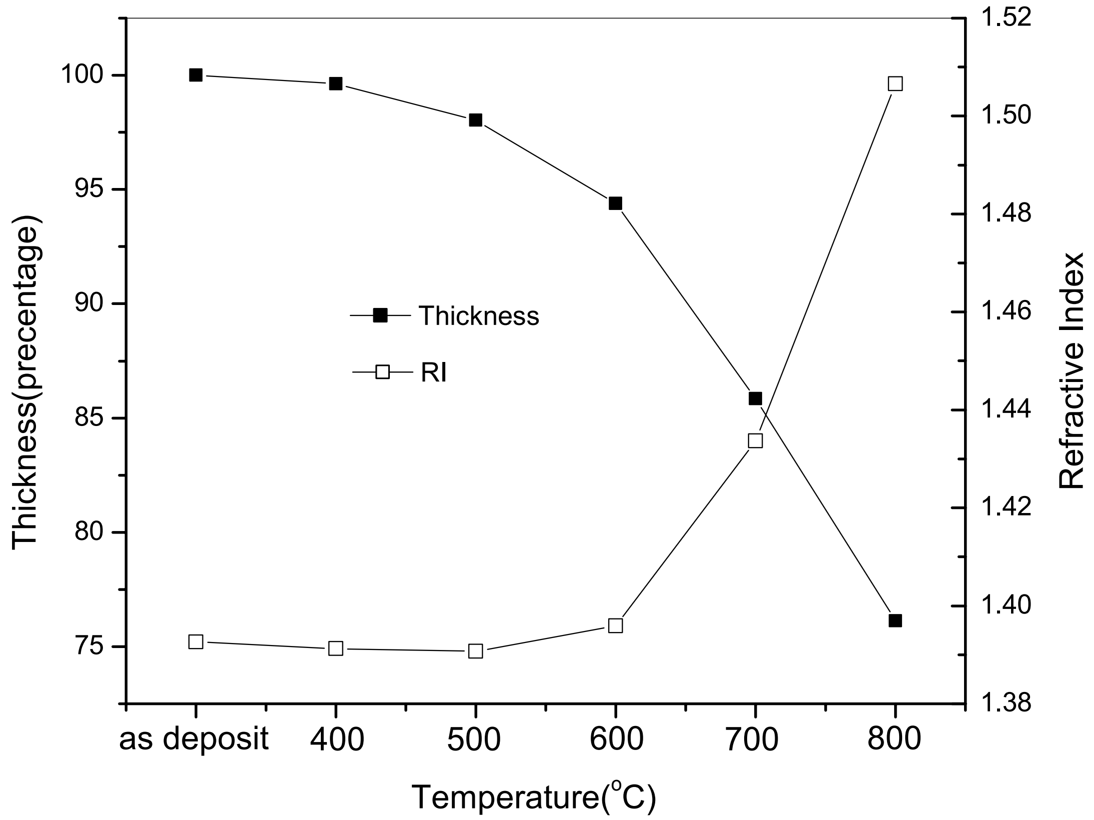

Figure 4-1 Thickness and RI of CORAL after annealing

600°C could be due to the breakage of Si-CH_3, Si-C and Si-H bonds at such high temperatures. The TGA profile in Fig. 4-3 shows that the weight loss of CORAL film is about 0.5% from 500°C to 600°C, while it is about 1.25% from 600°C to 700°C and 2% from 700°C to 800°C. The destruction and outgassing of the films result in the film shrinkage after the high temperature annealing.

With the increase of annealing temperature from 500 to 800°C, the refractive index of the films increases from 1.39 to about 1.51. This may indicate that the density of CORAL

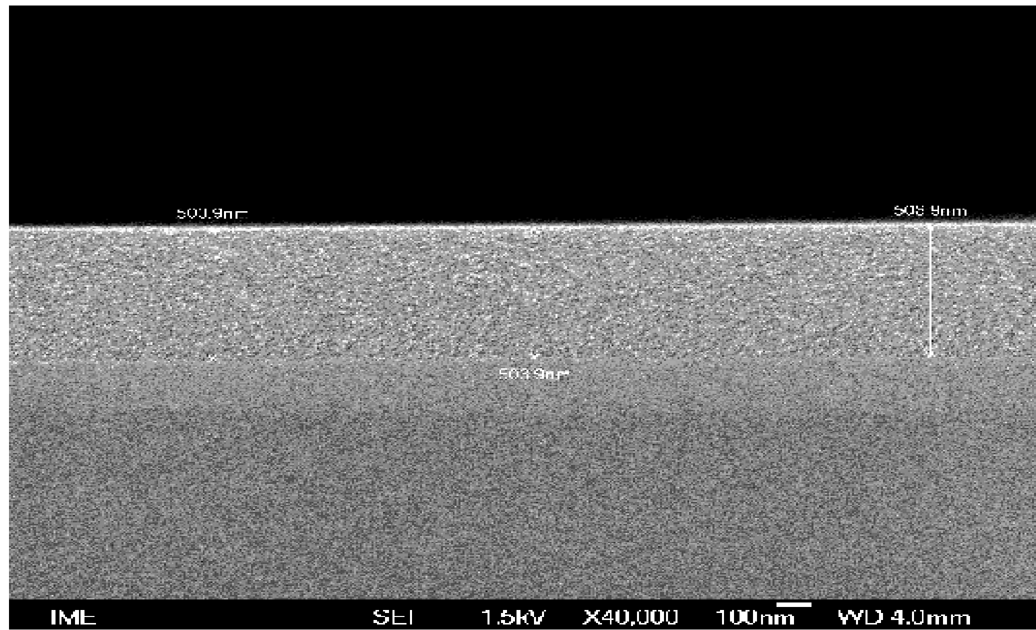

(a)

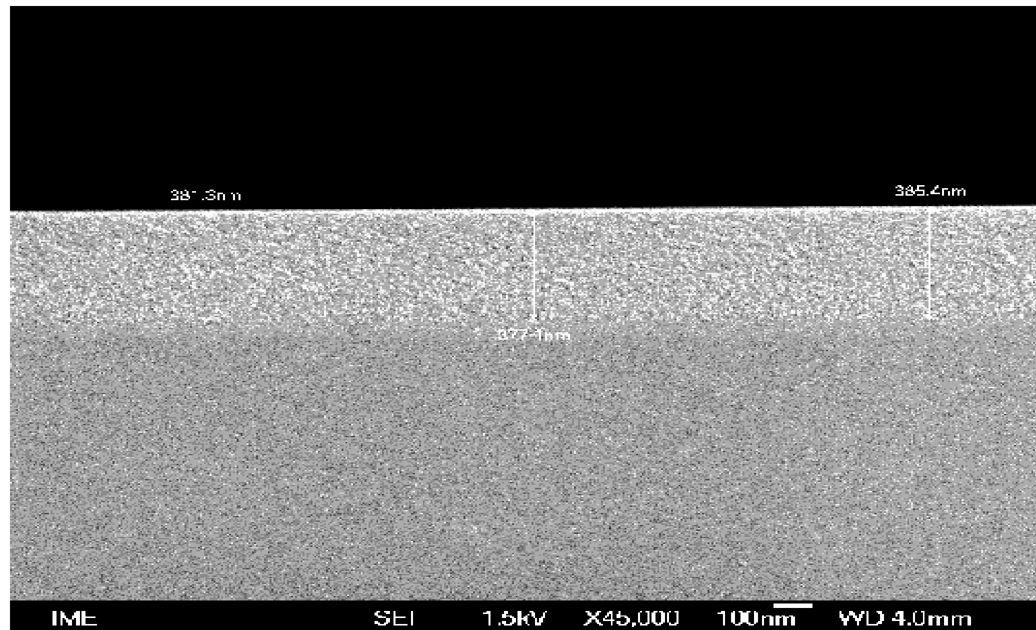

(b)

Picture 4-1 SEM cross section thickness analysis of CORAL film
(a) As deposit(b) After 800°C annealing in N_2 30 minutes

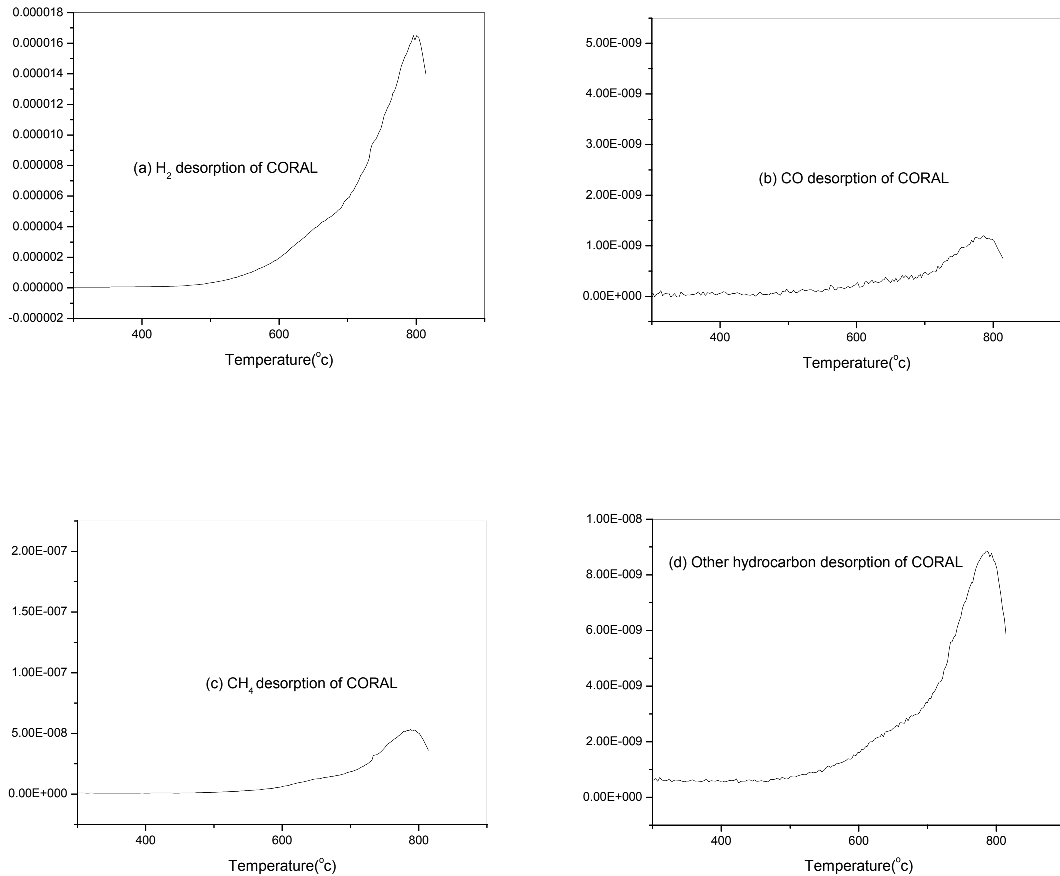

Figure 4-2 Gas desorption of CORAL

film increases after annealing according to the formula which relates the refractive index n to the film density N and the molecular polarization constant α: $n = 1 + (\alpha N / 2\varepsilon_0)$. [18]

Fig. 4-4 and Fig. 4-5 show the thickness and RI after each thermal cycle at 425°C respectively. It is found that the thickness and RI are very stable at this annealing temperature even after ten thermal cycles. It means that CORAL film can withstand many thermal cycles and keep thickness and RI constant at the interesting temperature that is used in microelectronics processes.

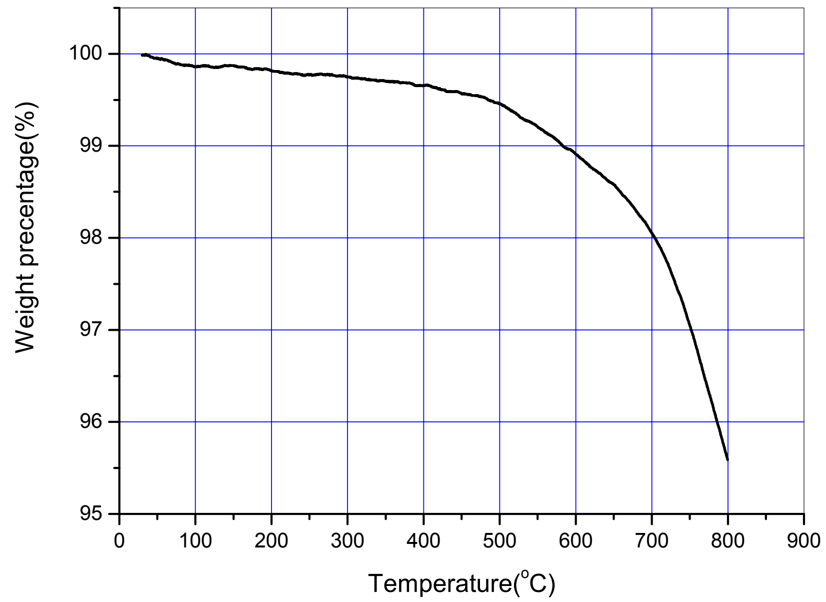

Figure 4-3 TGA from RT to 800°C of CORAL

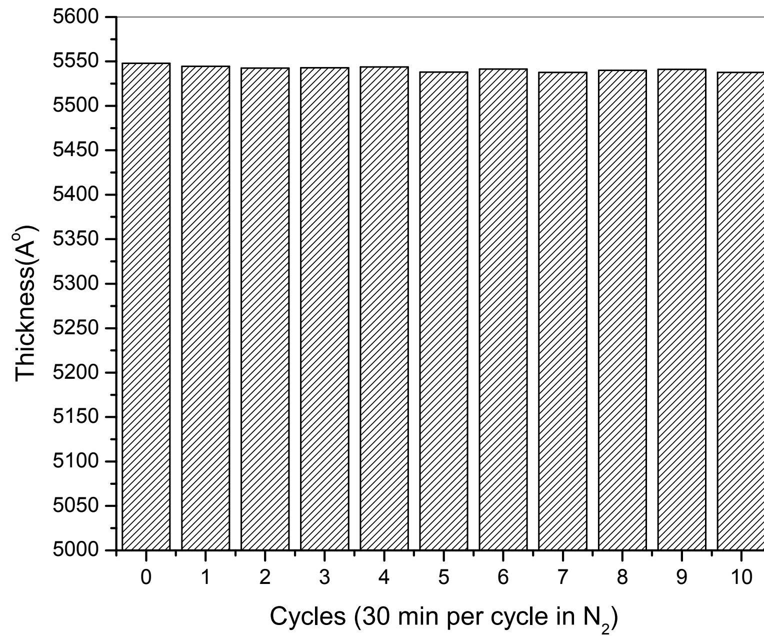

Figure 4-4 Thickness after 10 thermal cycles at 425°C of CORAL

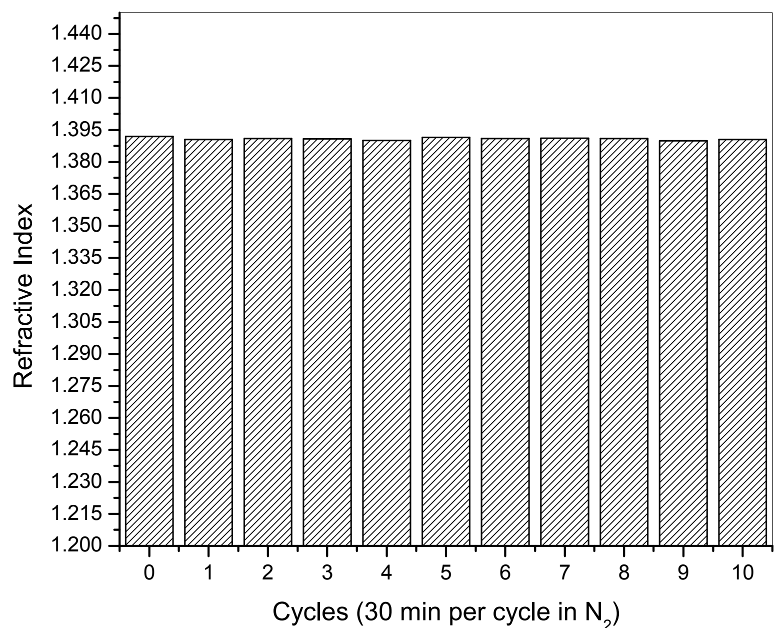

Figure 4-5 RI trend after thermal cycle at 425°C of CORAL

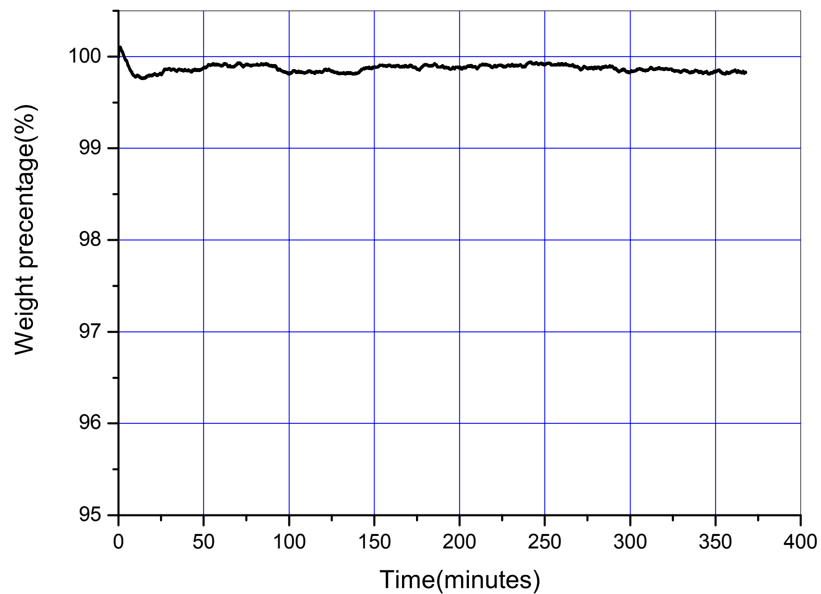

Fig. 4-6 TGA @ 425°C for 6 hours of CORAL film

TGA is also done on CORAL film at 425°C for 6 hours. Fig. 4-6 shows this result. It is found that the weight loss of CORAL film less than 0.5% at this temperature. In other words, outgasing of CORAL film at this temperature is low.

4.2.2 Chemical bonding in CORAL films

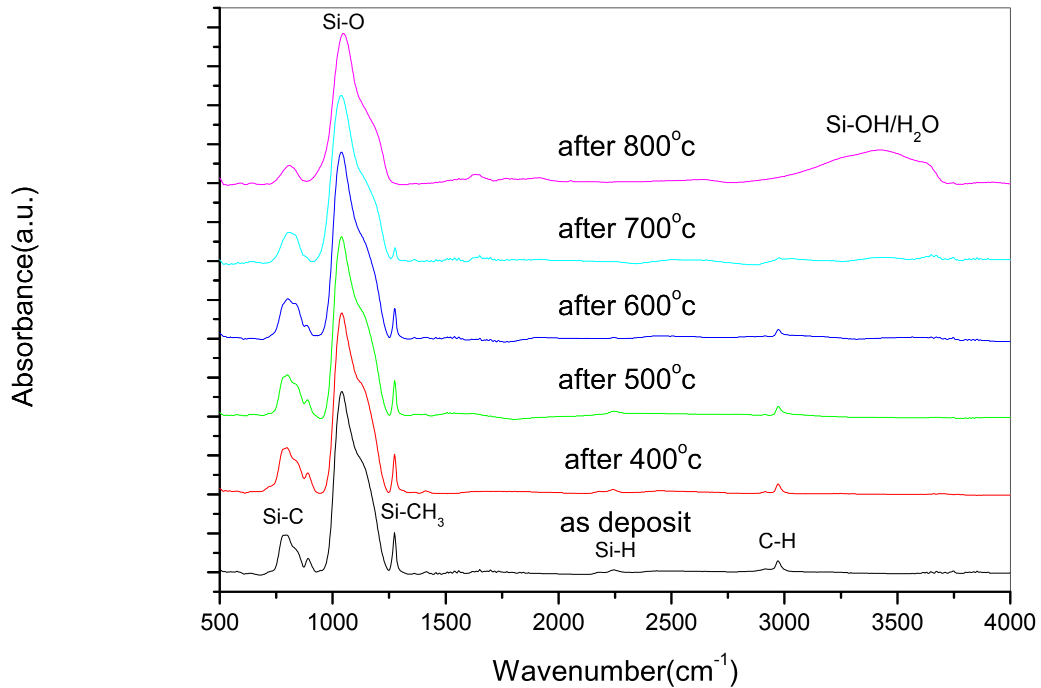

Figure 4-7 FTIR spectra of CORAL after annealing

FTIR was performed to monitor the change in chemical composition and bond structure of CORAL film upon the thermal annealing. Fig. 4-7 shows the FTIR spectra of the as-deposit CORAL and the films after annealing at different temperatures. The dominant i.r. absorption band at 1040cm^{-1} is attributed to small angle Si-O-Si stretching vibration. Its strong shoulder at about 1130cm^{-1} is due to large angle Si-O-Si stretching vibration, corresponding to the Si-O-Si chains in a cage structure which can generate constitutive

microporosity and contribute to a lower film density and lower k value.[15,18] This shoulder shrinks, as shown in Fig. 4-8, meaning that the microporous structure and

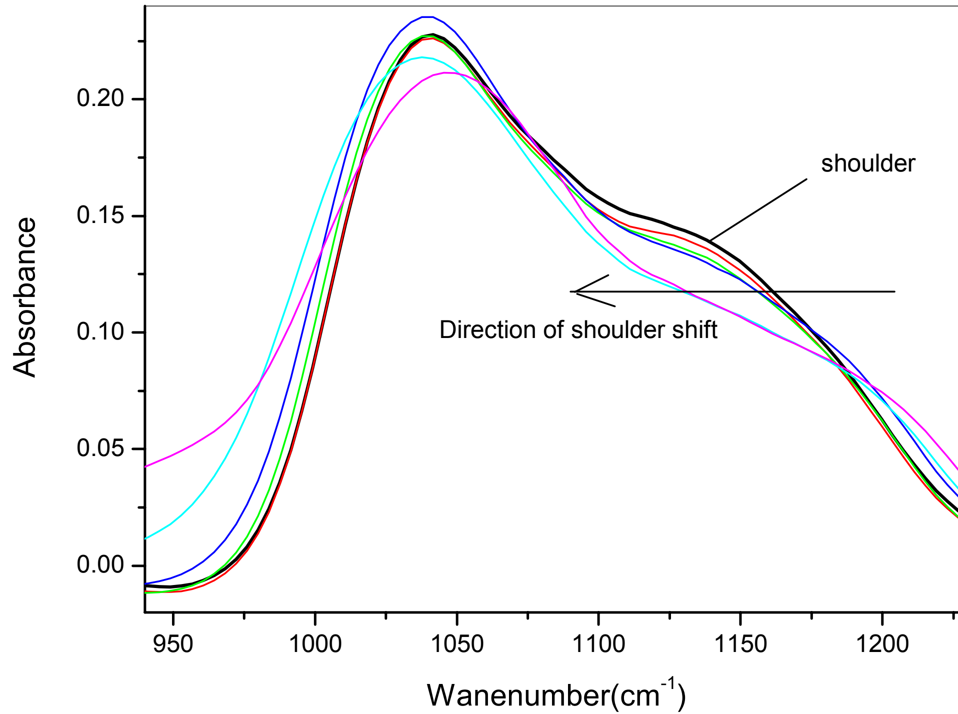

Figure 4-8 Shoulder shift after annealing of CORAL

density of CORAL film change after annealing.[18] Clearly, the as-deposit film spectrum has other vibrational modes, including (a) Si-C stretching mode at ~800cm^{-1}, (b) Si-H stretching in the range of 2100-2300cm^{-1}, (c) Si-CH_3 bending mode at ~1270cm^{-1}, and (d) C-H stretching mode at ~2900cm^{-1}.[28] With increasing annealing temperature the Si-CH_3 peak at 1273cm^{-1} decreases. The band ratio of Si-CH_3 (1273cm^{-1}) to Si-O (1042cm^{-1}) in the CORAL film changes slightly at temperatures below 600°C, but drops sharply when the annealing temperature ramps up above 600°C. It totally vanishes at 800°C. The same trend applies to the C-H (2900cm^{-1}) and Si-C (800cm^{-1}) bonds as

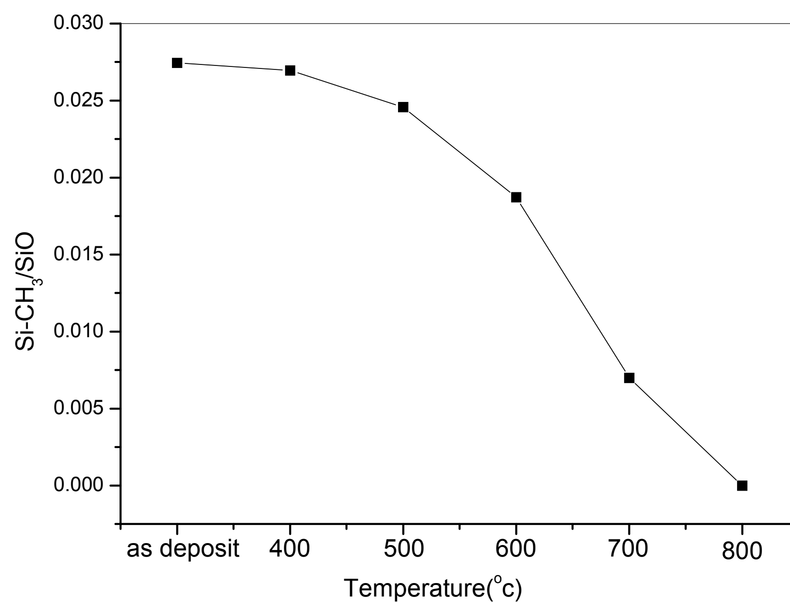

Figure 4-9 Si-CH_3 to Si-O peak area ratio as determined from FTIR spectra after annealing of CORAL

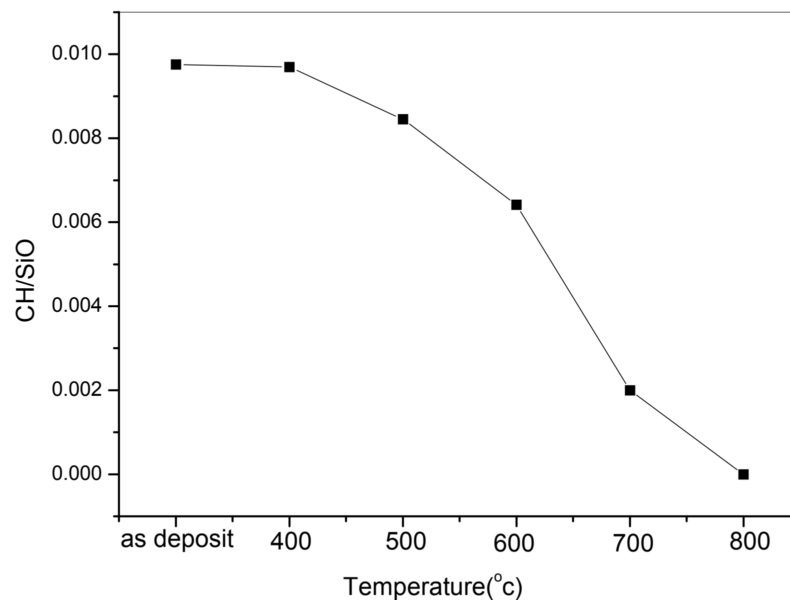

Figure 4-10 C-H to Si-O peak area ratio as determined from FTIR spectra after annealing of CORAL

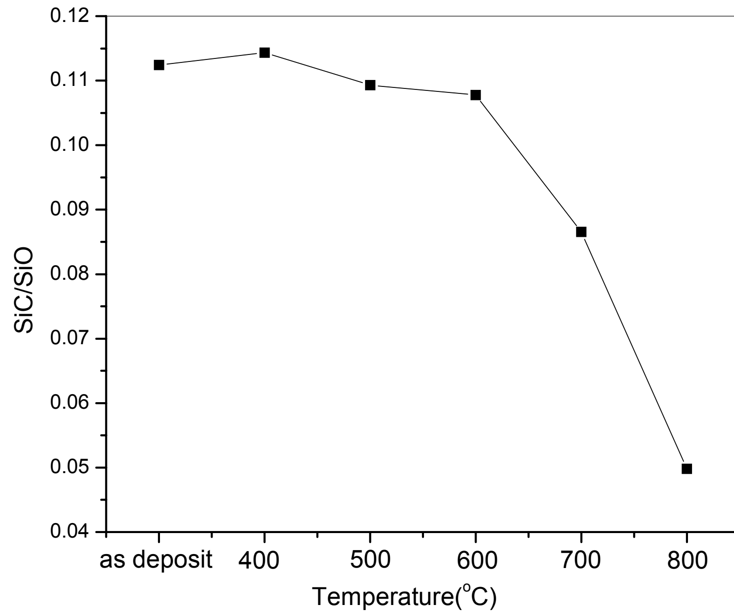

Figure 4-11 Si-C to Si-O peak area ratio as determined from FTIR spectra after annealing of CORAL

shows in Fig.4-9, 4-10 and 4-11 respectively. These results agree well with the TPD test mentioned above, indicating that degradation of the CORAL film property, for example, k value, break down voltage etc, can be expected at temperature above 600°C.

The spectrum after annealing at 800°C shows a broad band corresponding to the Si-OH and H-OH (from 3200 to 3700cm^{-1}) bonds. The formation of Si-OH bond may have two possible causes. One is that when the thermal energy breaks Si-H and Si-CH_3 bonds, oxygen in the ambient (due to the purity of nitrogen) may convert Si-H and Si-CH_3 bonds into Si-OH bonds. The other is that the silicon dangling bonds generated due to the breaking of Si-CH_3 and Si-H bonds can react easily with moisture in the atmosphere when the CORAL film after annealing is exposed to air, forming Si-OH bonds.[42] The

Si-OH bonds in the CORAL film lead to moisture uptake, which is responsible for the increase of k value and leakage current.[28]

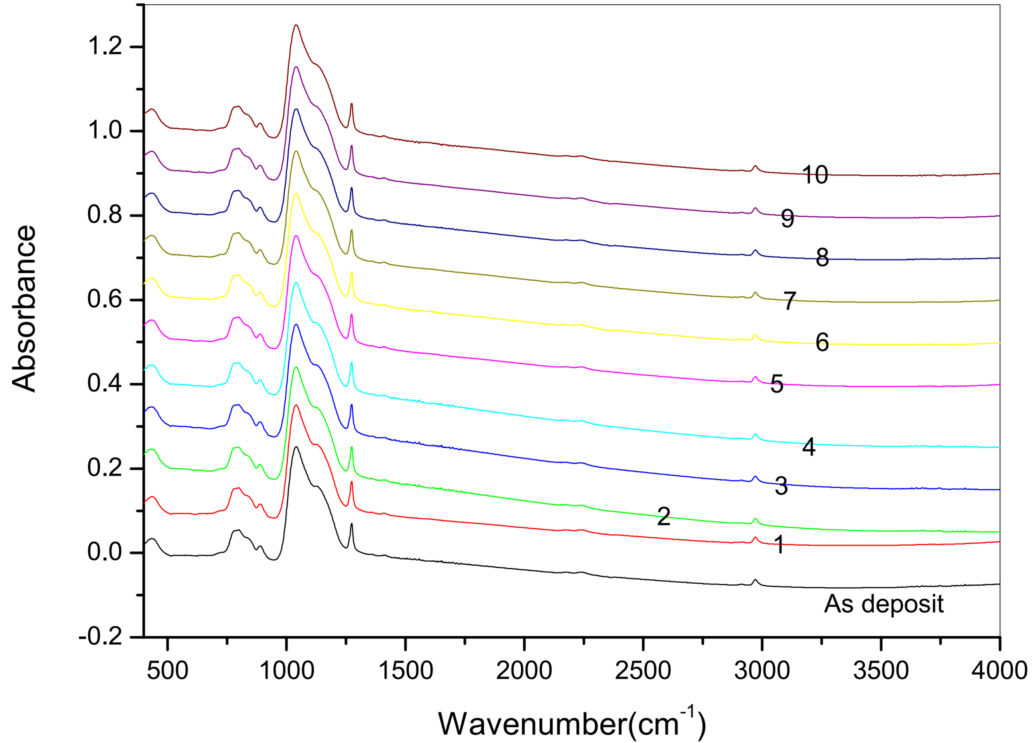

Figure 4-12 FTIR spectra of CORAL after 10 thermal cycles @ 425°C

Fig. 4-12 shows the FTIR spectra after each thermal cycle at 425°C. The results show that the chemical bonding of CORAL film remains the same as that of the as-deposited film after ten thermal cycles. It indicates that there is no chemical structure change in CORAL film after ten thermal cycles.

4.2.3 Roughness and stress

As measured by AFM and shown in Fig. 4-13, the surface roughness of CORAL film changes after annealing. The surface of the film becomes rough after low temperature

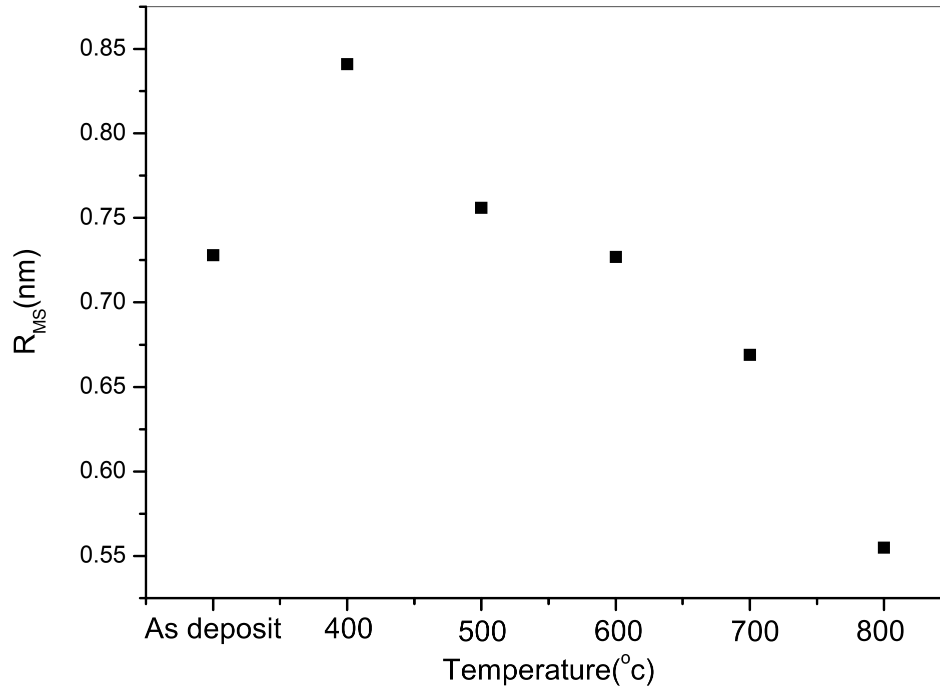

Figure 4-13 Surface roughness (R_{MS}) of CORAL film after annealing

thermal treatment but becomes smooth after high temperature treatment. The root-mean-square roughness (rms) of this film changes from ~0.728 to ~0.841nm after 400°C annealing. However after 800°C annealing the R_{MS} decreases to ~0.555nm. Pictures 4-2 (a) to (f) show the AFM images of the as-deposit CORAL film and the annealed films. It seems that the particle grain becomes small after annealing and the "ball like" grain of as-deposit film transform to "cloud like" grain after high temperature treatments. This change of grain's shape results in the smoothness of the film surface after annealing. For lower temperature annealing the thermal energy is too low to change the shape of the film

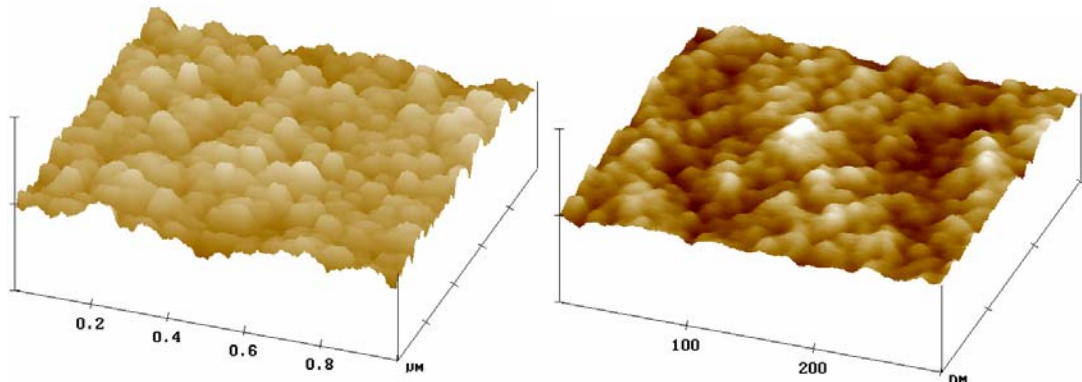

(a) (b)

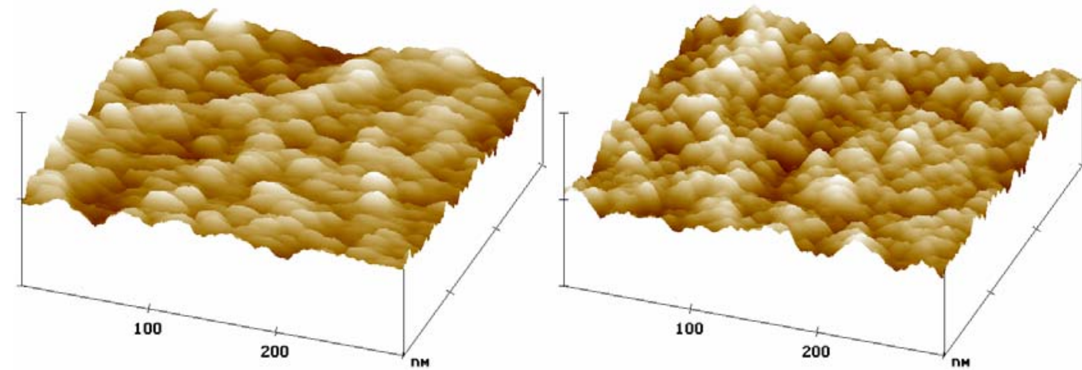

(c) (d)

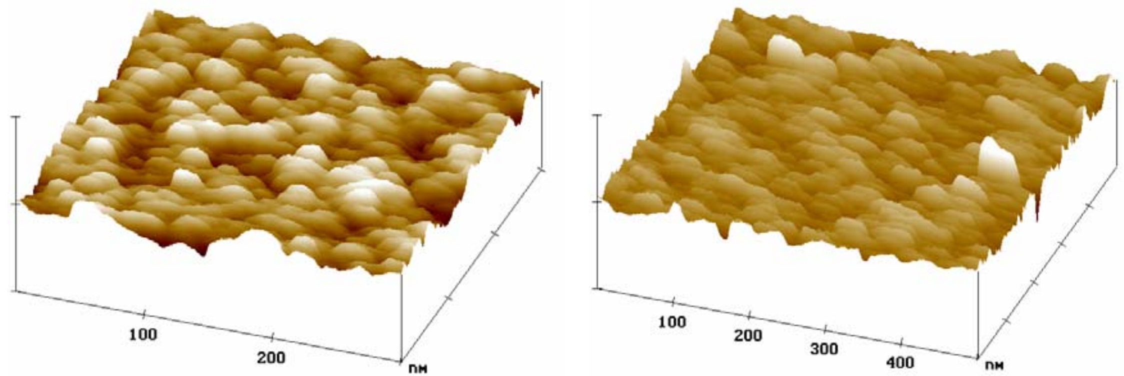

(e) (f)

Picture 4-2 AFM images of CORAL film surface after annealing
(a) As deposit film (b) After 400°C annealing (c) After 500°C annealing (d) After 600°C annealing (e) After 700°C annealing (f) After 800°C annealing

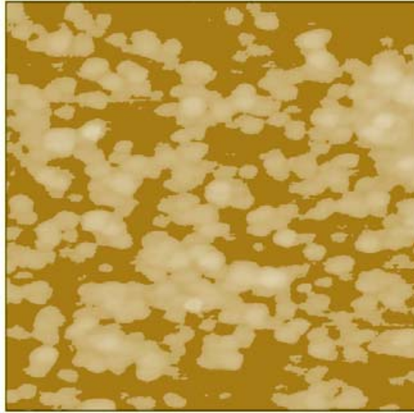

(a)

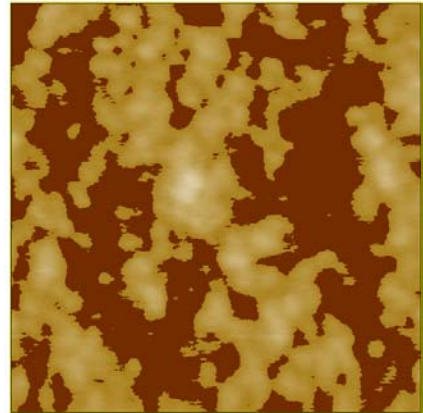

(b)

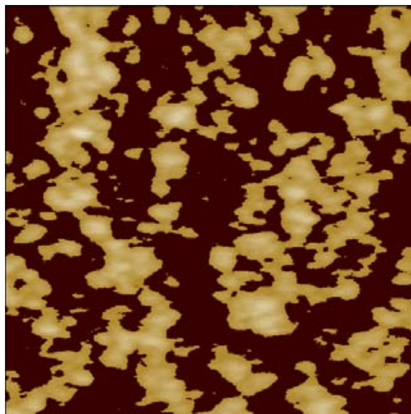

(c)

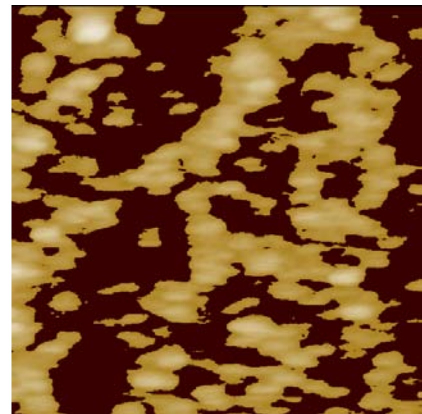

(d)

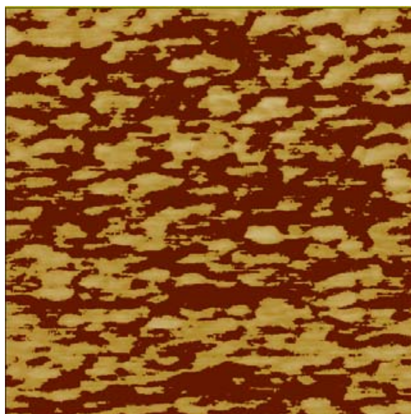

(e)

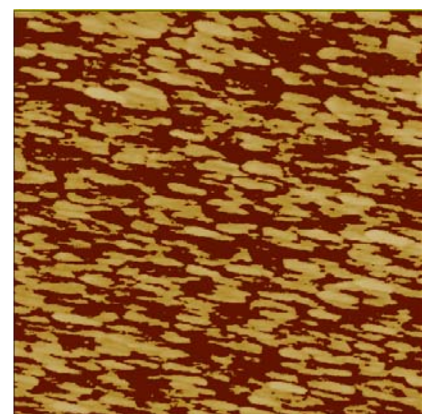

(f)

Picture 4-3 AFM images of CORAL film grain after annealing
(a) As deposit CORAL film(b) After 400^oC annealing(c) After 500^oC annealing (d) After 600^oC annealing (e) After 700^oC annealing (f) After 800^oC annealing

grain, but it can lead the "ball like" grains aggregate, resulting in rough film surface. Picture 4-3 (a) to (f) shows the film grain AFM images after annealing in N_2 for 30 minutes.

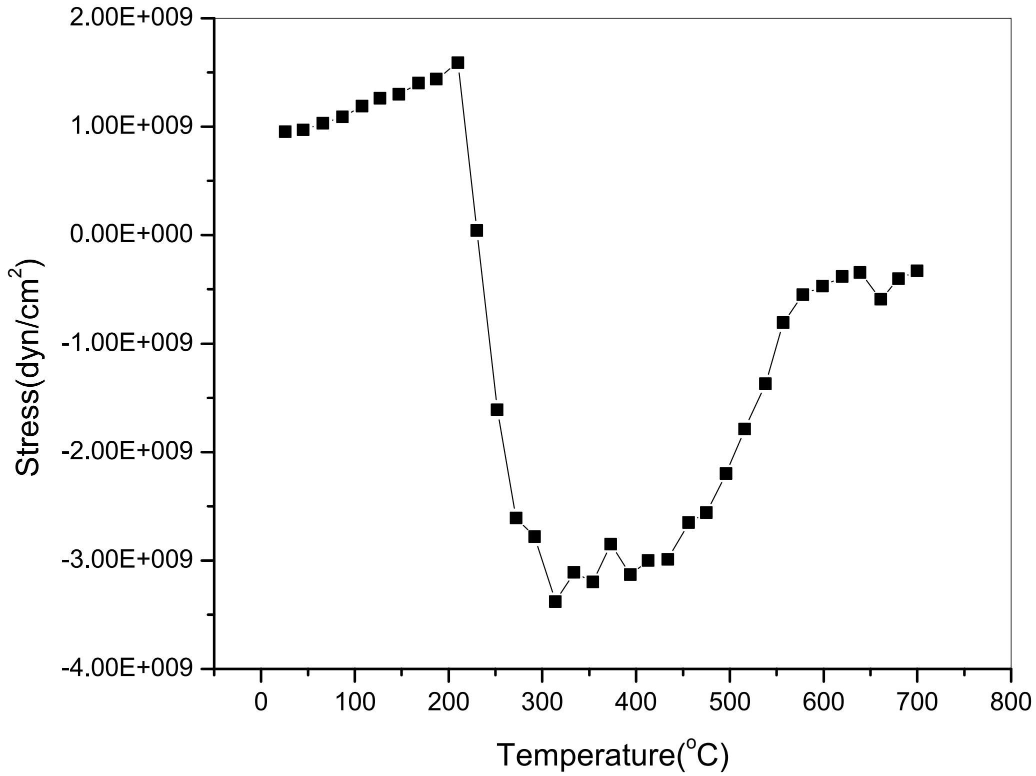

Figure 4-14 Dependence of stress on annealing temperature of CORAL film

The film stress was measured by FSM 7800TC stress measurement system. Fig. 4-14 is the result of film stress vs. annealing temperature. The tensile stress of CORAL film increases with increasing annealing temperature. With temperature elevates to about 230°C, the compressive stress reaches to maximum then released. CORAL film was deposited at 400°C, both the silicon and CORAL film at expanded status. After the as-deposit film wafer was taken out from the process chamber, and cooled to room

temperature, CORAL film tends to be "smaller" than the silicon substrate as it has higher coefficient of thermal expansion (CTE) (~30 ppm/^{o}C) than silicon (~3 ppm/^{o}C) has.[43] Therefore, at room temperature CORAL film indicates tensile stress. At temperatures below 230°C the stress of the film still remains tensile because intrinsic stress of CORAL film dominates. However, when annealing temperature ramps up further, thermal stress dominates, and CORAL film tends to be "larger" than the substrate, resulting in compressive stress due to its high CTE.

4.2.4 Chemical composition of CORAL films

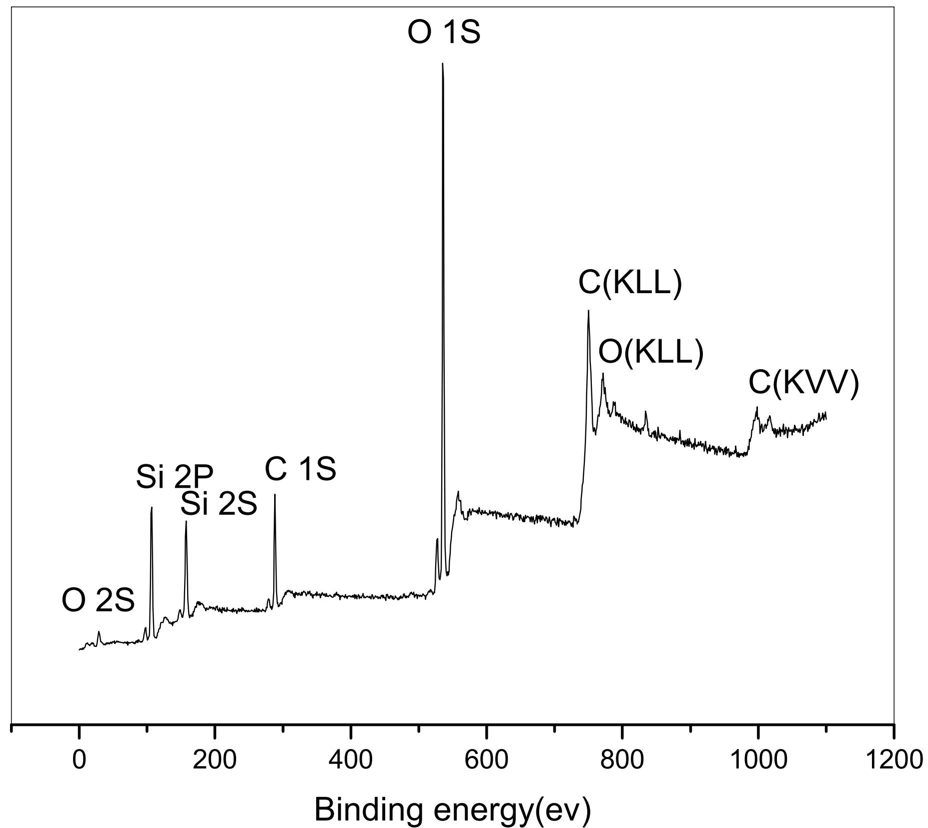

Figure 4-15 XPS wide scan of as-deposit CORAL film

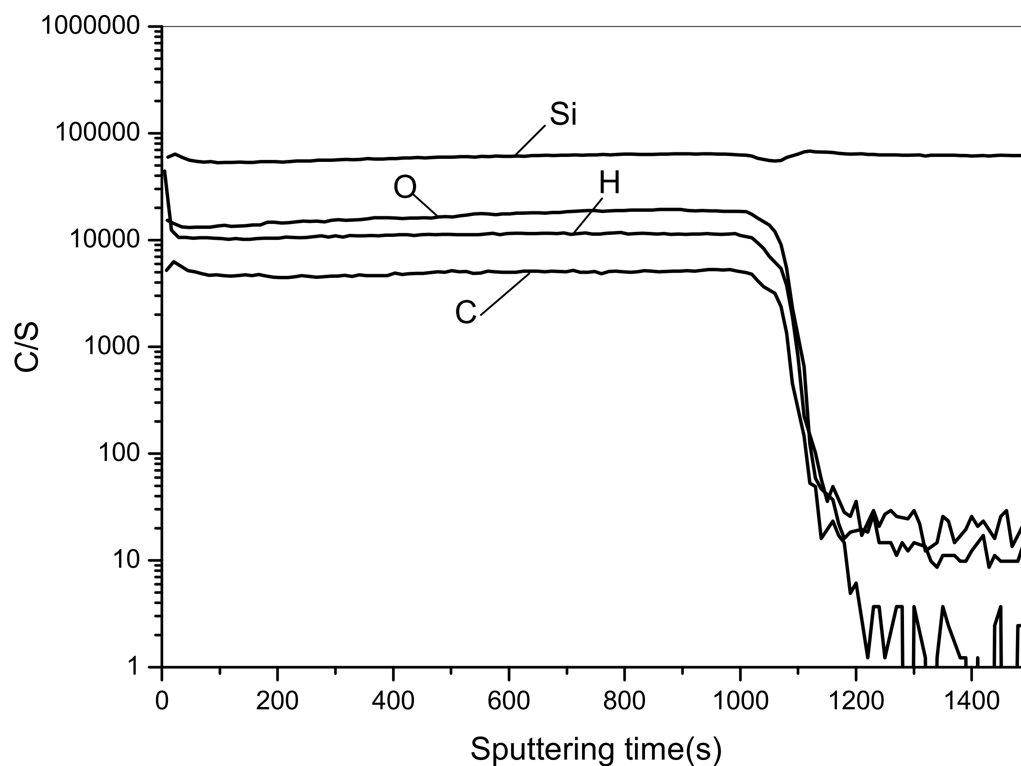

Figure 4-16 SIMIS depth profile of as-deposit CORAL film

The surface chemical composition of CORAL films was investigated by XPS and SIMS. Fig. 4-15 and Fig. 4-16 are the wide scan XPS spectrum and the SIMS depth profiles of the as-deposit CORAL film respectively, both of which reveal that CORAL film primarily consists of Si, C, O and H. The XPS spectra of the films after annealing at different temperatures are basically the same as that shown in Fig. 4-15, with some changes in relative peak intensities only. As summarized in Table 4-1, the O/Si ratio increases with increasing the annealing temperature, whereas the C/Si ratio decreases. The trend of the changes in these ratios is consistent with our SIMS results. As shown in

Fig. 4-17 for the oxygen to silicon ratio (at various annealing temperatures) and Fig. 4-18

Table 4-1 Element concentration of CORAL film after annealing

Temperature(°C)	C	O	O/Si	C/Si
As deposit	0.24	0.47	1.62	0.83
400	0.23	0.48	1.65	0.79
500	0.24	0.50	1.76	0.82
600	0.20	0.51	1.77	0.69
700	0.18	0.53	1.87	0.64
800	0.16	0.57	2.08	0.59

for the carbon to silicon ratio (at various temperatures), the concentration of carbon remains almost constant (~23 at.%) for the film after annealing at temperature below 600°C. However, after the temperature ramps up above 600°C, the carbon concentration becomes lower and lower. At 800°C the carbon concentration decreases to ~16 at.%. It is noted that the carbon loss is more evident on the top layers. The change of carbon concentration against the annealing temperature can well explain the change of the k value of the film. As will be discussed below, upon low temperature (below 600°C) annealing, the K value of CORAL film changes slowly, whereas it increases very quickly when the annealing temperature higher than 600°C.

The oxygen gain at high annealing temperatures above 600°C is shown in Fig. 4-17. Higher O/Si ratios indicate the incorporation of oxygen in CORAL film, which will

degrade the reliability of the film. In CORAL film, some of oxygen atoms in the SiO_2

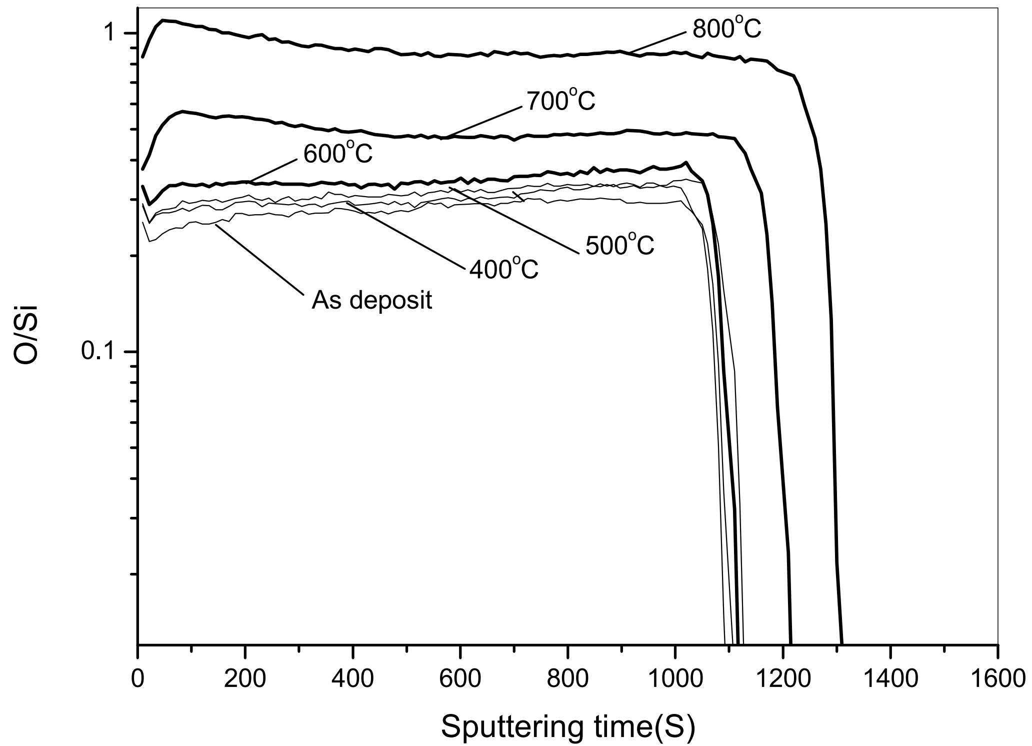

Figure 4-17 Oxygen to silicon ratio of CORAL film after annealing

network are replaced by carbon atoms. Upon high temperature annealing, some carbon loss is accompanied by the oxygen incorporation after the annealing. But these oxygen atoms may not form skeletal SiO_2 structure as they are in ideal SiO_2 film. Most of them would constitute Si-OH bonds, as observed from the FTIR spectra (see Fig. 4-7 after 800°C annealing). As mentioned above, the Si-OH bonds result in degradation of the film reliability.[44]

It is worthy to note that relative oxygen abundance occurs in the top layers whereas the relative carbon surface depletion occurs only for the annealing at 700-800°C. The relative

oxygen abundance in the top layers of CORAL film could be because when the annealing

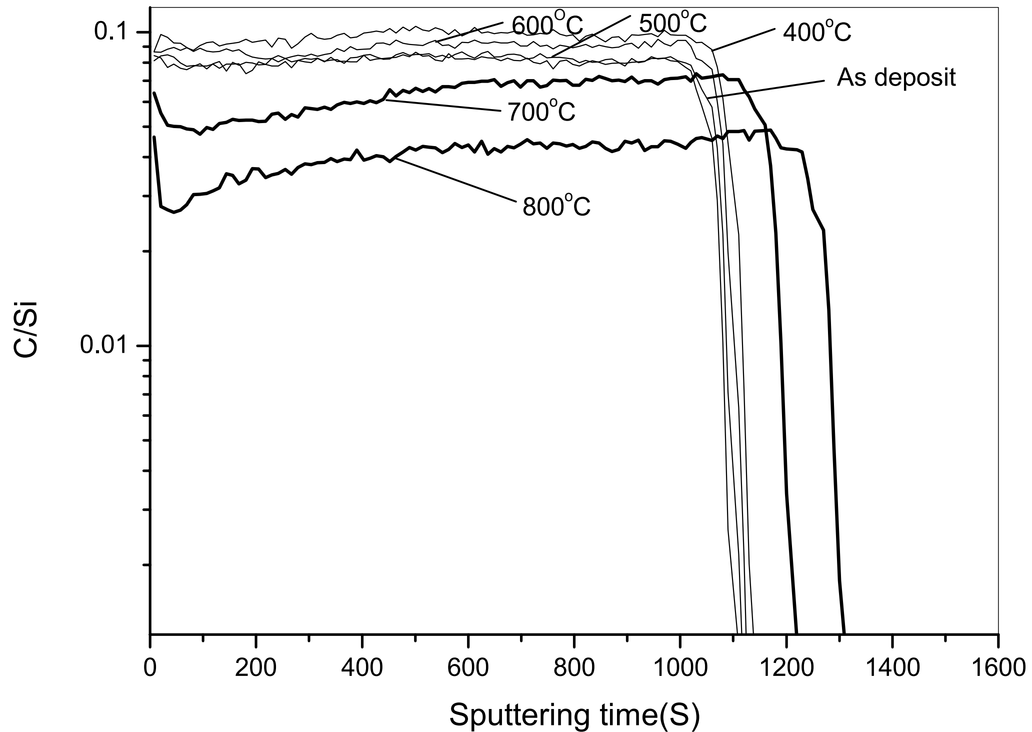

Figure 4-18 Carbon to silicon ratio of CORAL film after annealing

temperature ramps over 600°C, Si dangling bonds are generated resulting in CORAL film absorbs water easily, as discussed above. Abundant oxygen atoms can be observed after such high temperature annealing. The oxygen atoms cannot diffuse into the film so quickly after annealing. Therefore, the top layer has more oxygen atoms than the bottom layer. On the other hand, during annealing at 700-800°C, tremendous of carbon in the CORAL film was lost in the form of gas desorption. The top layers can desorb gases easily than the bottom layers. Carbon loss in the top layers of CORAL film results in carbon surface depletion after 700-800°C annealing.

Si 2p and C 1s XPS narrow scans shown in Fig. 4-19 and Fig. 4-20 can provide information on the detail chemical structure of CORAL film. Figs. 4-19 (a) to (f) show the Si 2p spectra of as-deposit film and films after annealing at different temperature respectively. The Si 2p spectrum can be deconvoluted into two different moieties using Gaussian-Lorentzian curve fitting method. The correction of charging shifts of these peaks is done by referring to C-C binding energy of 284.6eV. As shows in these figures, the peak at binding energy 103.4eV is assigned to SiO_4 skeletal structure. The other peak at binding energy 102.2eV, is assigned to CH_3-Si-O_3 in which one of the oxygen atoms is replaced by methyl group.[15] The intensity of the latter peak becomes lower and lower with the increase of annealing temperature, which means that Si-CH_3 bonds break, and is consistent with the FTIR results.

The C 1s spectra in Fig. 4-20 show that for annealing below 700°C the C 1s spectrum can be fitted by three Gaussian-Lorentzian peaks. The first peak at binding energy 283.6eV is assigned to Si-C carbide, while the second peak at 284.6eV is due to C-C or C-H, and the third one at 286.0eV to C-OH. The C 1s spectrum after 800°C annealing in Fig. 16f is evidently broadened at higher binding energy side, and needs to be fitted with an extra peak at 288.8eV, which is assigned to C-O. Note that the Si-C carbide peak grows remarkably at annealing temperatures higher than 500°C, which may appear to correspond to the increase of the cross-link structure (i.e. the cage structure) in the film, as already shown in the above FTIR study. Also the area of the C-OH component peak increases distinctly after 700-800^oC annealing indicating that CORAL film can absorb water easily after high temperature annealing. The C-O bond cannot be detected in the

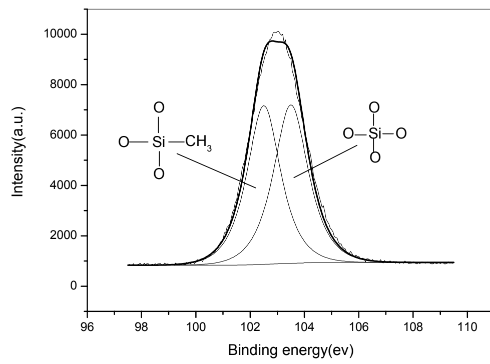

(a)

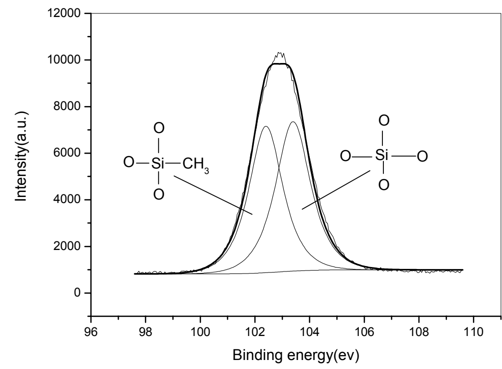

(b)

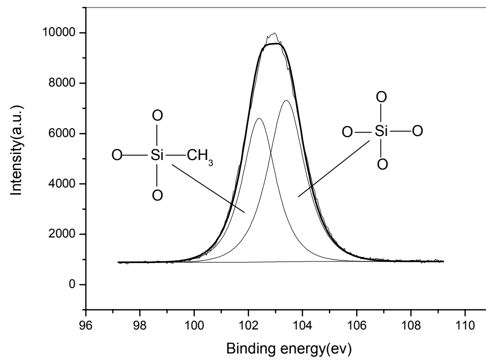

(c)

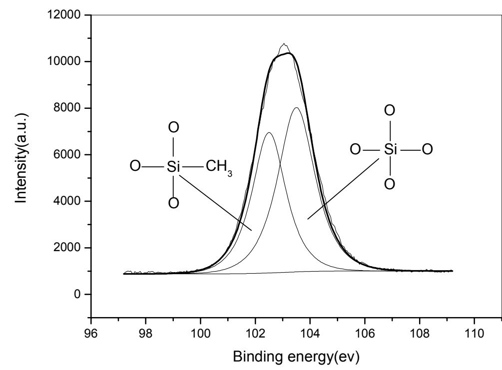

(d)

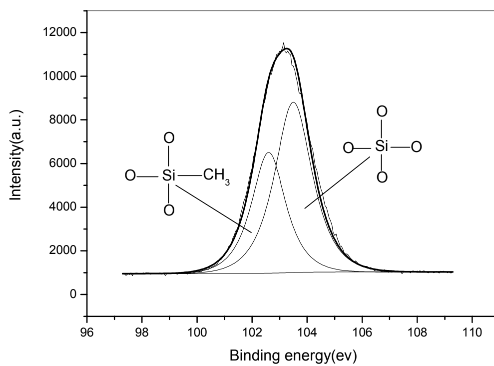

(e)

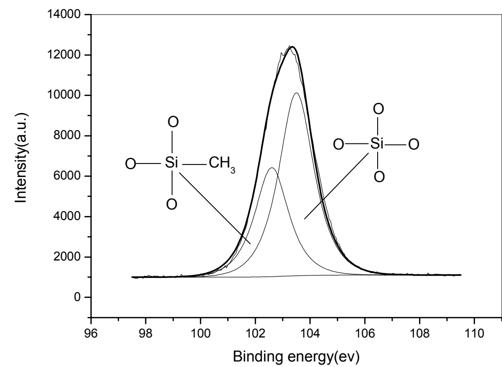

(f)

Figure 4-19 XPS narrow scan Si 2p of CORAL film after annealing
(a) As deposit (b) After 400°C annealing (c) After 500°C annealing (d) After 600°C annealing (e) After 700°C annealing (f) After 800°C annealing

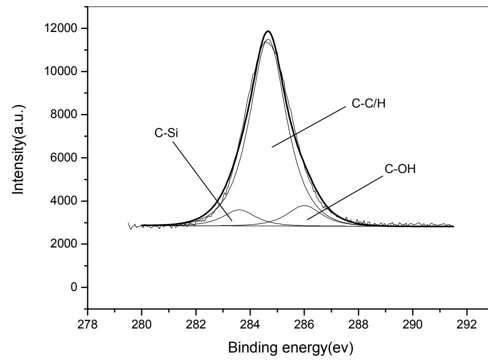

(a)

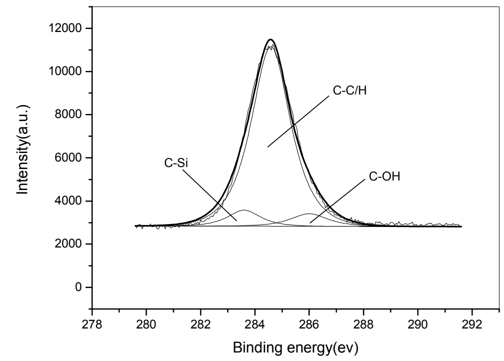

(b)

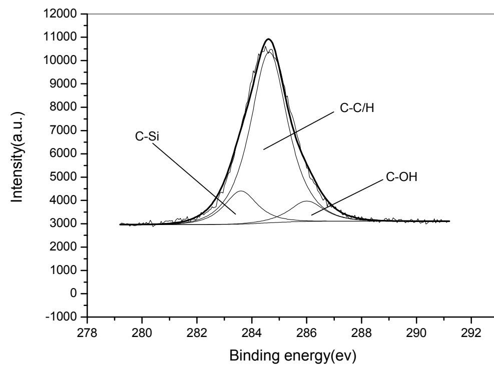

(c)

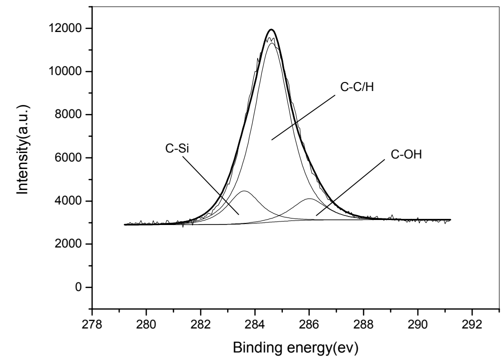

(d)

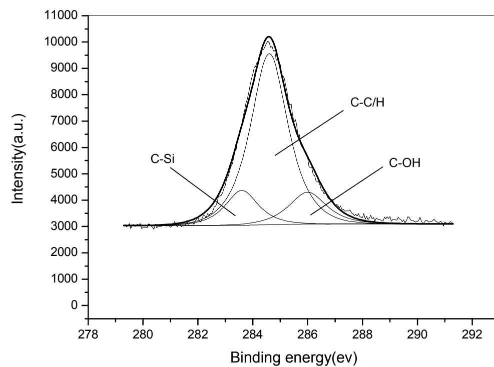

(e)

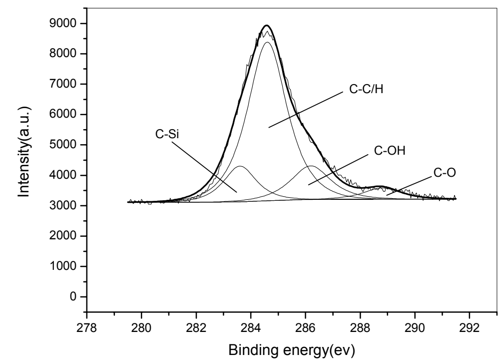

(f)

Figure 4-20 XPS narrow scan C 1s of CORAL film after annealing
(a) As deposit (b) After 400°C annealing (c) After 500°C annealing (d) After 600°C annealing (e) After 700°C annealing (f) After 800°C annealing

FTIR spectrum after 800°C annealing because the C-O bond located at 1000-1200 cm^{-1} is overlapped by and indistinguishable from the strong Si-O stretching band.[15] Carbon lost was indicated by the smaller and smaller total intensity of the C peaks after annealing at increasing temperatures.

4.2.5 K value and leakage current

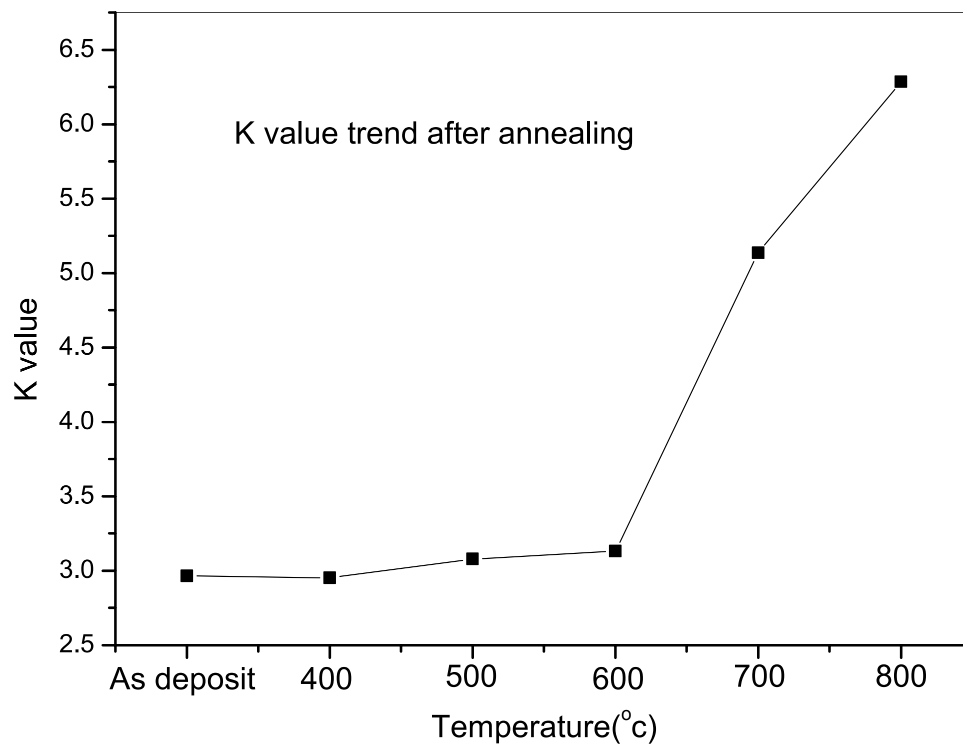

Figure 4-21 K value of CORAL after annealing

K value and leakage current are the two most important properties of interest. They were determined by using SSM 495 C-V system. Fig. 4-21 shows the change of the k value of CORAL film as function of the annealing temperature. It is found that below 600°C the k value increases very slowly with increasing annealing temperature. It increases about

5.6% after annealing at 600^oC in N_2 for 30 minutes. It could be because most of the Si-CH_3 and Si-C bonds in the film cannot be broken at below 600^oC treatment. For the annealing temperatures above 600^oC, the k value increases rapidly. At 700-800^oC, the k value is 2 times that of the as-deposit film. Obviously at such high temperature, the thermal energy is sufficiently high to easily break Si-CH_3 and Si-C bonds, resulting in the formation of dangling bonds Si- that can react easily with H_2O or oxygen to generate Si-OH bonds. The Si-OH bond has higher polarizability than Si-C bond. Therefore, the film annealed at temperatures 700-800^oC has a significantly high k value.

Leakage current is one of the most important electrical parameter of a low-k dielectric film. We test the leakage current of the CORAL films as-deposited and after annealing at different temperatures. No change was detected after 400^oC annealing. The increase in leakage current was found after annealing above 500^oC. At the field break-down voltage of 4 MV/cm, the leakage current increases from $\sim10^{-9}$ A/cm^2 for 400^oC annealing (as well as for as-deposit) to $\sim10^{-8}$ A/cm^2 for 500^oC and 10^{-7} A/cm^2 for 600^oC annealing. However, after above 600^oC annealing, the leakage current increases very fast (from $\sim10^{-7}$ to $\sim10^{-4}$ A/cm^2) (see Fig. 4-22), which could be due to the appearance of Si-OH bonds, the increase of film density, the reduction in porosity, and the change of film composition. If we define the current-to-breakdown is 0.001Amps, it is seen in Fig. 18 that V_{FB} decreases after annealing, from ~5MV/cm (400^oC) to ~4.3MV/cm (500^oC). The decreasing rate is very slow. But when annealing temperature is above 600^oC, V_{FB} decreases very fast. After 800^oC annealing, V_{FB} decreases about 77% to ~1.13MV/cm

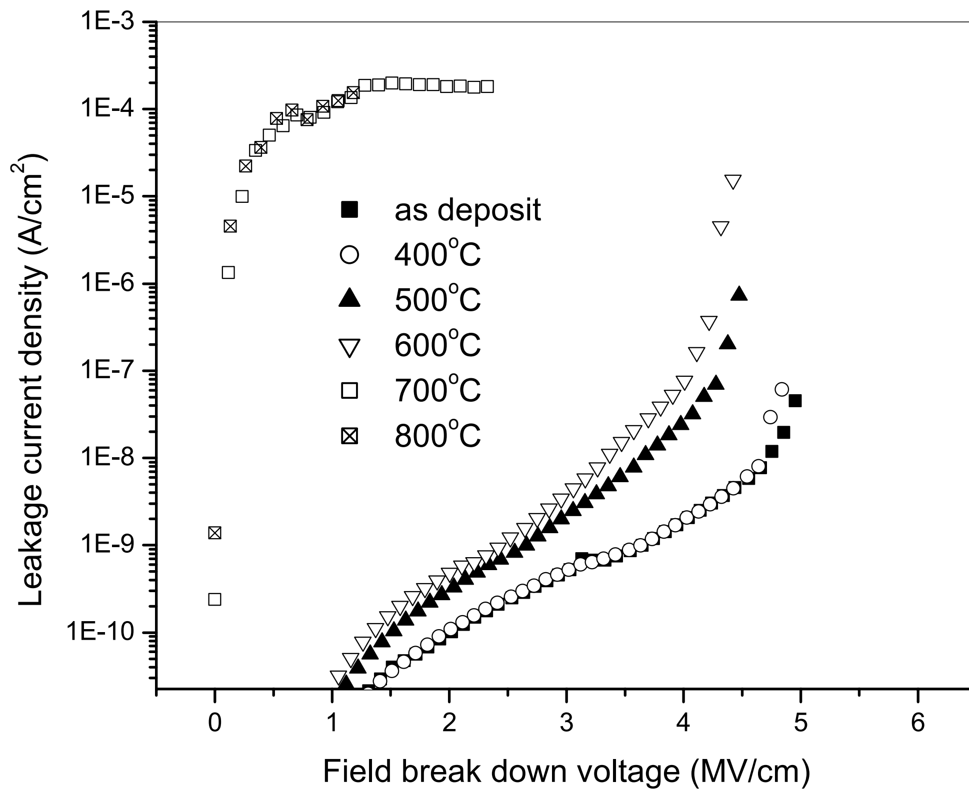

Figure 4-22 Field break down voltage of CORAL after annealing

compare to the as-deposit film. This could be due to the composition change and moisture uptake of the film.

4.3 Dilute HF treatment

Dilute HF has been shown to be an effective mean to increase the porosity of the SiO_2-based materials.[9,19] Here the effect of dilute HF treatments was studied to exam if it can reduce the k value of the CORAL films.

4.3.1 Thickness and Refractive Index (RI)

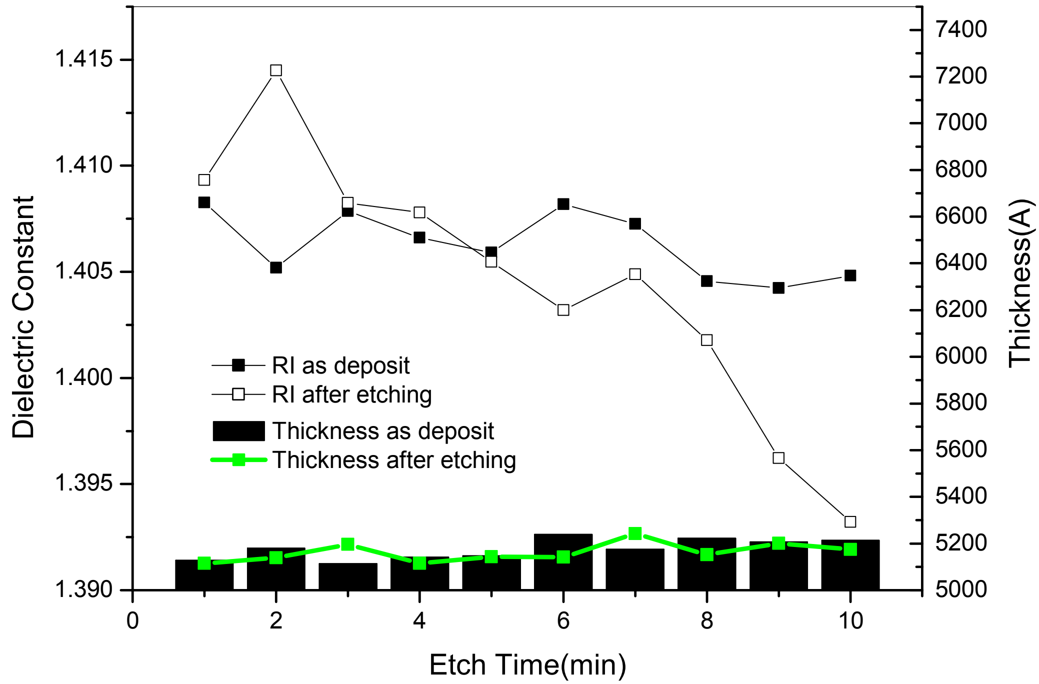

Figure 4-23 Thickness and RI of CORAL film after etching in 1% dilute HF

Fig. 4-23 shows the thickness and RI of CORAL film after etching in 1% dilute HF at room temperature from 1 minute to 10 minutes respectively. It is found that after about 5 minutes etching, RI begins to decrease whereas film thickness keeps constant up to 10 minutes. The reason could be dilute HF can only attack the SiO_2 skeletons of CORAL film. Therefore pores are introduced into CORAL film but thickness of the bulk films has no obvious change after etching. Because the concentration of HF is very low, film density changes due to pores are introduced i.e. RI changes can only be observed after a few minutes etching. Thus, decreasing dielectric constant of CORAL film can be expected by introducing pores in it.

4.3.2 Surface roughness

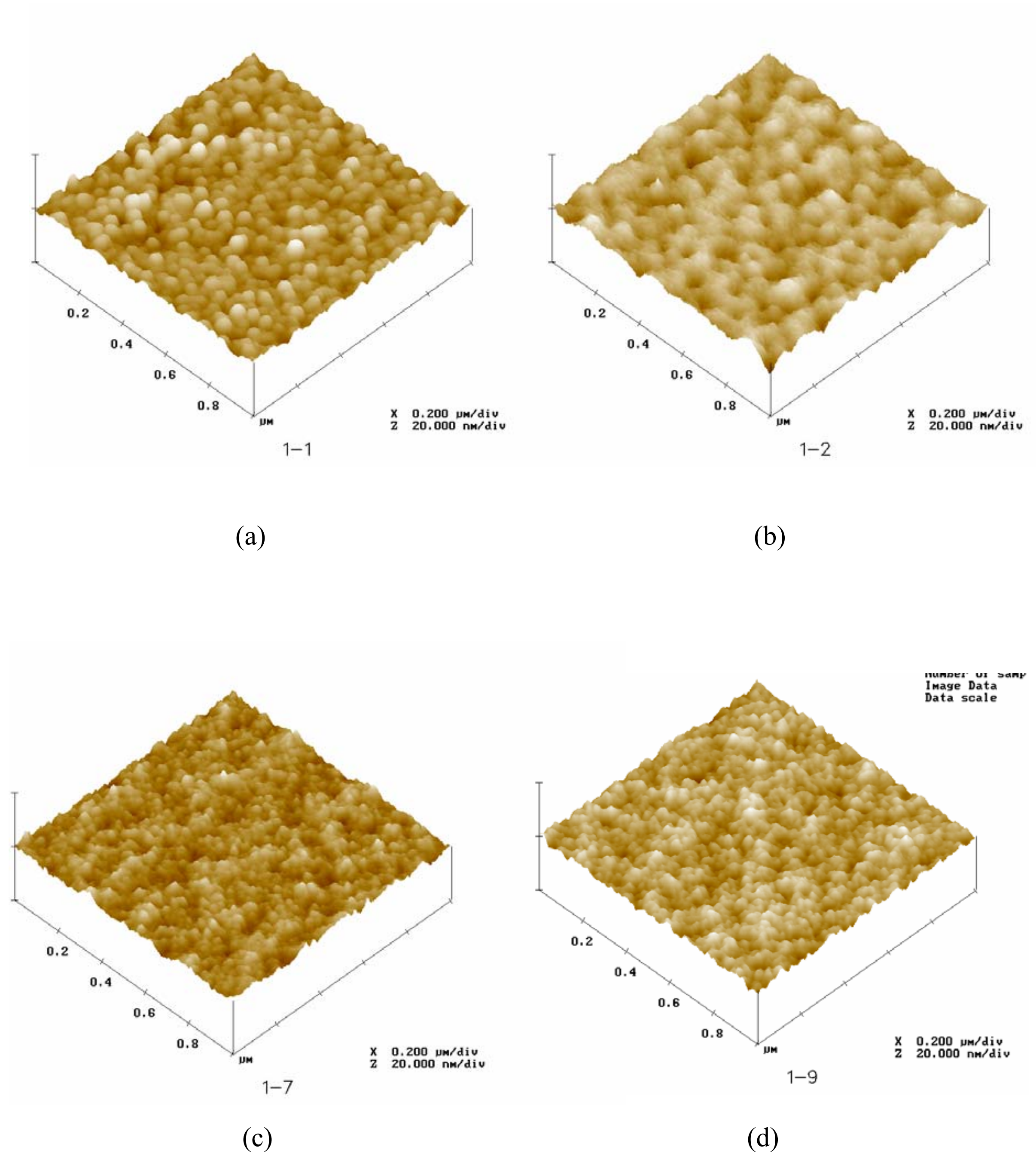

Figure 4-24 AFM images of CORAL surface after 1% dilute HF treatment
(a) After 1 minute (b) After 2 minutes (c) After 7 minutes (d) After 9 minutes

Fig. 4-24 shows the AFM image of CORAL film surface after different etching time in 1% dilute HF. Fig. 4-25 shows the surface roughness trend of CORAL film after dilute

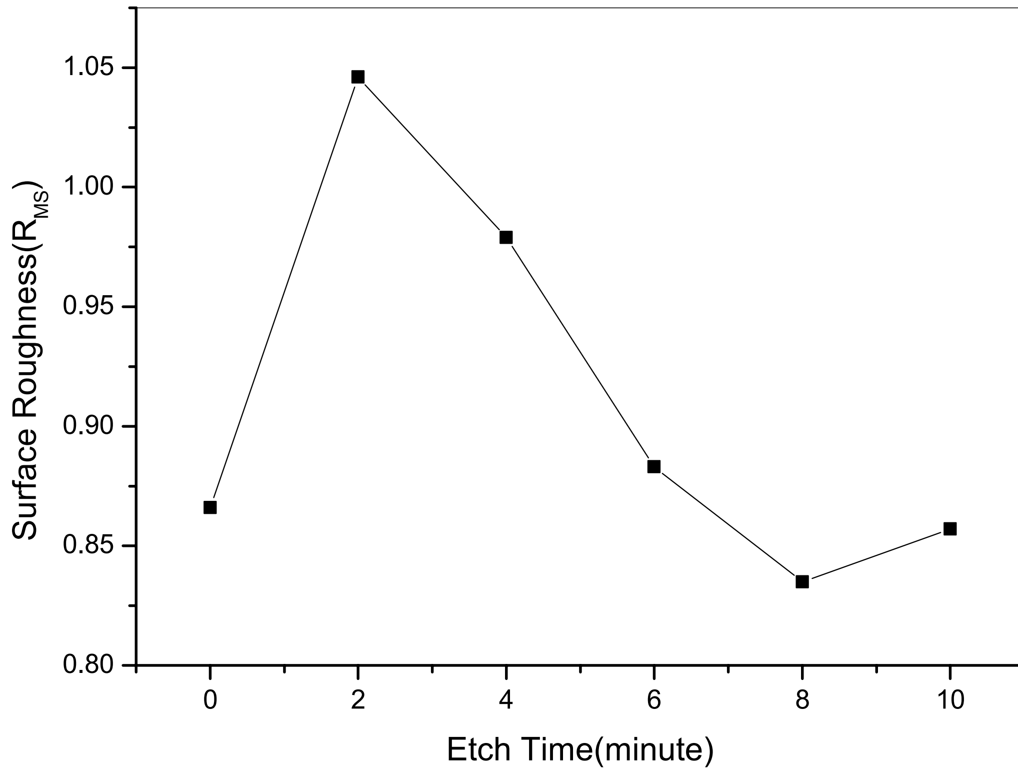

Figure 4-25 Surface Roughness of CORAL film after dilute HF treatment

HF treatment. It is found that surface roughness (R_{MS}) of CORAL film has the maximum value after etching for 2 minutes in dilute HF. The possible reason could be at the beginning, dilute HF attack CORAL film and introduce many pores in the film. Thus, the surface roughness of CORAL film in 1x1μm range becomes rougher and rougher. With increasing etch time, the pore size becomes big resulting in CORAL film surface smooth in a small range.

4.3.3 Chemical bonding

FTIR spectra show that no new peaks are observed after etching. The chemical bonding of CORAL film remains almost the same as that of the as-deposit film except the Si-O bond slightly decreases after up to 10 minutes etching in 1% dilute HF at room temperature. Fig. 4-26 shows Si-O bond decreases after etching. The results mean that CORAL film is stable in dilute HF except the skeleton Si-O is slightly attacked. Thus, the main properties of CORAL film can be maintained.

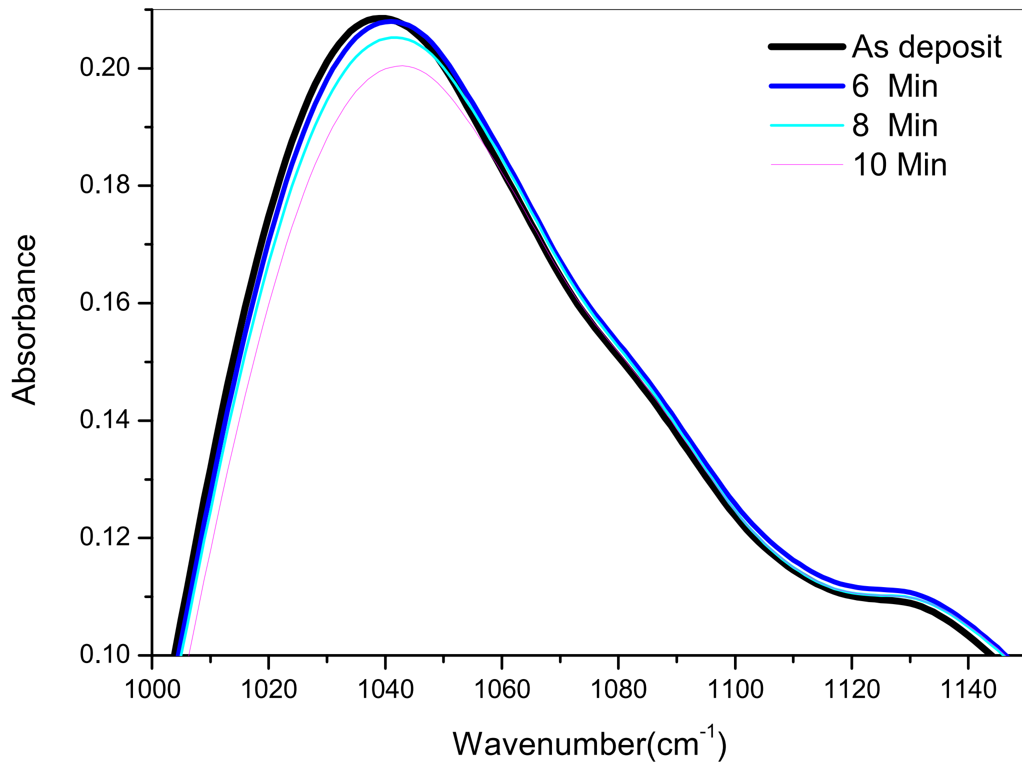

Figure 4-26 Si-O peak of CORAL film decreases after dilute HF etching

4.3.4 K value and leakage current

Fig. 4-27 shows the k value trend of CORAL film after dilute HF treatment under different time. Generally, the k value of CORAL film decreases after dilute HF etching.

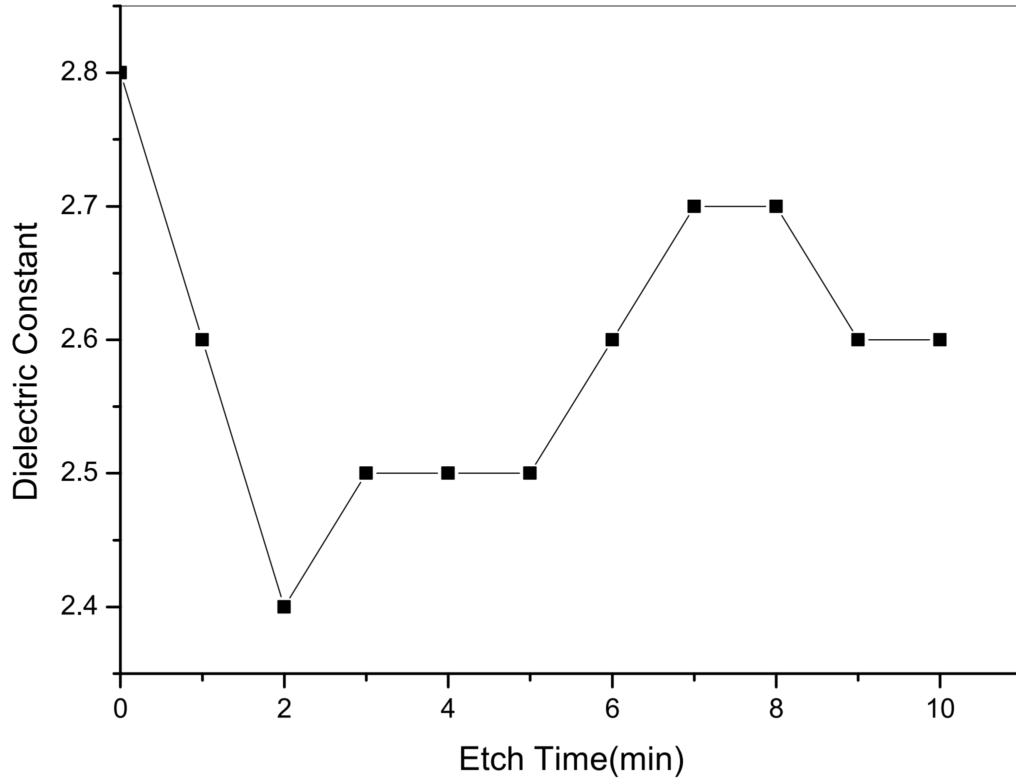

Figure 4-27 K value trend of CORAL film after1% dilute HF treatment

But it does not follow the rule that more etching time, lower k value. It is noticed that after about 2 minutes etching, the dielectric constant of CORAL film has the lowest value ~2.4, around 86% of the as-deposit film. Increasing etch time results in the k value is constrained in a certain range. This result corresponds to the surface roughness trend of CORAL film after dilute HF treatment. Two possible reasons can explain this

phenomenon: 1) Pores that contribute to reduce the k value decreases with the increasing etch time. In other words, in order to reduce the k value of CORAL film use dilute HF, the size of the pores introduced could be in a certain range. Otherwise, reduction of k value use this method is not effective. 2) When the pores introduced increase to a certain size, the interaction between mercury probe and this dilute HF treatment CORAL film is not clear, it needs further investigation. Therefore, the results obtained using this method is subjected to discuss. [18]

C-V curve hysteresis of CORAL film after dilute HF etching is shown in Fig. 4-28. It is found that more etching time on CORAL film more hysteresis of the C-V curve. The C-V curve shows significant hysteresis of 32V for V_{fb} (flat band voltage) shift after 10 minutes etching. This hysteresis can be interpreted by hole trapping mechanism at the Si/CORAL interface. In the forward curve, when the gate voltage is varied from -150V to 0 V so that the Si interface goes from accumulation to weak inversion, the Si interface is under high accumulation state at the beginning. There could be a high density of hole trapping sites at the Si/CORAL interface after a certain time HF etching, and these trapping sites could be filled with majority carrier holes at the accumulation state. The excess positive charge thus trapped at the interface will give rise to the negative V_{fb} shift of the forward C–V curve according to the formula: $V_{fb} = \Phi_{MS} - \frac{Q_0}{C_{ox}}$ where Q_0 is effective interface charge, C_{ox} is the CORAL capacitance per unit area and Φ_{MS} is the contact potential of body material (Silicon) to gate material (Hg). [33] When the gate voltage is brought to the weak inversion region (~0 V) de-trapping of the trapped holes will occur by charge exchange with the Si substrate. Although the band structure at weak

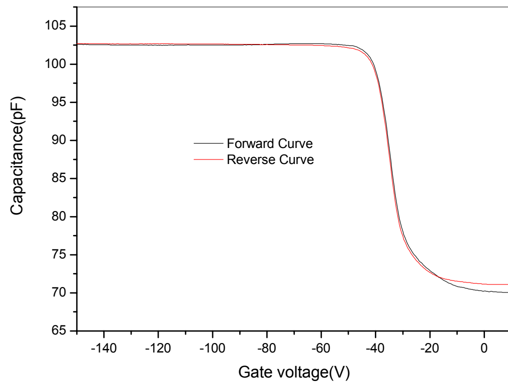

(a)

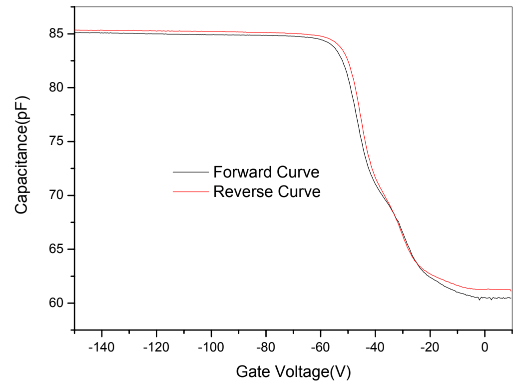

(b)

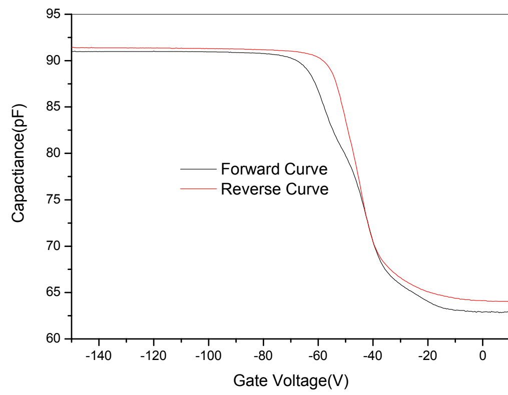

(c)

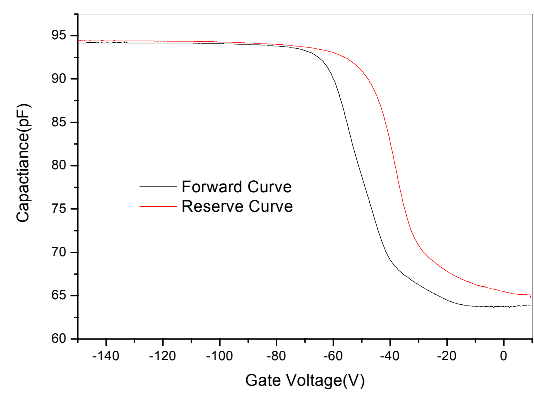

(d)

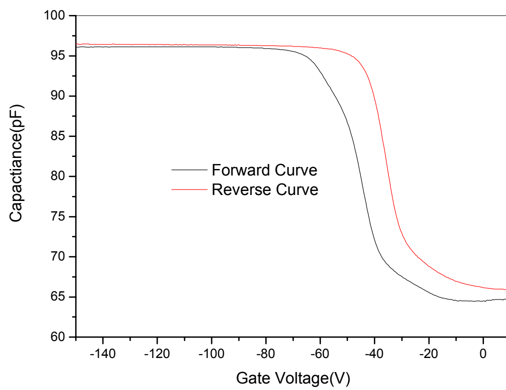

(e)

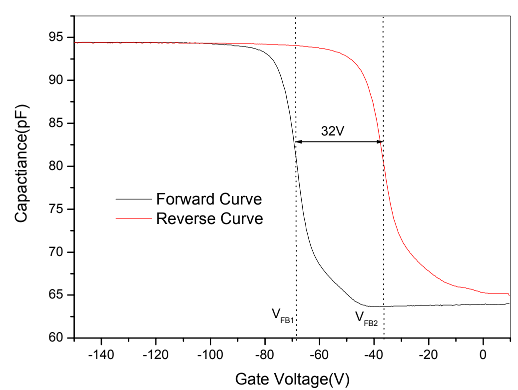

(f)

Figure 4-28 C-V curve of CORAL after etching in dilute HF
(a) As-deposit (b) After 2 minutes etch (c) After 4 minutes etch (d) After 6 minutes etch (e) After 8 minutes etch (f) After 10 minutes etch

inversion does not favor a strong hole de-trapping process, the amount of the positive charge de-trapped will be sufficient to cause the positive V_{fb} shift observed in the reverse curve in comparison to the forward curve. Thus, the hystersis of C-V curve indicates that hole trapping sites are introduced into Si/CORAL interface after dilute HF treatment.[45]

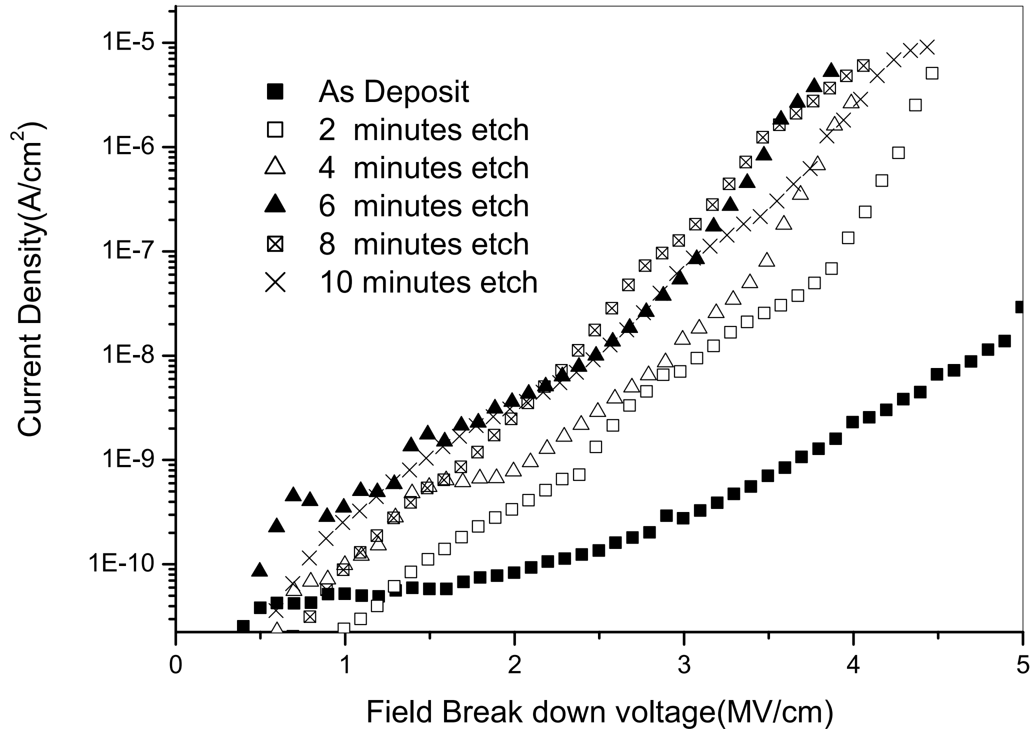

Figure 4-29 Leakage current of CORAL after 1% dilute HF etching

On the other hand, reducing k value by dilute HF etching leads to increasing leakage current of CORAL film. Fig. 4-29 shows the result of leakage current of CORAL film after dilute HF treatment. Leakage current increases from ~10^{-9}A/cm^2 to ~10^{-6}-10^{-8}A/cm^2 under field breakdown voltage 4MV/cm after etching in 1% dilute HF at room temperature up to 10 minutes. The reason can be attributed to introduction of hole trapping sites after dilute HF etching.[45]

4.4 Plasma treatment

Plasma treatment may possibly change the chemical composition of CORAL, hence its k value. The plasma treatments using various gases such as H_2/N_2, O_2, NH_3, He and Fluoride gas were performed in Applied Materials Centural 5200 PECVD system D_XZ chamber and Mattson photoresist strip (PRS) system. As presented below, the plasma treatments have indeed affected the k value of CORAL films.

4.4.1 Forming gas (4%H_2+N_2) plasma treatment

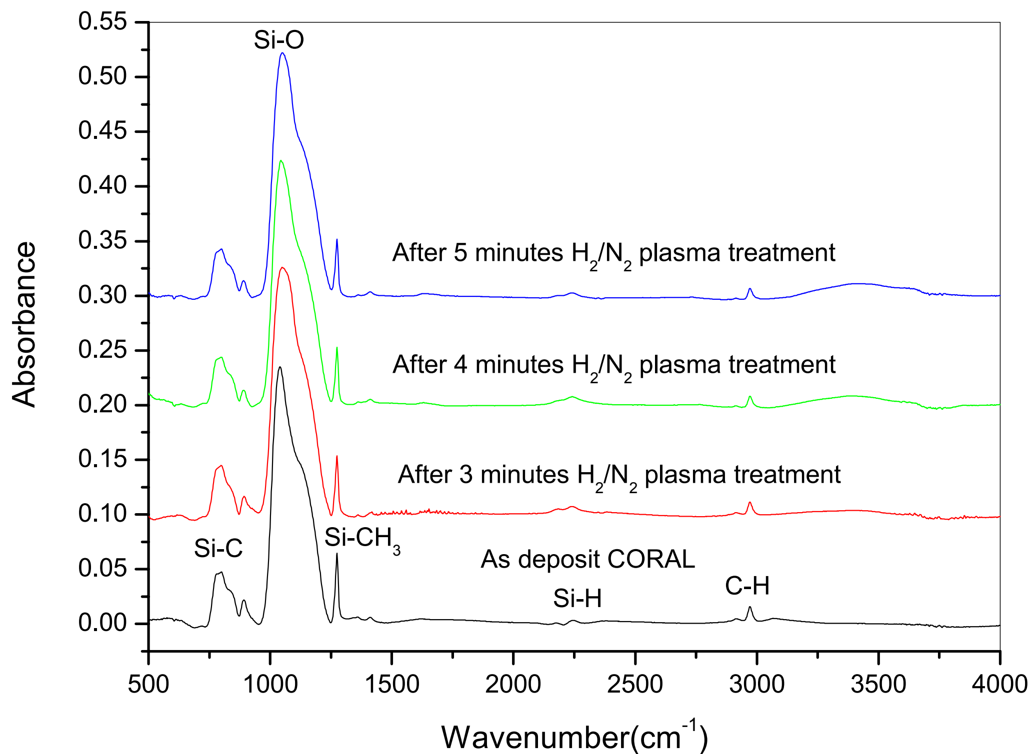

Figure 4-30 FTIR spectra of CORAL film after forming gas plasma treatment

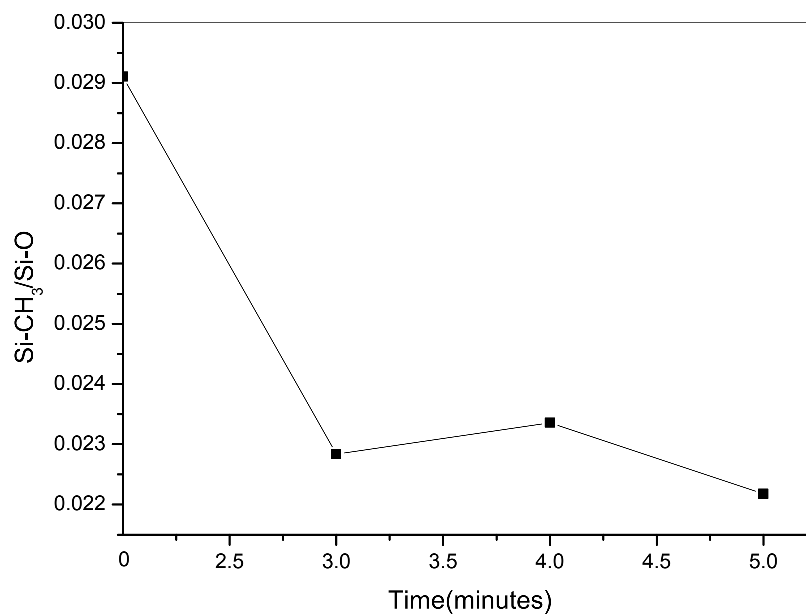

Figure 4-31 Peak area ratio of Si-CH_3 to Si-O as determined from FTIR spectra after forming gas plasma treatment

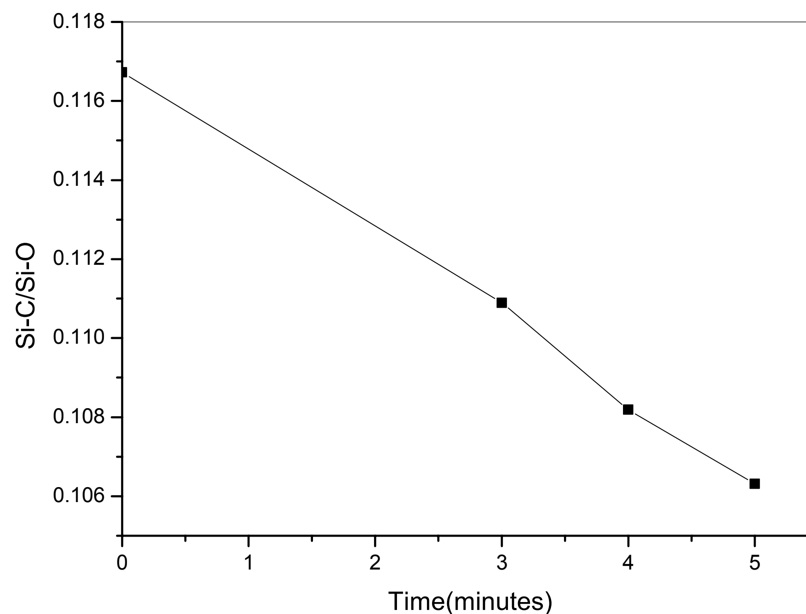

Figure 4-32 Peak area ratio of Si-C to Si-O as determined from FTIR spectra after forming gas plasma treatment

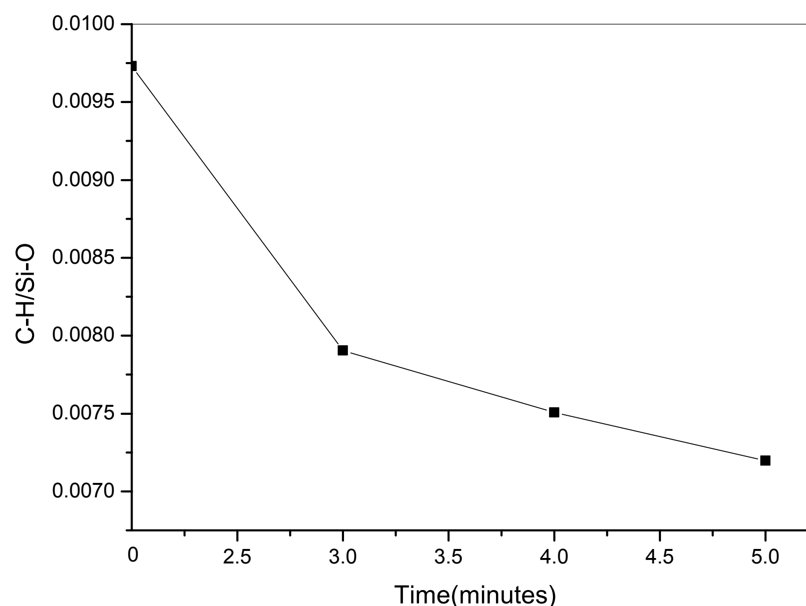

Figure 4-33 Peak area ratio of C-H to Si-O as determined from FTIR spectra after forming gas plasma treatment

Forming gas plasma treatment time was set to 3, 4 and 5 minutes respectively. The thickness of CORAL and RI remains stable after treatment. Fig. 4-30 shows the FTIR spectra of the CORAL film after forming gas plasma treatment. In Fig. 4-31 to Fig. 4-33 careful measurements shows that the area ratios of Si-CH_3, Si-H and C-H to Si-O decrease after forming gas treatment. This may mean that with increasing treatment time, the active species in forming gas plasma can attack Si-CH_3, Si-H and C-H bonds, resulting in the formation of Si dangling bonds. Because H^+ ions are too light to bombard the CORAL film, it is believed that N^+ ions bombardment in this process is very important. Nevertheless H^+ ions and moisture uptake can transfer Si dangling bonds to OH bonds easily, so OH broad bond at ~3000 to 3700cm^{-1} can be observed after 4 minutes plasma treatment.

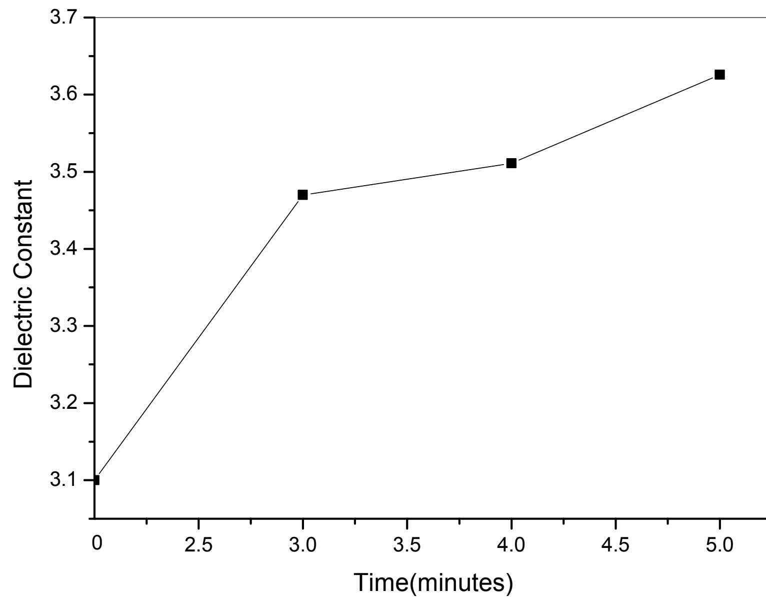

Figure 4-34 K value of CORAL after forming gas plasma treatment

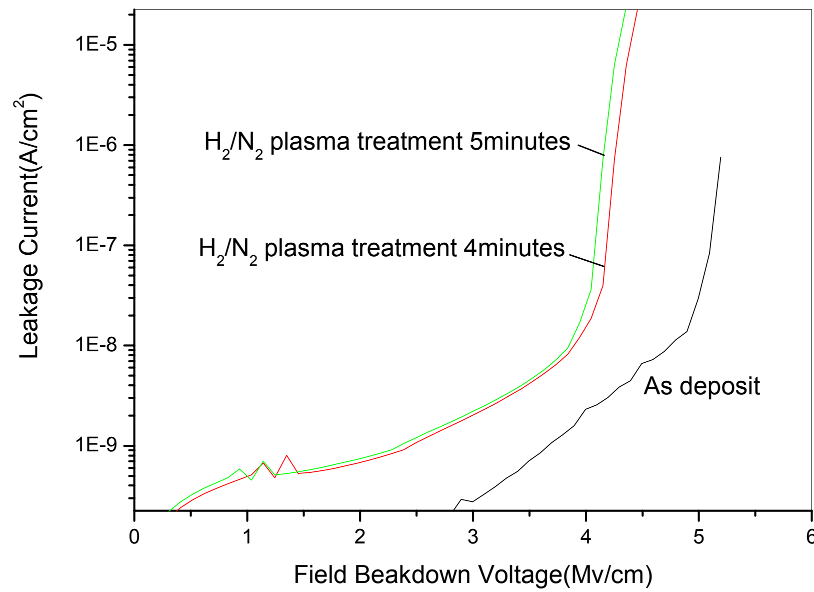

Figure 4-35 Leakage current of CORAL film after forming gas plasma treatment

As shown in Fig. 4-34 and Fig. 4-35, k value and Leakage current of CORAL film increases after forming gas plasma treatment. After 4 or 5 minutes plasma treatment, the k value increases from ~17% to 20% while the leakage current increases from ~10^{-9} A/cm^2 to ~10^{-8} A/cm^2 at field breakdown voltage 4MV/cm. It is attributed to incorporation of OH bonds.

4.4.2 Oxygen plasma treatment

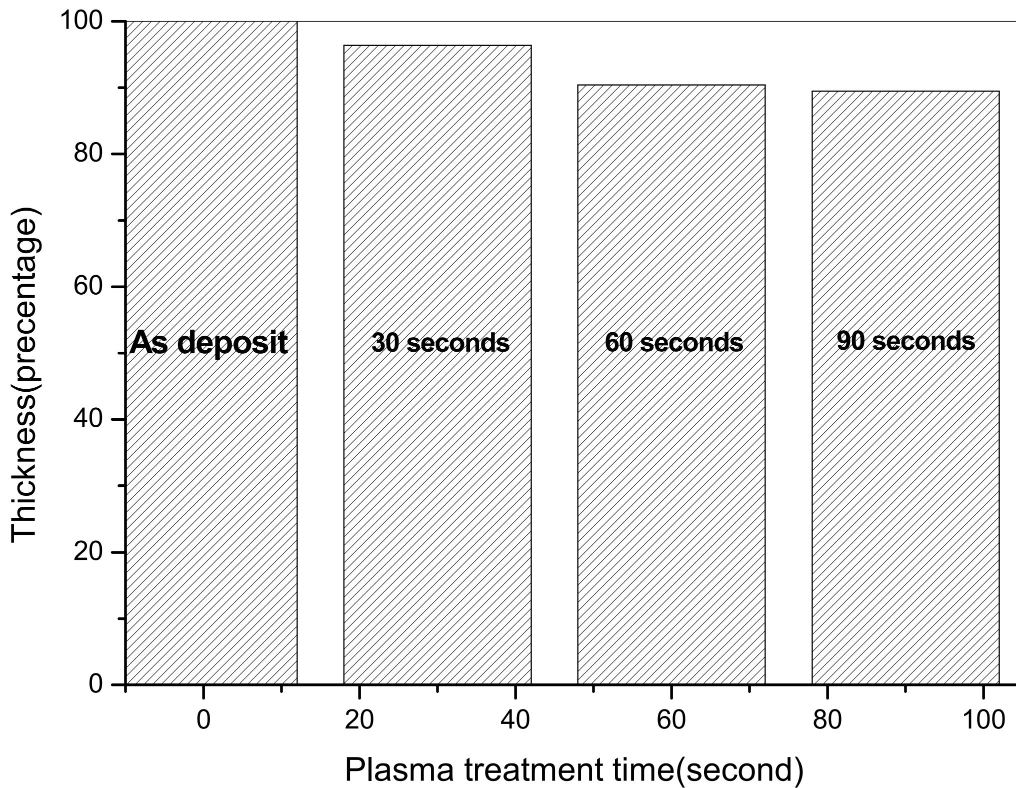

Figure 4-36 Thickness of CORAL after Oxygen plasma treatment

Oxygen plasma treatment time is set to 30 seconds, 60 seconds and 90 seconds respectively. Fig. 4-36 shows that the thickness of CORAL film decreases after 30

seconds of O_2 plasma treatment. After 90 seconds O_2 plasma treatment, the thickness of CORAL film decreases ~11% compared with the as-deposit film. Nevertheless after O_2 plasma treatment, the RI of CORAL film keeps no change. The thickness shrinkage of CORAL film after O_2 plasma treatment is attributed to the oxidation of Si-CH_3, C-H and O-Si-H bonds. Gas desorption is the main reason for thickness decreases.

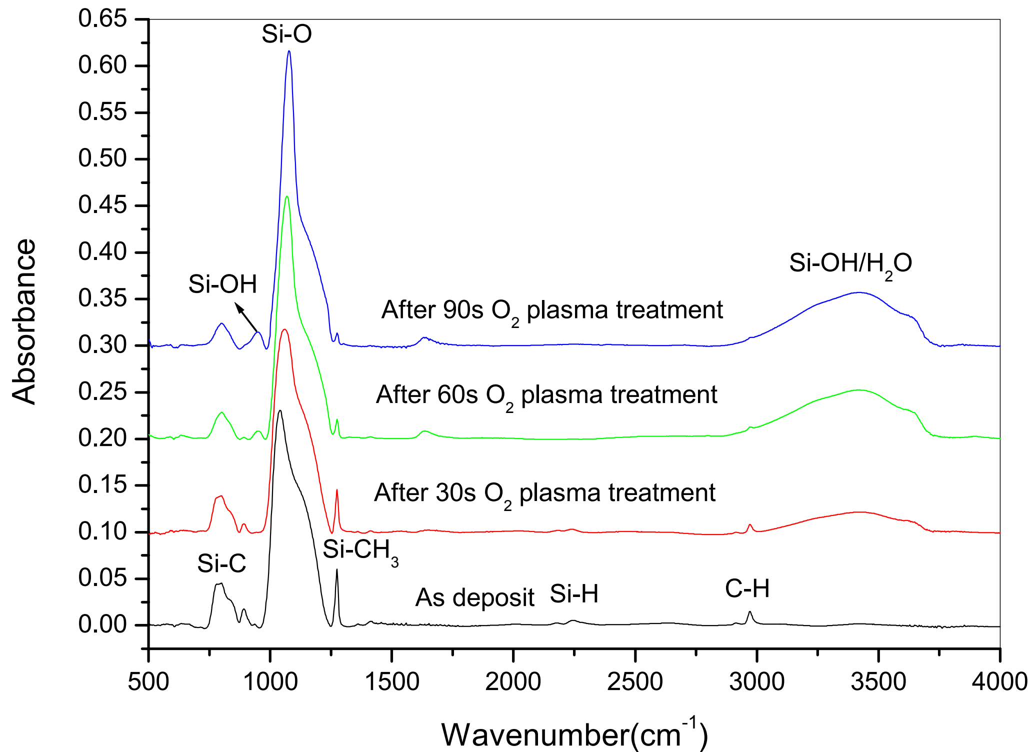

Figure 4-37 FTIR spectra of CORAL after Oxygen plasma treatment

Fig. 4-37 shows the FTIR spectra of the CORAL films after Oxygen plasma treatment for various time periods. It is seen that after 90 seconds of O_2 plasma treatment, Si-CH_3 and Si-H bonds almost completely disappear. It is also noticed that there are two new peaks appear at 965cm^{-1} and 3000-3700cm^{-1} respectively. The first peak at 965cm^{-1} is assigned to Si-OH bonds and the second one at 3000-3700cm^{-1} is assigned to Si-OH mixed with

H-OH bonds. After oxygen plasma treatment, plenty of functional groups are destroyed causing increasing Si dangling bonds in the CORAL film. Some of this dangling bond may form Si-O bonds, which is observable from the increase of the Si-O signal, and others convert into Si-OH bonds due to moisture uptake. [46]

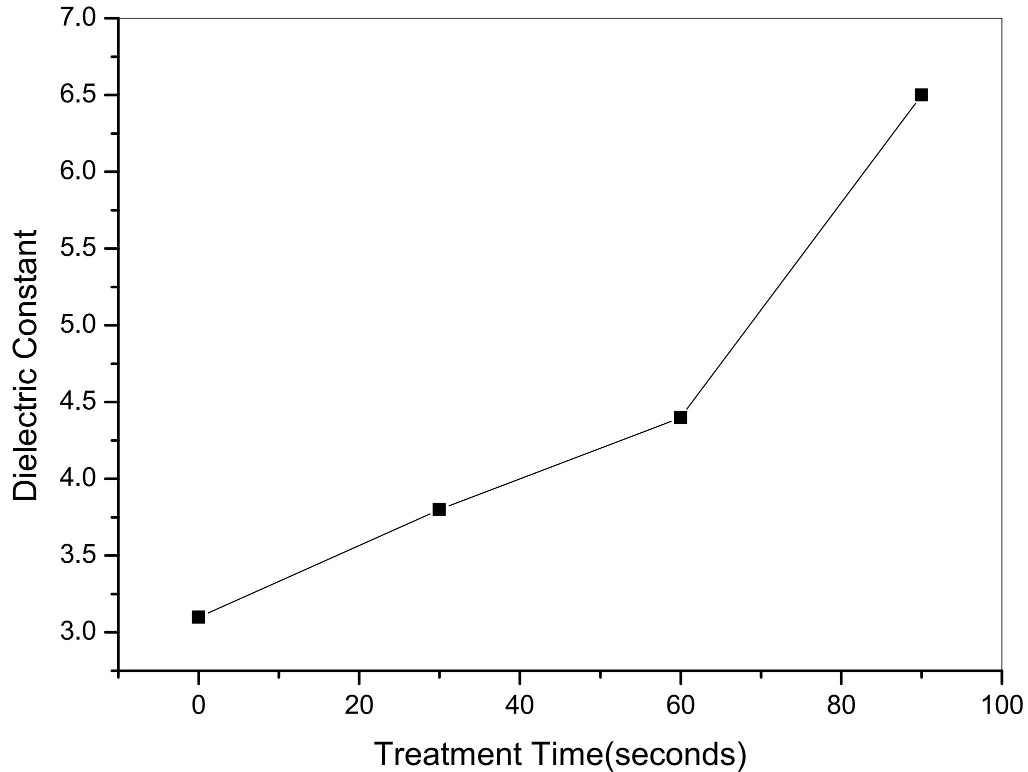

Figure 4-38 K value of CORAL after Oxygen plasma treatment

Fig. 4-38 and Fig. 4-39 show the k value and leakage current respectively of CORAL film after exposing to oxygen plasma for different time. The results are in good agreement with the FTIR spectra. K value increases dramatically due to the break-down of functional groups and moisture uptake. It is found that after 90 seconds of oxygen plasma treatment, the k value of CORAL film increases to ~6.5, double of that the as-deposit film. Accordingly, the leakage current of CORAL film increases from $\sim 10^{-8}$

A/cm^2 to ~10^{-3}-10^{-4} A/cm^2 at field breakdown voltage 4MV/cm after 90 seconds oxygen plasma treatment. Oxygen plasma treatment should be avoided in processing.

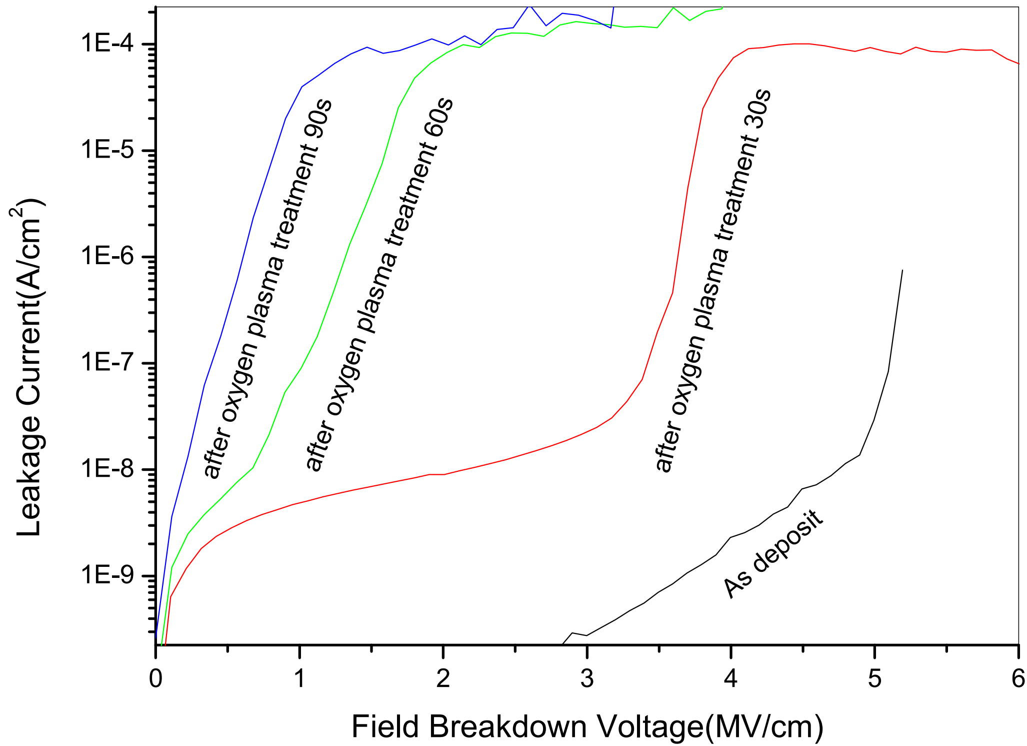

Figure 4-39 Leakage current of CORAL after Oxygen plasma treatment

4.4.3 Fluoride gas plasma treatment

An etch recipe (CHF_3+CF_4+Ar+O_2) was used to test the effect of the fluoride gas plasma treatment on CORAL film. At etch time of 15 seconds, about 100nm CORAL was etched. FTIR and k value measurement show that there are no chemical and dielectric constant change after etching. The main properties of CORAL film after etch is maintained. Although oxygen plasma treatment can change the properties of CORAL

film dramatically, the partial pressure and flow rate of oxygen in this process are optimized to avoid this negative effect. The main function of oxygen here is to accelerate the etching rate. Since the reaction of oxygen with CF_x radicals would form CO, CO_2 and COF_2, and produce more free fluorine. This effect, in combination with the lowering of the concentration of CF_x radicals by oxygen reaction, reduces the recombination of F atoms with CF_x and increases the steady-state F atom density. [34] On the other hand, oxygen plasma bombard the CORAL surface to destroy the function groups and transfer the top surface to oxide like film which is etched by fluorine plasma easily. When the oxide-like film transfer rate matches the etching rate exactly, maximum etching rate is obtained. Thus, concentration of oxygen in this process is very important. [18]

4.4.4 Ammonia and Helium plasma treatment

CORAL film is very stable upon NH_3 and He plasma treatments. FTIR results indicate that no obvious chemical change while k value measurement shows that dielectric constant and leakage current of CORAL film keep stable after 60 seconds NH_3 and He plasma treatment.

Chapter 5 Conclusion

By using PECVD process, carbon-doped low-k oxide CORAL film has been successfully synthesized using tetramethylcycloterasiloxane (TMCTS) as precursor. The effects of thermal treatment, dilute HF treatment and plasma treatment on the structural, chemical bonding and optical properties of CORAL have been carefully studied.

5.1 Thermal treatment

The properties of CORAL film are found to be stable up to 600^oC in N_2. However when annealing temperature ramps over 600^oC the carbon doped low-k material becomes unstable.

Above 600^oC annealing, the thermal energy is sufficiently high to break $Si\text{-}CH_3$, C-H and Si-H bonds, resulting in the formation of Si dangling bonds and outgassing of hydrogen, methane and carbon oxides. The Si dangling bonds can easily react with oxygen or H_2O in atmosphere to form Si-OH bonds increasing the k value and leakage. The outgasing leads to the film weight loss, thickness shrinkage (up to 25%) and carbon loss. The thermal annealing can also change the shape of the particle grains in the film and result in the surface roughness change.

The compositional change of the CORAL films, especially the carbon loss upon annealing, is an important reason for the increase of the k value. When carbon concentration decreased from ~24 at% to ~16 at% the k value increased from ~2.9 to ~7. Incorporation of oxygen atoms in CORAL film can degrade its reliability extremely. The incorporation of oxygen atoms in the film due to annealing may not form skeletal SiO_2 structure as they are in ideal SiO_2 film. Most of them constitute Si-OH bonds that result in the rise of leakage current from ~10^{-9} to ~10^{-4} A/cm^2.

Hence it is extremely important that thermal treatment should not exceed 600°C.

5.2 Dilute HF treatment

The dilute HF wet etching method was employed in order to reduce dielectric constant of CORAL films. It was found that the chemical structure of CORAL film remained stable after dilute HF etch except that Si-O bond concentration decreased, which was attributed to the interaction of HF with the main structure Si-O skeleton of CORAL film.

This method can reduce k value of CORAL film about 14% by introducing pores in it. On the other hand, this method may also introduce of hole trapping sites at the interface of Si/CORAL. These sites can increase leakage current of the dilute HF treated CORAL film.

5.3 Plasma treatment

The properties of CORAL film after H_2/N_2, O_2, fluoride gas, NH_3 and He plasma treatment were investigated. It was found that CORAL film was unstable after H_2/N_2 and O_2 plasma treatment whereas it remains stable after fluoride gas, NH_3 and He plasma treatment.

In H_2/N_2 plasma, the effect of N^+-ion bombardment the CORAL film was obvious due to its heavy mass. This bombardment results in the bond-breakage of certain functional groups in CORAL film, forming Si dangling bonds. The H^+ ions and water in the atmosphere then transferred the Si dangling bonds to OH bonds. The OH bonds can degrade film properties including increased k value and leakage current.

In O_2 plasma, the function groups of CORAL film were destroyed by oxygen radicals. This process results in thickness decreased which was attributed to gas desorption from CORAL film. The breakage of function groups result in Si dangling bonds, some of which may form Si-O bonds, and the others were transferred to OH bonds due to moisture uptake. The incorporated OH bonds result in k value and leakage current increased.

Therefore the comprehensive study of the effect of various treatments would suggest thermal annealing below 600^oC, dilute HF etching and plasma treatment with fluoride gas

(for film etching), NH_3 and He. The dilute HF treatment may lower the k value of CORAL films due to the increase of film porosity.

Reference:

[1] S.M.Sze , VLSI Technology 1988

[2] Laura Peters Semiconductor International May 2001 P.68

[3] Keith Buchanan, Solid State Technology August, 2003

[4] G. Maier Prog. Polym. Sci. 26 3-65 (2001)

[5] D. Shamiryan Microelectronic Engineering 64 361-366 (2002)

[6] Michael E. Clarke Introducing Low-k Dielectrics into Semiconductor Processing Online access on 28 November 2003 http://www.mykrolis.com/publications.nsf/0/dcc71529daa48c5e85256c4800744cf0/$FILE/Mal123.pdf

[7] Laura Peters, Semiconductor International June 2000 P108

[8] Michael Morgen Annu. Rev. Mater. Sci. 30:645-80 (2000)

[9] M. ONeill, A. Lukas, R. Vrtis, J. Vincent, B. Peterson, M. Bitner and E. Karwacki, " Low-k Materials by Design" Semiconductor International July 2002

[10] Y.L. Cheng , Y.L. Wang , C.W. Liu , Y.L. Wu , K.Y. Lo , C.P. Liu , J.K. Lan Thin Solid Films 398 –399 533–538 (2001)

[11] D. G. Shamiryan Electrochemical and Solid-State Letters, 4 (1) F3-F5(2001)

[12] Electronic News 27 August, 2003

[13] C.Y.Chang and S.M.Sze, ULSI Technology

[14] M.J. Loboda Microelectronic Engineering 50 15-23 (2000)

[15] Licheng M. Han Journal of The Electrochemical Society, 148 (7) F148-F153 (2001)

[16] Ravi K. Laxman Semiconductor International November 2000

[17] The International Technology Roadmap of Semiconductor 2002 update

[18] K. Maex, M. R. Baklanov, D. Shamiryan, F. Lacopi, S.H. Brongersma and Z.S. Yanovitskaya Journal of Applied Physics, Applied Physics Reviews—Focus Review Volume 93, Number 11 1 June 2003

[19] J.T. Rantala, W. McLaughlin, J.S. Reid, D. Beery, N.P. Hacher Solid State Technology Vol. 46, No. 12 December 2003

[20] Yoshimi Shioya, Kazuo Maeda, Tomomi Ishimaru, Toshiyuki Ohdaira and Ryoichi Suzuki Journal of The Electrochemical Society, 149 (9) F103-F109 (2002)

[21] H. Zhou, H. K. Kim, F. G. Shi, B. Zhao and J. Yota Microelectronics Journal 33 999-1004 (2002)

[22] Ben Pang et al. Semiconductor Fabtech—10th Edition

[23] Zhen-Cheng Wu Journal of The Electrochemical Society,148 (6) F127-F132 (2001)

[24] D.Shamiryan Microelectronic Engineering 64 361-366 (2002)

[25] Satoshi Sugahara, Tomohiro Kadoya, Koh-ichi Usami, Takeo Hattori and Masakiyo Matsumura Journal of The Electrochemical Society, 148 (6) F120-F126 (2001)

[26] H. Zhou, H. K. Kim, F. G. Shi, B. Zhao and J. Yota Microelectronics Journal 33 221-227 (2002)

[27] Takeshi Furusawa, Daisuke Ryuzaki, Ryo Yoneyama, Yoshio Homma and Kenji Hinode Electrochemical and solid-state Letters, 4 (3) G31-G34 (2001)

[28] Y.H.Wang Electrochemical and solid-state Letters, 6 (1) F1-F3 (2003)

[29] Jerry Healey "Current Technical Trends: Dual Damascene & Low-k Dielectrics" 2002 by Threshold Systems

[30] K.Mosig Microelectronic Engineering 64 11-24 (2002)

[31] O. Louveau Microelectronic Engineering 1 000-000 (2002)

[32] D.Louis Proceeding of IEEE IITC, p.289 2001

[33] T.Furusawa Proceeding of IEEE IITC, p.222 2000

[34] Stephen M. Rossnagel Handbook of plasma processing technology 1989

[35] Yannis Tsividis Operation and Modeling of The MOS Transistor 1999

[36] Bill George, Peter Mclntyre "Infrared Spectroscopy" by Wiley 1987

[37] http://www.uwo.ca/ssw/services/afmfiles/whatis.html

[38] http://www.lasurface.com/w_xps/Ag_xps_novis.htm

[39] http://www.uwo.ca/ssw/services/sims.html

[40] http://www.me.ust.hk/~mejswu/MECH343/SIMS-notes.pdf

[41] Mark O'Neill Semiconductor International June 2002

[42] T.C.Chang, P.T. Liu, F.Y. Shih, S.M. Sze Electrochemical and solid-state Letters, 2(8) 390-392(1999)

[43] Cu Technology HYNIX Semiconductor May 2002 Online access on October 2003 http:// www.postech.ac.kr/bk21/ece/Kor/Achieve/news/hynix/CU1.pdf

[44] B.K.Hwang Proc. ISMIC Conf. 104,113(1995)

[45] Rohana Perera, Akihiro Ikeda*, Reiji Hattori, Yukinori Kuroki Thin Solid Films 423 (2003) 212–217

[46] Po-Tsun, T.C.Chang, Y.S. Mor, C.W.Chen, T.M.Tsai, C.J.Chu, F.M.Pan and S.M.Sze Electrochemical and solid-state Letters, 5 (3) G11-G14(2002)